UNIVERSITY OF AMSTERDAM

UvA-DARE (Digital Academic Repository)

Search for Higgs bosons decaying into new spin-0 or spin-1 particles in four-lepton final states with the ATLAS detector with 139 fb^{-1} of pp collision data at √s = 13 TeV

The ATLAS Collaboration

DOI
10.1007/JHEP03(2022)041

Publication date
2022

Document Version
Final published version

Published in
Journal of High Energy Physics

License
CC BY

Link to publication

Citation for published version (APA):
The ATLAS Collaboration (2022). Search for Higgs bosons decaying into new spin-0 or spin-1 particles in four-lepton final states with the ATLAS detector with 139 fb^{-1} of *pp* collision data at $\sqrt{s}$ = 13 TeV. *Journal of High Energy Physics*, *2022*(3), Article 41. https://doi.org/10.1007/JHEP03(2022)041

General rights
It is not permitted to download or to forward/distribute the text or part of it without the consent of the author(s) and/or copyright holder(s), other than for strictly personal, individual use, unless the work is under an open content license (like Creative Commons).

Disclaimer/Complaints regulations
If you believe that digital publication of certain material infringes any of your rights or (privacy) interests, please let the Library know, stating your reasons. In case of a legitimate complaint, the Library will make the material inaccessible and/or remove it from the website. Please Ask the Library: https://uba.uva.nl/en/contact, or a letter to: Library of the University of Amsterdam, Secretariat, P.O. Box 19185, 1000 GD Amsterdam, The Netherlands. You will be contacted as soon as possible.

UvA-DARE is a service provided by the library of the University of Amsterdam (https://dare.uva.nl)

Download date:11 Oct 2026

Published for SISSA by Springer

Received: October 27, 2021
Revised: February 2, 2022
Accepted: February 9, 2022
Published: March 7, 2022

Search for Higgs bosons decaying into new spin-0 or spin-1 particles in four-lepton final states with the ATLAS detector with 139 fb^{-1} of pp collision data at $\sqrt{s} = 13$ TeV

The ATLAS collaboration

E-mail: atlas.publications@cern.ch

Abstract: Searches are conducted for new spin-0 or spin-1 bosons using events where a Higgs boson with mass 125 GeV decays into four leptons ($\ell = e, \mu$). This decay is presumed to occur via an intermediate state which contains two on-shell, promptly decaying bosons: $H \to XX/ZX \to 4\ell$, where the new boson X has a mass between 1 and 60 GeV. The search uses pp collision data collected with the ATLAS detector at the LHC with an integrated luminosity of 139 fb^{-1} at a centre-of-mass energy $\sqrt{s} = 13$ TeV. The data are found to be consistent with Standard Model expectations. Limits are set on fiducial cross sections and on the branching ratio of the Higgs boson to decay into XX/ZX, improving those from previous publications by a factor between two and four. Limits are also set on mixing parameters relevant in extensions of the Standard Model containing a dark sector where X is interpreted to be a dark boson.

Keywords: Beyond Standard Model, Hadron-Hadron Scattering, Higgs Physics

ArXiv ePrint: 2110.13673

Open Access, Copyright CERN,
for the benefit of the ATLAS Collaboration.
Article funded by SCOAP^3.

https://doi.org/10.1007/JHEP03(2022)041

JHEP03(2022)041

Contents

1 Introduction **1**

2 Benchmark models **2**
- 2.1 Dark bosons 2
- 2.2 Extended Higgs sectors 3

3 ATLAS detector **4**

4 Data and simulated event samples **5**

5 Event reconstruction and selection **7**
- 5.1 Lepton reconstruction 7
- 5.2 Invariant kinematic mass variables 8
- 5.3 Common event selection 8
- 5.4 HM event selection 10
- 5.5 LM event selection 11
- 5.6 ZX event selection 11

6 Systematic uncertainties **12**

7 HM analysis: $H \to XX \to 4\ell$ ($15\,\text{GeV} < m_X < 60\,\text{GeV}$) **13**
- 7.1 Background estimate 13
- 7.2 Background validation 14
- 7.3 Results 14

8 LM analysis: $H \to XX \to 4\mu$ ($1\,\text{GeV} < m_X < 15\,\text{GeV}$) **17**
- 8.1 Background estimate 17
- 8.2 Results 18

9 ZX analysis: $H \to ZX \to 4\ell$ ($15\,\text{GeV} < m_X < 55\,\text{GeV}$) **20**
- 9.1 Background estimate 20
- 9.2 Background validation 21
- 9.3 Results 21

10 Limits and interpretation **24**
- 10.1 Limits on fiducial and total cross sections 25
  - 10.1.1 HM and LM limits 26
  - 10.1.2 ZX limits 26
- 10.2 Limits on branching ratios 27
- 10.3 Limits on Higgs mixing 27

11 Conclusion **33**

A HM signal region optimization **34**

The ATLAS collaboration **46**

JHEP03(2022)041

1 Introduction

Although the Higgs boson was discovered at the Large Hadron Collider (LHC) in 2012 [1, 2], there is good reason to believe that the description of the Higgs sector of the Standard Model (SM) is still incomplete. Besides the well-known issues of naturalness and baryon asymmetry, astrophysical observations implying the existence of dark matter motivate extensions to the Higgs sector of the SM, particularly those that propose the existence of a 'dark' (i.e., hidden) sector, with its own hidden-sector particles [3, 4].

An attractive way to search for new physics in the Higgs sector is through non-standard ('exotic') decays of the Higgs boson. Existing precision measurements of the properties of the Higgs boson still allow a branching ratio of up to about 30% to non-standard decays (assuming that the couplings of the Higgs boson to the W and Z bosons are not larger than their SM values) [5–7]. Further, since the SM predicts a very narrow decay width for the Higgs boson, even a small coupling to a new light state could result in a significant branching ratio to that state. In addition, new hidden-sector particles may preferentially couple to the Higgs boson, making it a 'portal' to explore this new physics [8–11]. Such exotic decays of the Higgs boson are predicted by many proposed extensions to the SM, including models with a first-order electroweak phase transition [12, 13], models with neutral naturalness [14–16], and models with a hidden sector [17–27], as well as by several models of dark matter [3, 28–32], including some posited to explain observed excesses of astrophysical positrons [33–35]. They are also predicted by the Next-to-Minimal Supersymmetric Standard Model (NMSSM) [36–41].

This paper reports three related searches, each of which looks for a SM Higgs boson H decaying via a new boson into a final state consisting of four charged leptons ($\ell \equiv e$, μ). All use the full LHC Run 2 data set of about 139 fb^{-1} that the ATLAS detector collected from proton-proton collisions at a centre-of-mass energy of $\sqrt{s} = 13$ TeV. Following the models motivating these analyses, the new boson could be either a dark-sector vector boson or a scalar boson, denoted by X. The three searches considered are:

- High-mass (HM): $H \to XX \to 4\ell$ ($15\,\text{GeV} < m_X < 60\,\text{GeV}$).
- Low-mass (LM): $H \to XX \to 4\mu$ ($1\,\text{GeV} < m_X < 15\,\text{GeV}$).
- Single Z boson (ZX): $H \to ZX \to 4\ell$ ($15\,\text{GeV} < m_X < 55\,\text{GeV}$).

The LM analysis uses only the 4μ final state because the selection efficiency for isolated muons is significantly larger than that for isolated electrons in this mass range (see section 5.4). These searches are sensitive to any intermediate bosons within the considered mass ranges that are narrow, on-shell, and decay promptly. This paper provides model-independent fiducial cross-section limits, as well as limits based on the specific models described in section 2.

This work extends previous searches performed by ATLAS with 20 fb^{-1} of data collected at $\sqrt{s} = 8$ TeV [42] and with 36 fb^{-1} of data collected at $\sqrt{s} = 13$ TeV [43]. In addition to a larger data sample and improved lepton identification, the signal region selection of the HM analysis has been re-optimized. Other similar searches, including searches for pairs of

JHEP03(2022)041

light bosons decaying into muons, τ-leptons, photons, and/or jets, as well as searches for a single light boson decaying into a pair of muons, using both $\sqrt{s} = 8\,\text{TeV}$ and 13 TeV data, have been performed by ATLAS [44–48], CMS [49–52], and LHCb [53]. Further searches for a SM Higgs boson decaying into undetected particles are reported in refs. [54, 55].

This section is followed by a summary of the theoretical models used in the interpretation of the results (section 2). Next, the detector is described (section 3), followed by discussions of features that are common to all three analyses, including the samples of data and simulated events (section 4), the reconstruction of lepton candidates and of their combinations (sections 5.1 and 5.2), the event selections (section 5.3), and the common systematic uncertainties (section 6). Next, aspects specific to each analysis are described (sections 7 to 9). Finally, the ways the analyses are combined to extract limits, and the interpretations of the results in terms of the theoretical models, are presented in section 10, and a summary is given in section 11.

2 Benchmark models

2.1 Dark bosons

Many theories of dark matter posit a hidden sector [17–26, 56], which does not interact with SM particles except via a mediator or portal interaction (besides gravity). A concrete realization of such a mediator involves adding a field with a $\mathrm{U}(1)_\mathrm{d}$ dark gauge symmetry [21–26] which mixes kinetically with the SM $\mathrm{U}(1)_\mathrm{Y}$ hypercharge gauge field with some strength ϵ [57–59]. The gauge boson of this symmetry is the Z_d vector boson, also called a 'dark photon'.

The coupling strength of the Z_d boson to SM particles, and hence its lifetime (assuming no significant decays to non-SM particles), is determined by the mixing parameter ϵ. The decays of the Z_d boson, on the other hand, are determined by the gauge couplings, and the decay branching ratios are largely independent of ϵ for $\epsilon \ll 1$. Over the Z_d mass range $1\,\text{GeV} < m_{Z_\mathrm{d}} < 60\,\text{GeV}$, the branching ratio for decays into electron or muon pairs can be 10%–15% [21]. Over the same mass range, the decay is prompt for $\epsilon \gtrsim 10^{-5}$ [21]. For smaller values of ϵ, the decay vertex would be significantly displaced from the interaction point, while for $\epsilon \lesssim 10^{-8}$ the lifetime of the Z_d boson becomes long enough for it to likely escape the detector. Also, the decay width of the Z_d boson is very small ($\ll 1\,\text{GeV}$) for $\epsilon \ll 1$ and $m_{Z_\mathrm{d}} < 60\,\text{GeV}$. ATLAS and CMS have searched for these long-lifetime signatures in collisions at energies of both 8 TeV [60–63] and 13 TeV [64–68].

If the $\mathrm{U}(1)_\mathrm{d}$ symmetry is broken by an additional dark Higgs boson s, then there could be mixing with strength κ between the SM Higgs boson and the dark Higgs boson [21–26]. The observed Higgs boson would be one of the mass eigenstates and could also decay into dark-sector particles, including dark Higgs bosons that subsequentially decay into SM fermions. The dark Higgs boson would inherit the Yukawa couplings from the SM Higgs boson and decay preferentially into high-mass fermion pairs.

A further possibility is mass mixing between the Z_d boson and the SM Z boson [23, 24]. If the mass term for this mixing is written as $\epsilon_Z m_Z^2 Z Z_\mathrm{d}$, with $\epsilon_Z = \delta m_{Z_\mathrm{d}}/m_Z$, then δ is the model parameter describing the mixing.

JHEP03(2022)041

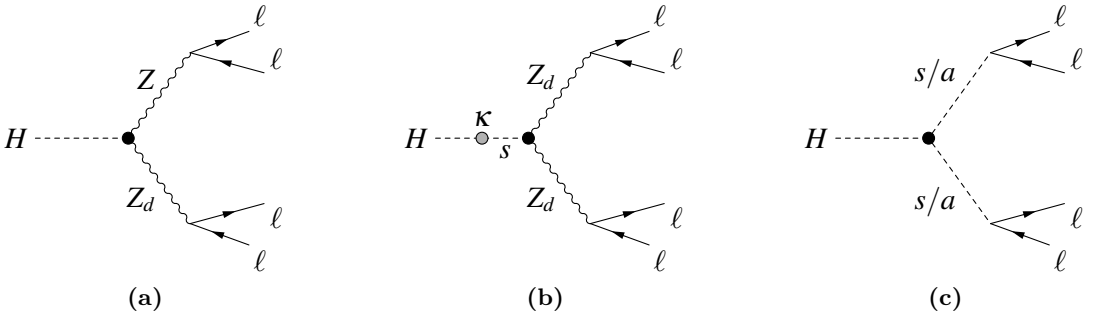

Figure 1. Exotic decays of the Higgs boson into four leptons induced by intermediate dark vector bosons via (a) the hypercharge portal (to which the ZX analysis is sensitive) and (b) the Higgs portal, where s is a dark Higgs boson [21] (to which the HM and LM analyses are sensitive). The Z_d gauge boson decays into SM particles through kinetic mixing with the hypercharge field (with branching ratios that are nearly independent of ϵ). The HZZ_d vertex factor is proportional to ϵ whereas the $HZ_\mathrm{d}Z_\mathrm{d}$ vertex factor is proportional to κ. (c) illustrates the decay of a Higgs boson into dark Higgs scalars s or pseudoscalars a that couple to SM particles through mixing with the SM Higgs field in models with an extended Higgs sector (section 2.2).

The processes probed in this paper that involve a SM Higgs boson decaying into Z_d bosons are depicted in figures 1(a) and 1(b) and are included in the Hidden Abelian Higgs Model (HAHM) [21]. The decay $H \to ZZ_\mathrm{d}$ is sensitive to the parameters ϵ and m_{Z_d}, but does not depend on κ. However, the presence of an irreducible background from the SM $H \to ZZ^*$ process means that this signal can be observed only as a peak in the dilepton mass spectrum over the background. The process $H \to Z_\mathrm{d}Z_\mathrm{d}$, in contrast, is much more easily separated from SM backgrounds and hence is potentially sensitive to smaller values of the kinetic mixing ϵ, where it is only required that the mixing be large enough for the Z_d boson to decay promptly. However, this process does require mixing between the SM and dark-sector Higgs bosons and thus depends on κ.

Limits on the kinetic mixing of $\epsilon \lesssim 0.03$ have been set from precision electroweak measurements [21, 69, 70] over the range $1\,\mathrm{GeV} < m_{Z_\mathrm{d}} < 200\,\mathrm{GeV}$. Searches for dilepton resonances, $pp \to Z_\mathrm{d} \to \ell\ell$, at the LHC for $m_{Z_\mathrm{d}} < m_Z$ imply that $\epsilon \lesssim 0.005$–0.020 for $20\,\mathrm{GeV} < m_{Z_\mathrm{d}} < 80\,\mathrm{GeV}$ [71]. Other searches rule out $\epsilon \gtrsim 10^{-3}$ for $10\,\mathrm{MeV} < m_{Z_\mathrm{d}} < 10\,\mathrm{GeV}$ [72–77]. The $H \to XX \to 4\ell$ analyses constrain the Higgs mixing parameter κ, while the $H \to ZZ_\mathrm{d} \to 4\ell$ analysis provides information about the kinetic mixing parameter ϵ.

2.2 Extended Higgs sectors

Models containing two Higgs doublets and an additional scalar field (2HDM+S) [22, 78] are also relevant for the search for $H \to XX \to 4\mu$. Two-Higgs-doublet models (2HDMs) generically contain two neutral scalars $H_{1,2}$, two charged scalars $H^\pm$, and one neutral pseudoscalar A. The lighter of the neutral scalars H_1 is identified as the observed Higgs boson H, while the other states are constrained to be heavy by existing data [79, 80]. Adding a complex scalar singlet that mixes weakly with $H_{1,2}$ gives two additional states, a scalar s and a pseudoscalar a. If these are lighter than $m_H/2$, then $H \to aa$ and $H \to ss$

JHEP03(2022)041

decays are allowed (figure 1(c)). This paper probes the process $H \to aa \to 4\mu$, but limits on $H \to aa \to 4\mu$ also apply to $H \to ss \to 4\mu$.

The decays of the scalar and pseudoscalar into fermions are determined by their Yukawa couplings [22], implying that the branching ratio to electrons is very small, and that the branching ratio to muons is smaller than that of the Z_{d} vector bosons described previously. Branching ratios for $H \to aa$ and $a \to \mu\mu$ can be significant in the range $2m_\mu < m_a < 2m_\tau$, ranging from 10^{-2} to 10^{-1} in some regions of parameter space [22]. In 2HDMs, there are several possible ways for the Higgs sector to couple to fermions. Of these, type-III models (in which leptons and quarks couple to different Higgs doublets) at large $\tan\beta$ (where $\tan\beta$ is the ratio of the vacuum expectation values of the two Higgs doublets) are particularly interesting for these analyses. A light pseudoscalar can correspond to the R-symmetry limit of the NMSSM [81, 82], which reduces the need for fine-tuning and addresses the μ-problem [83]. Searches for exotic decays of the Higgs boson into new light scalars or pseudoscalars have been carried out for a variety of mass ranges and final states with both LHC [42, 43, 45–50, 68, 84–89] and Tevatron [90] data.

3 ATLAS detector

The ATLAS detector [91] at the LHC covers nearly the entire solid angle around the collision point.[1] It consists of an inner tracking detector surrounded by a thin superconducting solenoid, electromagnetic and hadron calorimeters, and a muon spectrometer incorporating three large superconducting air-core toroidal magnets.

The inner-detector system (ID) is immersed in a 2 T axial magnetic field and provides charged-particle tracking in the range $|\eta| < 2.5$. The high-granularity silicon pixel detector covers the vertex region and typically provides four measurements per track, the first hit normally being in the insertable B-layer (IBL) installed before Run 2 [92, 93]. It is followed by the silicon microstrip tracker, which usually provides eight measurements per track. These silicon detectors are complemented by the transition radiation tracker (TRT), which enables radially extended track reconstruction up to $|\eta| = 2.0$. The TRT also provides electron identification information based on the fraction of hits (typically 30 in total) above a higher energy-deposit threshold corresponding to transition radiation.

The calorimeter system covers the pseudorapidity range $|\eta| < 4.9$. Within the region $|\eta| < 3.2$, electromagnetic calorimetry is provided by barrel and endcap high-granularity lead/liquid-argon (LAr) calorimeters, with an additional thin LAr presampler covering $|\eta| < 1.8$ to correct for energy loss in material upstream of the calorimeters. Hadron calorimetry is provided by the steel/scintillator-tile calorimeter, segmented into three barrel structures within $|\eta| < 1.7$, and two copper/LAr hadron endcap calorimeters. The

[1] ATLAS uses a right-handed coordinate system with its origin at the nominal interaction point (IP) in the centre of the detector and the z-axis along the beam pipe. The x-axis points from the IP to the centre of the LHC ring, and the y-axis points upwards. Cylindrical coordinates (r, ϕ) are used in the transverse plane, ϕ being the azimuthal angle around the z-axis. The pseudorapidity is defined in terms of the polar angle θ as $\eta = -\ln\tan(\theta/2)$, and the rapidity is defined in terms of energy E and momentum p as $y = (1/2)[(E + p_z)/(E - p_z)]$. Angular distance is measured in units of $\Delta R \equiv \sqrt{(\Delta\eta)^2 + (\Delta\phi)^2}$.

JHEP03(2022)041

solid angle coverage is completed with forward copper/LAr and tungsten/LAr calorimeter modules optimized for electromagnetic and hadronic energy measurements respectively.

The muon spectrometer (MS) comprises separate trigger and high-precision tracking chambers measuring the deflection of muons in a magnetic field generated by the superconducting air-core toroidal magnets. The field integral of the toroids ranges between 2.0 and 6.0 T m across most of the detector. A set of precision chambers covers the region $|\eta| < 2.7$ with three layers of monitored drift tubes, complemented by cathode-strip chambers in the forward region, where the background is highest. The muon trigger system covers the range $|\eta| < 2.4$ with resistive-plate chambers in the barrel, and thin-gap chambers in the endcap regions.

Interesting events are selected by the first-level trigger system implemented in custom hardware, followed by selections made by algorithms implemented in software in the high-level trigger [94]. The first-level trigger accepts events from the 40 MHz bunch crossings at a rate below 100 kHz, which the high-level trigger reduces in order to record events to disk at about 1 kHz.

An extensive software suite [95] is used in the reconstruction and analysis of real and simulated data, in detector operations, and in the trigger and data acquisition systems of the experiment.

4 Data and simulated event samples

The results in this paper are based on 139 fb^{-1} of $\sqrt{s} = 13$ TeV proton-proton (pp) collision data collected with the ATLAS detector over the period 2015–2018.

Monte Carlo (MC) simulation is used to determine expected contributions from both the signal processes and most background processes. For most samples, detector effects were included using a GEANT4 [96] simulation of the ATLAS detector [97]. The $H \to aa$, $H \to ZZ_{\mathrm{d}}$, and $H \to Za$ signal samples, as well as a portion of the $gg \to ZZ^*$ and triboson background samples, instead used a fast simulation [97] which relies on a parameterization of the calorimeter response [98]. The effects of pile-up (additional pp collisions in the same or a neighbouring bunch crossing) are included in the simulation. Weights are applied to the simulated events to correct for small differences between data and simulation in the reconstruction, identification, isolation, and impact parameter efficiencies for electrons and muons [99–101]. Further, the lepton momentum scales and resolutions in the simulation are adjusted to match the data [99, 101, 102]. Table 1 summarizes the samples and generators used, which include MADGRAPH5_aMC@NLO version 2.2.2 [103], POWHEG BOX v2 [104–108], PYTHIA 8.186 [109] (along with EVTGEN 1.2.0 [110] to decay heavy-flavour hadrons), and SHERPA 2.2.0, 2.2.1, and 2.2.2 [111].

Signal samples involving a Z_{d} vector boson were generated according to the HAHM [21, 22, 25, 26] implementation in MADGRAPH5_aMC@NLO, with the Higgs bosons being produced via gluon-gluon fusion (ggF) and the Higgs boson mass set to $m_H = 125$ GeV. For the $H \to Z_{\mathrm{d}}Z_{\mathrm{d}}$ process, ϵ and κ were both set to 10^{-4} and samples were generated with $m_{Z_{\mathrm{d}}} = 0.5$ GeV, 1 GeV, 2 GeV, and every 5 GeV in the range 5 GeV $\leq m_{Z_{\mathrm{d}}} \leq 60$ GeV. For the $H \to ZZ_{\mathrm{d}}$ process, κ was changed to 10^{-10}, and samples were generated every 5 GeV

JHEP03(2022)041

Process	ME generator	ME PDF	PS/UE/HF model	UE tune
$H \to Z_\mathrm{d}Z_\mathrm{d}$ / ZZ_d	MadGraph5_aMC@NLO	NNPDF2.3lo [112]	Pythia/EvtGen	A14 [113]
$H \to aa$	Powheg Box	PDF4LHC15nnlo [115]	Pythia/EvtGen	AZNLO [114]
$H \to Za$	Powheg Box	PDF4LHC15nnlo	Pythia/EvtGen	AZNLO
ggF	Powheg Box	PDF4LHC15nnlo	Pythia/EvtGen	AZNLO
VBF	Powheg Box	CT10nlo [116]	Pythia/EvtGen	AZNLO
VH	Pythia	NNPDF2.3lo [112]	Pythia/EvtGen	A14
$ggZH$	Powheg Box	NNPDF3.0nlo	Pythia/EvtGen	AZNLO
$b\bar{b}H$	MadGraph5_aMC@NLO	NNPDF2.3lo	Pythia/EvtGen	A14
$t\bar{t}H$	Powheg Box	NNPDF2.3lo	Pythia/EvtGen	A14
ZZ	Sherpa	NNPDF3.0nnlo	Sherpa	Sherpa default
VVV	Sherpa	NNPDF3.0nnlo	Sherpa	Sherpa default
$t\bar{t}Z$	Sherpa	NNPDF3.0nnlo	Sherpa	Sherpa default
$Z+$jets	Sherpa	NNPDF3.0nnlo	Sherpa	Sherpa default
$t\bar{t}$	Powheg Box	NNPDF3.0nlo	Pythia/EvtGen	A14
WZ	Powheg Box	CT10nlo	Pythia/EvtGen	A14

Table 1. Overview of the event generators used for the simulated signal and background samples. For each process, the table lists the matrix element (ME) generator used along with the parton distribution function (PDF), the model used to implement parton showering (PS), the underlying event (UE), and the decay of heavy-flavour hadrons (HF), as well as the set of tuned parameters used to model the UE. The text gives the full version numbers of the generators.

in the range $15\,\mathrm{GeV} \leq m_{Z_\mathrm{d}} \leq 55\,\mathrm{GeV}$. Final states with τ-leptons were not included; the change in signal region yield due to the omission of these decays was below 1% and thus neglected. The much smaller production of signal events by vector-boson fusion (VBF), VH, and $t\bar{t}H$ was also omitted.

Samples for $H \to aa$ were simulated using Powheg Box at next-to-next-to-leading order (NNLO) for arbitrary inclusive $gg \to H$ observables by reweighting the Higgs boson rapidity to that of HNNLO [104, 117–120]. Again, only the ggF production process was considered. Higgs boson decays into two scalars and thence into muons were simulated at leading order (LO) using Pythia. Samples were generated for $m_a = 0.5$, 1, 2, 2.5, 4, 6, 8, 10, 15, 30, 45, and 60 GeV. Samples for $H \to Za$ were generated similarly, for $m_a = 1$, 2, 4, 6, 8, 10, 15, 20, 25, and 30 GeV.

Prompt-lepton backgrounds are estimated directly from MC simulations. They arise primarily from the SM $H \to ZZ^* \to 4\ell$ process along with the non-resonant $ZZ^* \to 4\ell$ process. Smaller leptonic backgrounds arise from triboson production as well as $t\bar{t}+Z$ decays. Decays involving $Z \to \tau\tau$ were found to contribute negligibly to the background yields and are thus not included in the simulation. Backgrounds with jets misidentified as leptons are estimated with data-driven methods, detailed below in the individual analysis sections.

The $H \to ZZ^* \to 4\ell$ background process comprises various Higgs boson production modes. The ggF process $gg \to H$ [104–108, 121] was simulated in the same way as the

JHEP03(2022)041

$H \to aa$ signal sample described above. The prediction was normalized to the next-to-next-to-next-to-leading-order (N^3LO) cross section in QCD with next-to-leading-order (NLO) electroweak corrections [122–133]. The VBF process [106–108, 134] was simulated using POWHEG BOX at NLO. The prediction was normalized to an approximate-NNLO cross section in QCD with NLO electroweak corrections [135–137]. Associated production with a vector boson (VH) [138–145] was simulated at LO, while $t\bar{t}$ and $b\bar{b}$ associated production ($t\bar{t}H$, $b\bar{b}H$) [103, 146], as well as loop-induced Higgs and Z boson production ($ggZH$) [147], were simulated at NLO.

The non-resonant $q\bar{q} \to ZZ^* \to 4\ell$ background process [148] was simulated using SHERPA 2.2.2 at NLO for up to one additional parton and at LO for up to three additional partons. Matrix element calculations were matched and merged with the SHERPA parton shower based on the Catani-Seymour dipole factorization [149, 150] using the MEPS@NLO prescription [151–154]. The virtual QCD corrections are provided by the OPENLOOPS library [155–157]. The gluon-initiated process ($gg \to ZZ^* \to 4\ell$) was simulated in the same manner, except that it was at LO, and the s-channel H diagrams were omitted to avoid double-counting. The gluon-initiated process has a large QCD correction at NLO, so the cross section was scaled by a NLO/LO K-factor of 1.70 ± 0.15 [158]. Interference between the $gg \to ZZ^* \to 4\ell$ and $gg \to H \to ZZ^* \to 4\ell$ processes is neglected.

Higher-order electroweak processes include triboson production (VVV) and vector-boson scattering (VBS). These processes can yield final states with four leptons along with two additional particles. They were generated with SHERPA 2.2.2 at NLO for the inclusive processes and at LO for up to two additional partons, with the same treatment as for $q\bar{q} \to ZZ^* \to 4\ell$. Higgs boson production via VBF was subtracted from these samples in order to avoid double-counting.

The process $t\bar{t} + (Z \to \ell\ell)$ was generated with SHERPA 2.2.0 at LO with up to one additional parton emission.

Other, reducible, backgrounds have fewer than four prompt leptons in the final state, but can be accepted by the signal selection if there are additional leptons from heavy-flavour decay or jets misidentified as leptons. The Z + jets process was generated with SHERPA 2.2.1 using NLO matrix elements for up to two partons and LO matrix elements for up to four partons. The $t\bar{t}$ process was generated with POWHEG BOX at NLO with the h_{damp} parameter, which regulates the high-p_{T} radiation against which the $t\bar{t}$ system recoils, set to $1.5m_{\text{top}} = 258\,\text{GeV}$ [159]. The WZ process was also generated with POWHEG BOX at NLO with the CT10NLO PDF.

5 Event reconstruction and selection

5.1 Lepton reconstruction

For the analyses considered in this paper, the final-state objects of interest are electrons and muons.

Electrons are reconstructed and identified from charged-particle tracks in the ID that match energy deposits in the calorimeters [99]. The identification algorithm, based on a likelihood analysis, corresponds to the 'Loose' selection described in ref. [99]. The

JHEP03(2022)041

reconstruction and identification efficiency for electrons from $Z \to ee$ decays is about 90% per electron [99].

Muon reconstruction [101] begins by independently finding tracks in both the ID and MS. These track candidates are combined in a second step along with information from the calorimeters to form muon candidates of different types. Combined muons have matching tracks in both the MS and ID. Segment-tagged muons have an ID track but only a single-chamber track segment in the MS. Calorimeter-tagged (CT) muons have no MS track but have a pattern of energy deposition in the calorimeters consistent with a muon; this is used only in regions where the MS is not fully instrumented ($|\eta| < 0.1$). Finally, stand-alone (SA) muons have an MS track but no ID track, and are used in regions beyond the coverage of the ID, $2.5 < |\eta| < 2.7$. Due to the reduced performance of the latter two types, no more than one CT or SA muon may be used in an event. Muons are then identified by imposing quality requirements, corresponding to the 'Loose' selection in ref. [101]. The reconstruction and identification efficiency for muons from $W \to \mu\nu$ decays is greater than 98% [101].

To avoid identifying the same detector signature as multiple particles, an electron candidate that has the same ID track as a muon candidate is ignored, unless the muon is only calorimeter-tagged, in which case the muon is ignored instead. Electrons that have the same track or cluster as a higher-p_{T} electron are also ignored.

5.2 Invariant kinematic mass variables

All three analyses considered in this paper involve looking for mass resonances in final states consisting of a quadruplet of two same-flavour opposite-sign (SFOS) lepton pairs: $(e^+e^- + e^+e^-)$, $(e^+e^- + \mu^+\mu^-)$, or $(\mu^+\mu^- + \mu^+\mu^-)$. The invariant masses of the two pairs are denoted by m_{12} and m_{34}, where m_{12} is taken to be the one closer in mass to the Z boson, $|m_{12} - m_Z| < |m_{34} - m_Z|$.

If all four leptons have the same flavour, then for a given m_{12} and m_{34} labelling, alternative SFOS pairings can also be defined. An invariant mass m_{14} is constructed from the positively charged lepton of the m_{12} pair and the negatively charged lepton of the m_{34} pair. The other alternative pairing m_{23} is constructed analogously.

5.3 Common event selection

The analyses all involve a Higgs boson decaying into a pair of new bosons X, or into a new boson X along with a Z boson, which in turn decay into pairs of leptons. The X bosons are presumed to be on-shell, so the strategy is to search for resonances in the relevant dilepton mass distributions. Each analysis defines a signal region (SR) via a series of selections on measured quantities which maximizes the sensitivity to the signal.

All three analyses share a common preselection, but differ in the subsequent steps of selecting the candidate final-state leptons, forming them into quadruplets, selecting one of those quadruplets, and applying further requirements to the selected quadruplet. Table 2 shows the event selections of the different analyses.

The common preselection requires that events were recorded with the detector in good operating condition [161] and without excess calorimeter noise [162]. Each event must have an identified primary vertex with at least two tracks [163] and at least four lepton

JHEP03(2022)041

		Single Z (ZX) analysis $H \to ZX \to 4\ell$ ($\ell = e, \mu$)	High-mass (HM) analysis $H \to XX \to 4\ell$ ($\ell = e, \mu$)	Low-mass (LM) analysis $H \to XX \to 4\mu$
Mass range		$15\,\text{GeV} < m_X < 55\,\text{GeV}$	$15\,\text{GeV} < m_X < 60\,\text{GeV}$	$1\,\text{GeV} < m_X < 15\,\text{GeV}$
Baseline electrons		$p_\text{T} > 7\,\text{GeV}$ and $\lvert\eta\rvert < 2.47$; Loose identification with an IBL hit $\lvert z_0 \sin\theta\rvert < 0.5\,\text{mm}$		—
Baseline muons		$p_\text{T} > 5\,\text{GeV}$ ($15\,\text{GeV}$ if calo-tagged) and $\lvert\eta\rvert < 2.7$; Loose identification $\lvert z_0 \sin\theta\rvert < 0.5\,\text{mm}$ and $d_0 < 1\,\text{mm}$ (except for stand-alone muons)		
Quadruplet selection		Trigger-matched $e^+e^-e^+e^-$, $e^+e^-\mu^+\mu^-$, or $\mu^+\mu^-\mu^+\mu^-$; ≤ 1 SA+CT μ Three leading-p_T leptons satisfying $p_\text{T} > 20\,\text{GeV}$, $15\,\text{GeV}$, $10\,\text{GeV}$ Define pairs m_{12} and m_{34} such that $\lvert m_{12} - m_Z\rvert < \lvert m_{34} - m_Z\rvert$		
		$50\,\text{GeV} < m_{12} < 106\,\text{GeV}$ $12\,\text{GeV} < m_{34} < 115\,\text{GeV}$ $m_{14,32} > 5\,\text{GeV}$ ($4e/4\mu$)	—	
		$\Delta R(\ell, \ell') > 0.10\,(0.20)$ for same-flavour (different-flavour) ℓ, ℓ'		—
Quadruplet ranking		In order 4μ, $2e2\mu$, $2\mu2e$, $4e$ Smallest $\lvert m_Z - m_{12}\rvert$ Smallest $\lvert m_Z - m_{34}\rvert$	Select quadruplet with smallest $\Delta m_{\ell\ell} = \lvert m_{12} - m_{34}\rvert$	
Event selection	Isolation & impact parameter	Track and calorimeter isolation, excluding tracks/clusters from other leptons in the quadruplet $d_0/\sigma_{d_0} < 5$ for electrons and $d_0/\sigma_{d_0} < 3$ for muons		
	$m_{4\ell}$	$115\,\text{GeV} < m_{4\ell} < 130\,\text{GeV}$		$120\,\text{GeV} < m_{4\ell} < 130\,\text{GeV}$
	Z-veto	—	$10\,\text{GeV} < m_{12,34} < 64\,\text{GeV}$ For $4e$ and 4μ channels: $5\,\text{GeV} < m_{14,23} < 75\,\text{GeV}$	—
	Heavy-flavour veto	—	Reject event if $m_{12,34,14,23}$ in: $(m_{J/\Psi} - 0.25\,\text{GeV})$ to $(m_{\Psi(2S)} + 0.30\,\text{GeV})$, or $(m_{\Upsilon(1S)} - 0.70\,\text{GeV})$ to $(m_{\Upsilon(3S)} + 0.75\,\text{GeV})$	
	Signal region	—	$m_{34}/m_{12} > 0.85 - 0.1125 f(m_{12})$	$1.2\,\text{GeV} < m_{12,34} < 20\,\text{GeV}$ $m_{34}/m_{12} > 0.85$ Reject event if $m_{12,34}$ in: $2\,\text{GeV}$ to $4.4\,\text{GeV}$, or $8\,\text{GeV}$ to $12\,\text{GeV}$

Table 2. Summary of event selection requirements for the ZX, HM, and LM analyses. The quarkonia masses are taken to be $m_{J/\Psi} = 3.096\,\text{GeV}$, $m_{\Psi(2S)} = 3.686\,\text{GeV}$, $m_{\Upsilon(1S)} = 9.461\,\text{GeV}$, and $m_{\Upsilon(3S)} = 10.355\,\text{GeV}$ [160]. The text provides other definitions.

candidates. Events were triggered by requiring either one or two lepton candidates, where the candidates could be either electrons or muons [164–166]. The lepton candidates identified offline must match candidates identified by the trigger. The trigger p_T requirements range from $p_\text{T} > 7\,\text{GeV}$ to $p_\text{T} > 60\,\text{GeV}$, depending on lepton multiplicity and flavour. In either case, the trigger efficiency is above 95% (relative to signal region events surviving all other event selections).

Electron and muon candidates are reconstructed as described in section 5.1. Electrons must be within the central region of the detector ($\lvert\eta\rvert < 2.47$), have $p_\text{T} > 7\,\text{GeV}$, have a longitudinal impact parameter z_0 that satisfies $\lvert z_0 \sin\theta\rvert < 0.5\,\text{mm}$ with respect to the primary vertex, and have an additional associated hit in the insertable B-layer. Muons must be within the acceptance of the muon spectrometer, $\lvert\eta\rvert < 2.7$. All muons must have

JHEP03(2022)041

$p_{\mathrm{T}} > 5\,\mathrm{GeV}$, while CT muons must pass the stronger requirement $p_{\mathrm{T}} > 15\,\mathrm{GeV}$. Lastly, all muon candidates that are associated with a vertex, i.e. all except SA muons, must have a longitudinal impact parameter with respect to the reconstructed primary vertex satisfying $|z_0 \sin\theta| < 0.5\,\mathrm{mm}$ and a transverse impact parameter with respect to the position of the beam satisfying $d_0 < 1\,\mathrm{mm}$.

All possible quadruplets (section 5.2) are formed from the selected leptons. A quadruplet may contain no more than one SA or CT muon, and at least one lepton in the quadruplet must correspond to a lepton found by one of the triggers satisfied by the event. The three highest-p_{T} leptons must satisfy, respectively, $p_{\mathrm{T}} > 20\,\mathrm{GeV}$, $p_{\mathrm{T}} > 15\,\mathrm{GeV}$, and $p_{\mathrm{T}} > 10\,\mathrm{GeV}$. Except for the LM analysis, for which the angular separation between leptons can be very small, all pairs of same-flavour leptons in the quadruplet must satisfy $\Delta R(\ell, \ell') > 0.1$, while different-flavour pairs must satisfy $\Delta R(\ell, \ell') > 0.2$. At least one quadruplet per event is required. For the HM and LM analyses, if there is more than one quadruplet passing these requirements, the one with the smallest mass difference between the two pairs, $\Delta m_{\ell\ell} = |m_{12} - m_{34}|$, is chosen. The analogous procedure for the ZX analysis is described in section 5.6.

The leptons in the quadruplet must be isolated from other deposits in the calorimeter or ID tracks [100, 101]. This rejects backgrounds in which leptons arise from the decay of heavy-flavour jets, or in which hadronic jets are misidentified as leptons. For each lepton, the sum of the transverse energies of topological clusters [167] within a cone of $\Delta R = 0.2$ around it (excluding energy attributed to the lepton itself) must be less than 20% of its p_{T} for electrons, and less than 30% of its p_{T} for muons. The transverse momenta of tracks in a cone around the lepton are also summed, and must be less than 15% of its p_{T}. The η–ϕ radius of the cone depends on the momentum of the lepton. For electrons, the radius is $\Delta R = \min(0.2, 10\,\mathrm{GeV}/p_{\mathrm{T}})$, while for muons, it is $\Delta R = \min(0.3, 10\,\mathrm{GeV}/p_{\mathrm{T}})$. In both cases, tracks and energy clusters attributed to other leptons in the quadruplet are also excluded from the sums. This is particularly important for the LM analysis (section 5.5), where the angular separation between leptons may be very small.

In addition to the impact parameter requirements discussed earlier, each lepton in the quadruplet must have transverse impact parameter significance $d_0/\sigma_{d_0} < 5$ for electrons and $d_0/\sigma_{d_0} < 3$ for muons (with the exception of SA muons, which do not have an ID track), where σ_{d_0} is the estimated error in the reconstructed transverse impact parameter d_0.

5.4 HM event selection

The high-mass analysis applies a set of kinematic requirements to select events consistent with $H \to XX \to 4\ell$ decays. The invariant mass of the four-lepton system must be consistent with the SM Higgs boson: $115\,\mathrm{GeV} < m_{4\ell} < 130\,\mathrm{GeV}$. Also, the lepton pairs must not be consistent with the decays of Z bosons (Z-veto): $10\,\mathrm{GeV} < m_{12,34} < 64\,\mathrm{GeV}$. For the $4e$ and 4μ channels, it is possible that the leptons from a single X or Z decay are not paired together, but rather a lepton from one Z/X decay may be paired with a lepton from the other Z/X decay. Therefore, there are also requirements on the alternative lepton pairings, $5\,\mathrm{GeV} < m_{14,23} < 75\,\mathrm{GeV}$, in order to suppress ZZ^* background events in

JHEP03(2022)041

which the leptons are mispaired. Events with pairs consistent with J/ψ or Υ decay are also rejected with requirements on the lepton pair masses (see table 2).

The final requirement enforces consistency between m_{12} and m_{34}: $m_{34}/m_{12} > 0.85 - 0.1125 f(m_{12})$, where the function $f(m_{12})$ is defined in the appendix. Together with the relation $|m_{12} - m_Z| < |m_{34} - m_Z|$, this defines a wedge-shaped region in the m_{12}–m_{34} plane, as shown in figure 3(b).

5.5 LM event selection

The LM analysis is designed to be sensitive to the mass range $1\,\text{GeV} < m_X < 15\,\text{GeV}$. For these low masses, the angular separation between the two leptons in the $X \to \ell\ell$ decay can become very small ($\Delta R(\ell, \ell) < 0.1$ for $m_X = 1\,\text{GeV}$). In this case, the efficiency to select isolated electrons is significantly smaller than that for muons, so this analysis uses only the 4μ final state. Otherwise, the event selection is very similar to that of the HM analysis (section 5.4), except that a few kinematic criteria differ. The ΔR requirements between final-state leptons are removed, and the Z-veto requirement is not relevant. In addition to the HM heavy-flavour veto, the two lepton pair masses m_{12} and m_{34} must not be in the ranges 2–4.4 GeV or 8–12 GeV. The $m_{4\ell}$ requirement is narrowed to $120\,\text{GeV} < m_{4\ell} < 130\,\text{GeV}$, because muons have smaller radiative losses than electrons, and both lepton pairs must satisfy $1.2\,\text{GeV} < m_{12,34} < 20\,\text{GeV}$. Also, the final requirement for the signal region is simplified to $m_{34}/m_{12} > 0.85$.

5.6 ZX event selection

The selection for the ZX analysis differs from those of the HM and LM analyses as it is selecting a Z boson along with a new X boson. It is, however, very similar to the selection used for the ATLAS SM $H \to ZZ^* \to 4\ell$ analysis [168]. In addition to the common criteria described in section 5.3, each quadruplet must satisfy $50\,\text{GeV} < m_{12} < 106\,\text{GeV}$, $12\,\text{GeV} < m_{34} < 115\,\text{GeV}$, and, for the $4e$ and 4μ channels, the alternative pairings must satisfy $m_{14,23} > 5\,\text{GeV}$. The latter requirement suffices to remove mispaired J/ψ events. Backgrounds from Υ decays were found to be negligible after all selections. If there is more than one such quadruplet, quadruplets are ranked by the following criteria, applied in sequence:

- Rank by the flavours of the two lepton pairs according to the reconstruction efficiencies of the leptons. The reconstruction efficiency for muons is higher than that for electrons, especially at lower lepton momenta. Therefore, the final state lepton pairs in order of decreasing reconstruction efficiency are 4μ, $2e2\mu$, $2\mu2e$, and $4e$.
- Choose the quadruplet with the smallest $|m_Z - m_{12}|$.
- Choose the quadruplet with the smallest $|m_Z - m_{34}|$.

This is strictly applied to all quadruplets, even same-flavour ones, and thus differs slightly from the prescription used in the analysis of ref. [168], where the lower-ranked alternative pairing of a same-flavour quadruplet is prevented from being considered in the quadruplet

JHEP03(2022)041

selection. For this analysis, the alternative pairing is treated as a separate quadruplet and participates in the ranking and quadruplet selection.

Following the selection of the quadruplet, the tracks associated with all four leptons are required to be consistent with originating from a common vertex: $\chi^2/N_{\text{dof}} < 9$ (tightened to < 6 for the 4μ channel), where these upper bounds were chosen to give an efficiency of 99.5%. This removes additional reducible backgrounds, mainly $Z+\text{jets}$ and $t\bar{t}$. (These backgrounds are already very small for the HM and LM analyses, so this requirement is not applied in those cases.) Finally, the total invariant mass is required to be consistent with the decay of a Higgs boson, in the same manner as in the HM analysis: $115\,\text{GeV} < m_{4\ell} < 130\,\text{GeV}$. None of the other requirements of the HM analysis (Z boson/heavy-flavour veto and signal region requirements) are applied here.

6 Systematic uncertainties

Many systematic uncertainties are common to all the analyses considered here. The dominant ones include:

- *Luminosity and pile-up.* The uncertainty in the integrated luminosity is 1.7% [169], obtained using the LUCID-2 detector [170] for the primary luminosity measurements. Uncertainty due to pile-up arises from differences between the predicted and measured inelastic cross sections, as well as from the reweighting procedure described in section 4. This uncertainty is approximately 1%.

- *Lepton-related uncertainties.* The efficiency for events to pass the selection depends on the reconstruction and identification efficiencies for leptons, as well as the determination of their momentum scale. Tag-and-probe techniques are applied to the dilepton resonances $Z \to \ell^+\ell^-$, $J/\psi \to \ell^+\ell^-$, and $\Upsilon \to \mu^+\mu^-$ in order to measure the efficiencies and momentum scales and resolutions for electrons and muons. This leads to corrections, usually of the order of up to a percent, to account for differences observed between data and simulation, as well as an estimate of the residual uncertainty [99, 101]. As there are four leptons in the final state, small single-lepton uncertainties can result in larger uncertainties in the final yields, which range up to 15%, dominated by the uncertainty in the electron reconstruction and identification efficiency.

- *Theoretical uncertainties.* Uncertainties in the modelling of the simulated signal and background processes are estimated by varying the parton distribution functions, the factorization, renormalization, and QCD scales, and the modelling of hadronization and the underlying event. The total uncertainty in the acceptance of the signal is around 3%, and the uncertainty in the background yield is 3%–9% for the $H \to ZZ^* \to 4\ell$ process [171] and about 5% for $ZZ^* \to 4\ell$ [148–150, 152, 156, 158].

Uncertainties related to data-driven background estimates are discussed in the analysis-specific sections below.

JHEP03(2022)041

Each source of systematic uncertainty is considered to be uncorrelated with others: in the statistical description of the data, each source of systematic uncertainty is parameterized by several nuisance parameters that are constrained by Gaussian probability density distributions. The luminosity and lepton-related uncertainties are completely correlated among all Monte Carlo samples.

7 HM analysis: $H \to XX \to 4\ell$ ($15\,\text{GeV} < m_X < 60\,\text{GeV}$)

The high-mass analysis searches for decays of a SM Higgs boson into a pair of new bosons X, where X could be Z_d, a, or s, which in turn decay into pairs of electrons or muons (see figure 1). The event selection (detailed in section 5.4) seeks two same-flavour opposite-sign pairs of leptons of similar invariant mass that are consistent with the decay of a SM Higgs boson and inconsistent with the subsequent decay of Z bosons.

7.1 Background estimate

Backgrounds with four prompt leptons are estimated from simulation (see section 4) and validated using data from background-dominated control samples. The dominant backgrounds are $H \to ZZ^* \to 4\ell$ (about 72% of the total background) and $ZZ^* \to 4\ell$ (about 24% of the total background). Other such processes include $t\bar{t}Z \to 4\ell$ and processes with three gauge bosons. These are found to be negligible.

Reducible backgrounds include those from processes with leptons originating from the decay of heavy-flavour jets, or with jets misidentified as leptons. The background from the $Z+\text{jets}$ process is estimated using data. Control regions enriched in misidentified leptons are defined by selecting quadruplets with one or two of its subleading leptons satisfying 'inverted' criteria but otherwise passing the signal region selection. 'Inverted' electrons fail either the Loose electron selection or the isolation requirement, but not both. 'Inverted' muons fail either the isolation requirement or the transverse impact parameter significance requirement ($d_0/\sigma_{d_0} < 3$), or both. Two samples are defined, both requiring two leptons consistent with the decay of a Z boson. The 'good' sample requires at least one extra lepton passing the nominal selection, while the 'inverted' sample requires at least one extra lepton passing the 'inverted' selection. Since both samples are highly enriched in $Z \to \ell\ell$ decays, the extra leptons originate mostly from jets misidentified as leptons. Transfer factors are defined as the ratio of the number of extra leptons passing the 'good' selection to the number passing the 'inverted' selection. These transfer factors are applied to events in the 'inverted' control regions in order to extrapolate to the signal region. The systematic uncertainties in this procedure are estimated by propagating the statistical uncertainties in the transfer factors as well as comparing the results from several different definitions of 'good' and 'inverted' leptons. This yields an estimate of the background due to the $Z+\text{jets}$ process in the signal region compatible with zero.

Other reducible backgrounds are estimated from simulation. The dominant contribution is from $t\bar{t}$, with about 3% of the total background. Other such backgrounds, including those from diboson production and heavy-flavour processes, are found to be negligible.

JHEP03(2022)041

7.2 Background validation

The background estimates are validated using four dedicated background-enriched validation regions, defined so that they do not overlap with the HM signal region:

- VR1: the Z-veto requirement on the alternative pairings is inverted, requiring $m_{14,23} \geq 75\,\text{GeV}$, and the compatibility requirement on m_{34}/m_{12} is removed. This produces a sample enriched in the $H \to ZZ^* \to 4\ell$ process as well as the non-resonant $ZZ^* \to 4\ell$ process. Only the $4e$ and 4μ final states contribute to this region.

- VR2: the requirements on the four invariant mass pairings are removed and replaced with $m_{12} \geq 64\,\text{GeV}$, and the compatibility requirement on m_{34}/m_{12} is removed. This sample is also enriched in both the $H \to ZZ^* \to 4\ell$ and $ZZ^* \to 4\ell$ processes. All final states contribute to this region.

- VR3: both the Higgs boson mass window requirement ($115\,\text{GeV} < m_{4\ell} < 130\,\text{GeV}$) and the final m_{34}/m_{12} compatibility requirement are inverted, producing a sample dominated by $ZZ^* \to 4\ell$.

- VR4: the final m_{34}/m_{12} compatibility requirement is inverted, and all four dilepton mass requirements are changed to $m_{\ell\ell} < 55\,\text{GeV}$. This sample mainly consists of $H \to ZZ^* \to 4\ell$, but has a significant contribution from $ZZ^* \to 4\ell$.

Although these validation regions are constructed so that they do not overlap with the signal region for the HM analysis, there is some overlap of VR1 and VR2 with the signal region of the ZX analysis. However, given the cross-section limits found for the $H \to ZZ_\text{d} \to 4\ell$ process (figure 17(a)), the contribution of ZX signal events to either of these regions is less than 5% of the SM background expectation.

Figure 2 compares the predicted backgrounds in these regions with the data for the variable $\langle m_{\ell\ell} \rangle = \frac{1}{2}(m_{12} + m_{34})$. Good agreement is found in all cases. In these validation regions, the Z + jets background is estimated from MC simulations, while for the signal region it is estimated from data.

7.3 Results

The resulting $\langle m_{\ell\ell} \rangle$ distribution for this analysis is shown in figure 3(a), while table 3 summarizes the final yields and uncertainties in the signal region as defined in table 2. A total of 20 events are observed, with a total predicted background of 15.6 ± 1.3 events. The p-values for the background-only hypothesis as a function of m_X are shown in figure 4. The profile-likelihood ratio ($-2\log[L(\mu = 0, \hat{\hat{\theta}})/L(\hat{\mu}, \hat{\theta})]$) is used as the test statistic, and the likelihood used is described in section 10. Different final states are not distinguished in the fit; distributions used are summed over all channels. The largest deviation from SM expectations occurs around $m_{Z_\text{d}} = 28\,\text{GeV}$, corresponding to the two events with $\langle m_{\ell\ell} \rangle \approx 28\,\text{GeV}$, with a local significance of 2.5σ. Following procedures fixed before the data in the signal region were examined, the one event with $\langle m_{\ell\ell} \rangle < 15\,\text{GeV}$ and the two with $\langle m_{\ell\ell} \rangle > 60\,\text{GeV}$ are not considered when setting limits and do not affect figure 4. The distribution of m_{34} versus m_{12} for the selected events is shown in figure 3(b).

JHEP03(2022)041

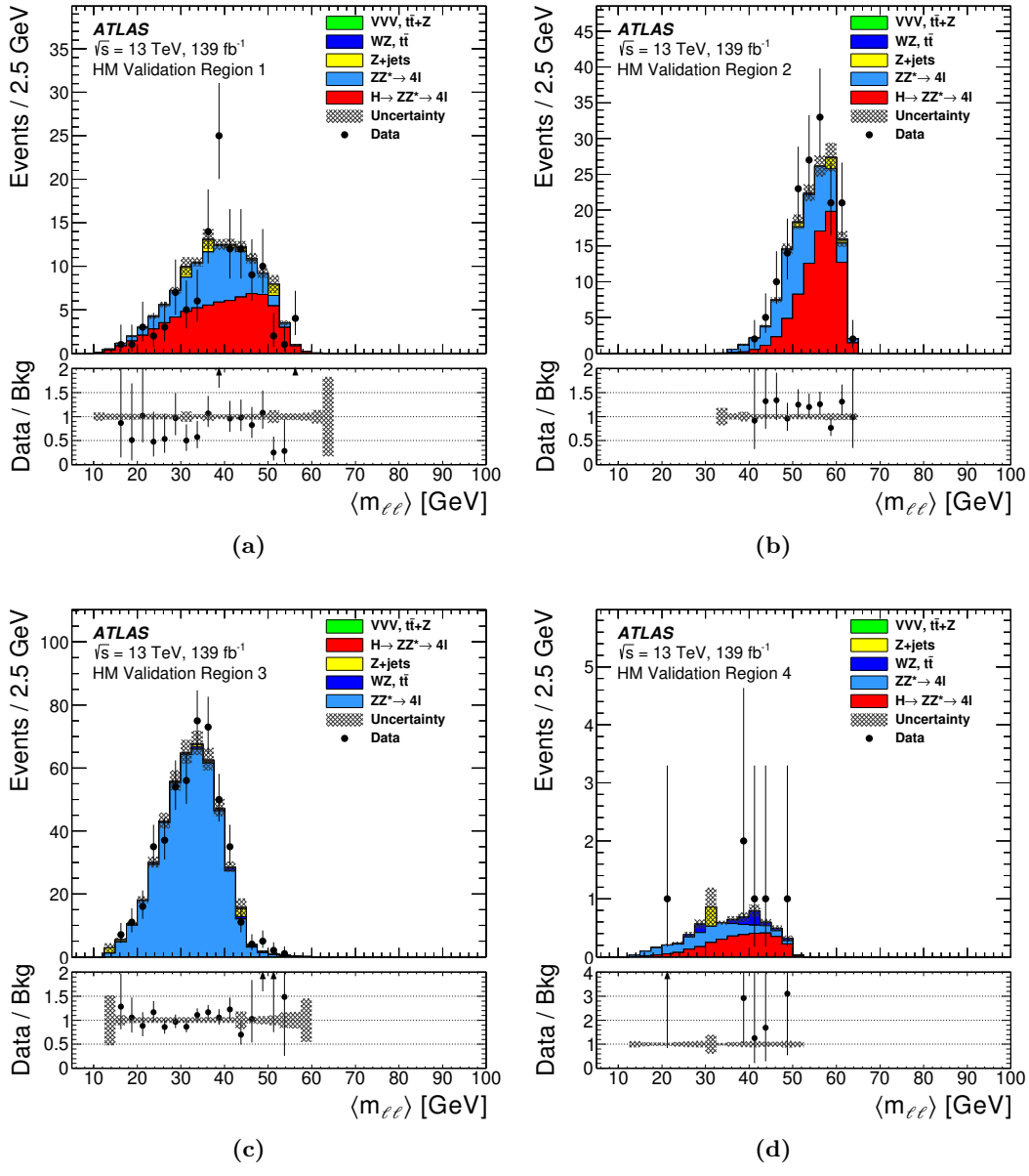

Figure 2. Distributions of $\langle m_{\ell\ell}\rangle = \frac{1}{2}(m_{12}+m_{34})$ in the validation regions for the HM $H \to XX \to 4\ell$ ($15\,\text{GeV} < m_X < 60\,\text{GeV}$) analysis: for (a) VR1, (b) VR2, (c) VR3, and (d) VR4 (see text for definitions). The signal contribution to these regions is negligible. The shaded band represents the total uncertainty of the prediction. The lower panels show the ratio of the observed data to the (pre-fit) MC predictions; the arrows at the upper edge indicate data points that fall outside of the y-axis range. The uncertainties of the plotted data are asymmetric and are calculated using eqs. (40.76) of ref. [160].

JHEP03(2022)041

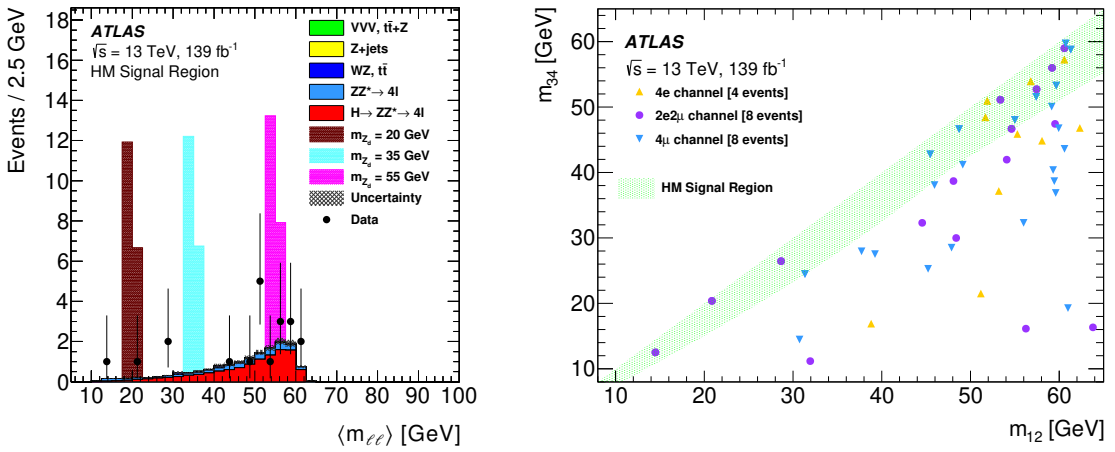

(a) **(b)**

Figure 3. Distribution of (a) $\langle m_{\ell\ell}\rangle$ and (b) m_{34} vs m_{12}, for events selected in the HM $H \to XX \to 4\ell$ ($15\,\text{GeV} < m_X < 60\,\text{GeV}$) analysis. In the $\langle m_{\ell\ell}\rangle$ distribution (a), the (pre-fit) background expectations are also shown; the hatched band contains the statistical and systematic uncertainties. The expectations for the signal are also shown, for several masses. The signal histograms are stacked on top of the background histograms, and expected yields are normalized with $\sigma(pp \to H \to Z_\text{d}Z_\text{d} \to 4\ell) = \frac{1}{10}\sigma_\text{SM}(pp \to H \to ZZ^* \to 4\ell) = 0.60\,\text{fb}$ (ggF process only). The uncertainties of the plotted data are asymmetric and are calculated using eqs. (40.76) of ref. [160]. For the m_{34} vs m_{12} distribution (b), each marker corresponds to an event that passed the Higgs boson window requirement and Z boson veto. The markers (differentiated by channel) that fall inside the green shaded area correspond to the events of the signal region.

Process	Yield ($\pm$stat. $\pm$ syst.)
$H \to ZZ^* \to 4\ell$	$11.1 \quad \pm 0.1 \quad \pm 1.0$
$ZZ^* \to 4\ell$	$3.38 \pm 0.05 \pm 0.25$
$t\bar{t}$	$0.47 \pm 0.13 \pm 0.09$
Z + jets	$0.43 \pm 0.39\ ^{+\ 0.17}_{-\ 0.01}$
$Z + t\bar{t} \to 4\ell$	$0.09 \pm 0.02 \pm 0.02$
WZ	$0.05 \pm 0.03\ ^{+\ 0.05}_{-\ 0.00}$
VVV/VBS	Negligible
Heavy flavour	Negligible
Total	$15.6 \quad \pm 0.4 \quad \pm 1.2$
Data	20

Table 3. Expected event yields of the SM background processes and data yield for the HM $H \to XX \to 4\ell$ ($15\,\text{GeV} < m_X < 60\,\text{GeV}$) selection. Three of the 20 observed events are outside the range $15\,\text{GeV} < \langle m_{\ell\ell}\rangle < 60\,\text{GeV}$ and are thus not considered when setting limits. The systematic uncertainties of the background estimates are highly correlated between the different sources of background (see section 6).

JHEP03(2022)041

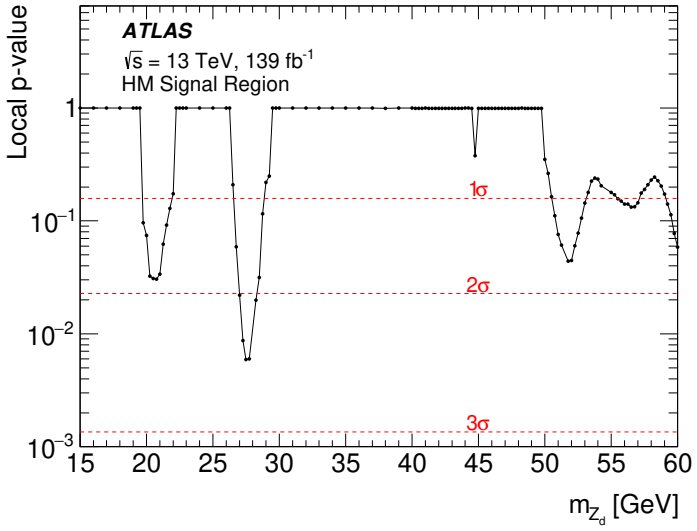

Figure 4. Observed local p-values under the background-only hypothesis for the process $H \to XX \to 4\ell$ in the high-mass range. For the limit determination, the distributions of $\langle m_{\ell\ell} \rangle$ in the signal region are binned with a width of 1 GeV. The p-values are plotted in steps of 0.25 GeV in the vicinity of observed data and 1 GeV elsewhere. The most significant excess corresponds to a local significance of 2.5σ at $m_{Z_\mathrm{d}} = 28$ GeV.

8 LM analysis: $H \to XX \to 4\mu$ ($1\,\mathrm{GeV} < m_X < 15\,\mathrm{GeV}$)

The LM analysis extends the HM analysis to the region $1\,\mathrm{GeV} < m_X < 15\,\mathrm{GeV}$, where $X = Z_\mathrm{d}$, a, or s. Only the 4μ final state is considered for this analysis. The event selection is detailed in section 5.5 and is similar to that of the HM analysis, with some adjustments for the different kinematic region.

8.1 Background estimate

Backgrounds involving four prompt leptons are estimated directly from MC simulations (see section 4). The $H \to ZZ^* \to 4\mu$ and $ZZ^* \to 4\mu$ processes together comprise about two thirds of the total background estimate. Higher-order electroweak processes, including triboson production and vector-boson scattering, are found to be negligible.

The remaining backgrounds involve non-prompt leptons, primarily from decays of heavy-flavour hadrons in events with multiple b-quarks such as $b\bar{b}$. A leading part of this contribution comes from double semileptonic decays, where a b-hadron decays into a muon and a c-hadron, which further decays into another muon and light hadrons. Resonances produced in the b-hadron decay chain (i.e., ω, ρ, ϕ, J/ψ) are also an important background but are almost completely suppressed by the heavy-flavour vetoes on dilepton masses required as part of the LM event selection. There is also a small contribution from $b\bar{b}b\bar{b}$, where each muon originates from an independent b-quark. As the muons selected here are all isolated, b-jet tagging is not useful for reducing these backgrounds. The backgrounds from these processes are estimated together using a data-driven method [43, 49].

JHEP03(2022)041

The first step is to find the shape of the background in the m_{12}–m_{34} plane. The invariant mass distribution of each muon pair is modelled separately to account for the different kinematic selections imposed on the leading, subleading, and remaining muons. Two distinct control samples are used, each of which contains an opposite-sign muon pair plus a third muon. The first sample, used to model m_{12}, requires a muon pair with $p_{\mathrm{T}1} > 20\,\mathrm{GeV}$ and $p_{\mathrm{T}2} > 10\,\mathrm{GeV}$ satisfying a dimuon trigger, and a third muon with $p_{\mathrm{T}3} > 5\,\mathrm{GeV}$. The second sample, used to model m_{34}, requires a muon pair with $p_{\mathrm{T}1,2} > 5\,\mathrm{GeV}$ and a third muon with $p_{\mathrm{T}3} > 27\,\mathrm{GeV}$, satisfying a single-muon trigger. In both cases, the muons must pass the same isolation and quality requirements as for the signal region. Ninety-seven percent of signal events pass both these selections, with the m_{12} and m_{34} pairs passing the requirements of the muon pair in the first and second samples, respectively. The invariant masses of the muon pairs are taken from the two control samples and used to form a 2D template in the m_{12}–m_{34} plane as the direct product of the two distributions.

A correction to the m_{12}–m_{34} template is made to account for a correlation between the kinematics of the two muon pairs, which is introduced by the Higgs boson mass requirement. Another control sample is defined by inverting the isolation and vertex requirements on the muons in the signal event selection, defining a sample enriched in events with muons from heavy-flavour quark decays. Comparing the distributions of muon pair invariant masses before and after the Higgs boson mass requirement yields the correction to the background shape as a function of m_{12} and m_{34}.

Finally, the overall normalization for the background from non-prompt leptons is determined from data in regions defined by inverting several selection criteria. As shown in figure 5, region B is defined by inverting the compatibility requirement $m_{34}/m_{12} > 0.85$. In order to improve the statistical precision of the background prediction, additional regions are defined by inverting the Higgs boson mass requirement (region C in figure 5) and also the isolation and vertex requirements (regions D and E in figure 5). The regions with $81\,\mathrm{GeV} < m_{4\ell} < 101\,\mathrm{GeV}$ are excluded in order to reduce contributions from Z bosons. The contribution with prompt muons, mostly ZZ^* in regions B and C, is subtracted from the data. The background with non-prompt leptons in region B is then estimated using $B = C \cdot D/E$. The 2D template is then used to scale from the estimate in region B to the signal region satisfying the compatibility requirement, region A.

The uncertainty in the heavy-flavour background estimate is found by varying each parameter of the background shape model up and down by 2σ and taking the largest change in yield for each bin, giving an uncertainty of 38%. Statistical uncertainties in the normalization of the signal region are also propagated to the heavy-flavour background yield, giving an uncertainty of 33%. Adding these uncertainties in quadrature gives a total systematic uncertainty of 50% in the heavy-flavour background yield.

8.2 Results

The $\langle m_{\ell\ell} \rangle$ distribution in the LM signal region is shown in figure 6(a). The distribution of m_{12} vs m_{34} is shown in figure 6(b), while table 4 summarizes the final yields and uncertainties. No events are observed, with a total background prediction of 0.89 ± 0.15 events.

JHEP03(2022)041

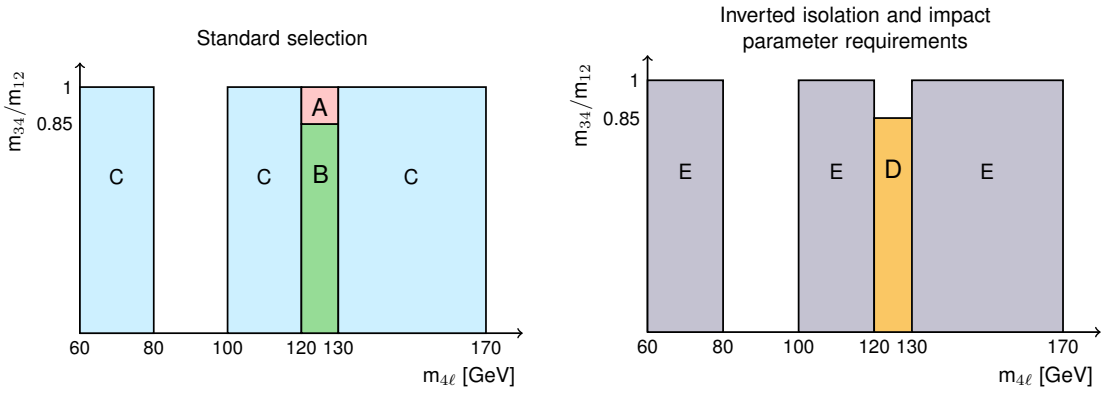

(a) **(b)**

Figure 5. Definition of regions used in the normalization of the heavy-flavour background in the LM analysis. (a) Region A is the signal region. The $m_{34}/m_{12} > 0.85$ compatibility requirement is inverted in region B, and the Higgs boson mass requirement is inverted in region C. The isolation and impact parameter requirements are inverted in regions D and E shown in (b).

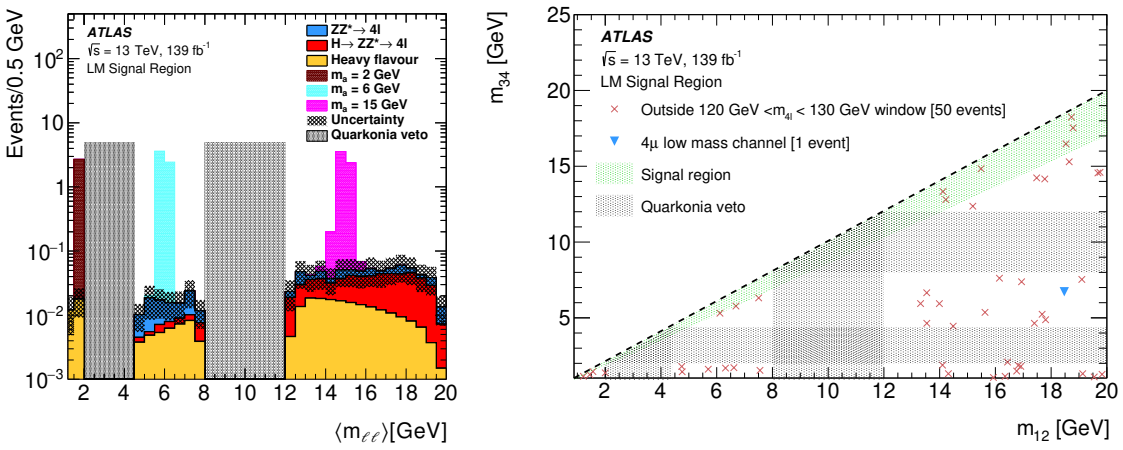

(a) **(b)**

Figure 6. Distribution of (a) $\langle m_{\ell\ell} \rangle$ and (b) m_{34} vs m_{12}, for events selected in the LM $H \to XX \to 4\mu$ ($1\,\text{GeV} < m_X < 15\,\text{GeV}$) analysis. No data events pass this selection. The expectation for a $H \to aa \to 4\mu$ signal is also shown, for several masses. The signal histograms are stacked on top of the (pre-fit) background histograms, and expected yields are normalized with $\sigma(pp \to H \to aa \to 4\mu) = \frac{1}{10}\sigma_{\text{SM}}(pp \to H \to ZZ^* \to 4\mu) = 0.15\,\text{fb}$ (ggF process only). The shaded band represents the total uncertainty of the prediction. The crossed-through points in (b) correspond to the 50 events that are outside the $m_{4\ell}$ mass window of $120\,\text{GeV} < m_{4\ell} < 130\,\text{GeV}$. The events outside the green signal region are events that fail the $m_{34}/m_{12} > 0.85$ requirement and include one event within the $m_{4\ell}$ mass window.

JHEP03(2022)041

Process	Yield (±stat. ± syst.)
$H \to ZZ^* \to 4\mu$	$0.41 \pm 0.01 \pm 0.03$
$ZZ^* \to 4\mu$	$0.22 \pm 0.04 \pm 0.04$
VVV/VBS	Negligible
Heavy flavour	$0.26 \pm 0.09 \pm 0.10$
Total	$0.89 \pm 0.10 \pm 0.11$
Data	0

Table 4. Expected event yields of the SM background processes and data yield for the LM $H \to XX \to 4\mu$ ($1\,\text{GeV} < m_X < 15\,\text{GeV}$) selection. The systematic uncertainties of the background estimates are highly correlated between the different sources of background (see section 6).

9 ZX analysis: $H \to ZX \to 4\ell$ ($15\,\text{GeV} < m_X < 55\,\text{GeV}$)

The ZX analysis searches for decays of a SM Higgs boson into a Z boson along with a new boson X, where both bosons in turn decay into pairs of electrons or muons. The event selection is detailed in section 5.6. Like the previous analyses, it involves finding two same-flavour opposite-sign lepton pairs with an overall invariant mass consistent with the decay of a SM Higgs boson. Unlike the other analyses, the leading pair must be broadly consistent with the decay of a Z boson, and the analysis then searches for a peak in the invariant mass distribution of the other pair. For $m_{Z_\text{d}} > 55\,\text{GeV}$, the invariant mass distribution for $Z_\text{d} \to \ell\ell$ starts to overlap significantly with that for $Z \to \ell\ell$. Since this analysis accepts events with the leading lepton pair consistent with the decay of a Z boson, it relies much more on the invariant mass distribution of the other lepton pair to reject the $ZZ \to 4\ell$ background than does the HM analysis. Therefore, the upper search range for this analysis is limited to 55 GeV, rather than 60 GeV as for the HM analysis.

9.1 Background estimate

The dominant backgrounds in this analysis are $H \to ZZ^* \to 4\ell$ (about 65% of the total) and non-resonant $ZZ^* \to 4\ell$ (about 33% of the total). Additional prompt backgrounds include the triboson processes ZZZ, WZZ, and WWZ. These are estimated from simulation (see section 4), but the $ZZ^* \to 4\ell$ background estimate is checked using background-enriched validation samples.

Other, reducible, backgrounds, such as those from Z+jets, $t\bar{t}$, and WZ processes, contain either additional non-isolated leptons from heavy-flavour decay or objects misidentified as leptons and constitute only a few percent of the background. The procedure used to estimate the total yield of these backgrounds is identical to that of the ATLAS SM $H \to ZZ^* \to 4\ell$ analysis [168, 172].

The reducible background is estimated separately for the cases where the second lepton pair (m_{34}) decays into muons ($\ell\ell\mu\mu$) and those where it decays into electrons ($\ell\ell ee$). For the $\ell\ell\mu\mu$ case, a number of mutually exclusive control regions are defined by inverting or relaxing

JHEP03(2022)041

some of the lepton identification requirements, including the isolation and impact parameter requirements for the subleading muon pair. A fit to the m_{12} distribution is then performed to estimate the amount of background due to each of $t\bar{t}$, Z + heavy-flavour (having b- or c-quark content), and Z + light-flavour. Transfer factors derived from simulation are then used to extrapolate the fitted yield of each background in the control regions to the signal region. The contribution from WZ production is estimated using simulation.

The $\ell\ell ee$ background from Z + jets, $t\bar{t}$, and WZ production is classified into processes with jets being misidentified as electrons (f), electrons from photon conversions (γ), and electrons from semileptonic decay of heavy-flavour hadrons (q). The q component is estimated from simulation. The other two components are estimated from a control region in which the identification requirements of the lowest-p_{T} electron are relaxed. Further, to suppress the ZZ^* contribution, the two subleading electrons must have the same sign. The expectations for the f and γ components are obtained by fitting to the distribution of the number of inner pixel detector hits associated with the track of the lowest-p_{T} electron. The estimated yields of all three components are then extrapolated to the signal region using transfer factors derived from simulation.

Finally, the shape of the m_{34} distribution for the reducible background is taken from simulation. An additional 10% systematic uncertainty is assigned to the reducible background estimate to account for differences in the lepton isolation requirements between this analysis and that of refs. [168, 172].

9.2 Background validation

The estimate of the non-resonant $ZZ^* \to 4\ell$ background is further validated in control samples that are enriched in this process. Two validation regions are defined by replacing the requirement $115\,\mathrm{GeV} < m_{4\ell} < 130\,\mathrm{GeV}$ with either $m_{4\ell} < 115\,\mathrm{GeV}$ (VR5) or $130\,\mathrm{GeV} < m_{4\ell} < 170\,\mathrm{GeV}$ (VR6). The latter validation region also requires $|m_{12} - m_Z| < 6\,\mathrm{GeV}$. For consistency with the ATLAS SM $H \to ZZ^* \to 4\ell$ analysis [168, 172], the requirement on m_{34} is also changed for both validation regions:

- $m_{34} > 5\,\mathrm{GeV}$ for $m_{4\ell} < 100\,\mathrm{GeV}$;
- $m_{34} > 1.4(m_{4\ell} - 100\,\mathrm{GeV}) + 5\,\mathrm{GeV}$ for $100\,\mathrm{GeV} < m_{4\ell} < 105\,\mathrm{GeV}$;
- $m_{34} > 12\,\mathrm{GeV}$ for $105\,\mathrm{GeV} < m_{4\ell} < 140\,\mathrm{GeV}$;
- $m_{34} > 0.76(m_{4\ell} - 140\,\mathrm{GeV}) + 12\,\mathrm{GeV}$ for $140\,\mathrm{GeV} < m_{4\ell} < 170\,\mathrm{GeV}$.

These requirements are illustrated in figure 7. Distributions of m_{34} for the two validation regions are shown in figure 8. Good agreement is found with background expectations.

9.3 Results

The final m_{34} distribution for this analysis is shown in figure 9, while table 5 summarizes the final yields and uncertainties. The dominant systematic uncertainty in final states that contain electrons arises from the modelling of the electron identification efficiency. For the 4μ channel, the dominant systematic uncertainty arises from the modelling of muon isolation.

JHEP03(2022)041

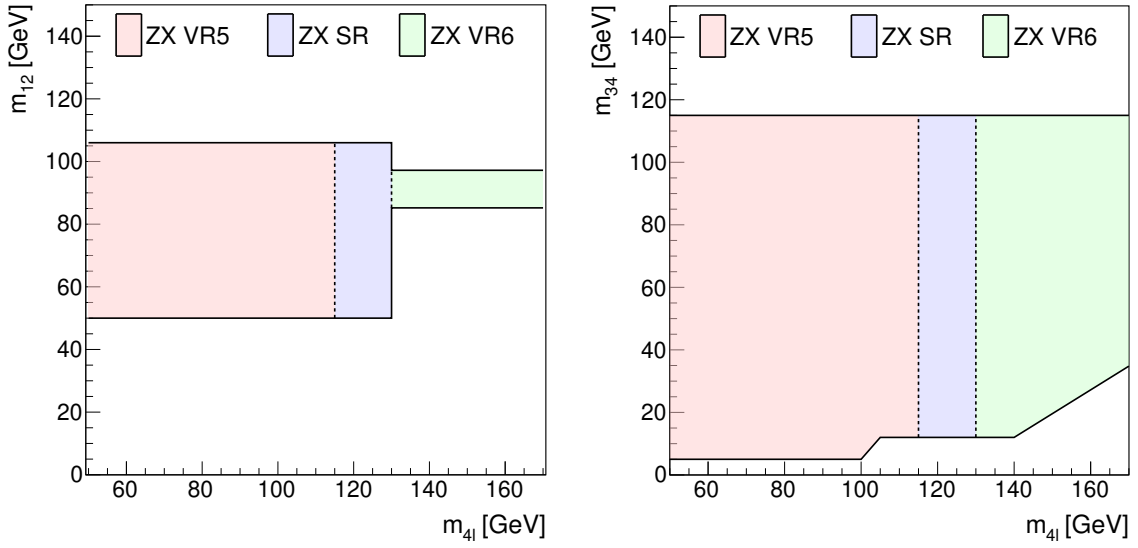

(a) (b)

Figure 7. Illustration of the validation region definitions for the $H \to ZX \to 4\ell$ analysis. Shown are the selections in the (a) m_{12} vs $m_{4\ell}$ and (b) m_{34} vs $m_{4\ell}$ planes for the two validation regions as well as the signal region. Details of the selections are given in the text.

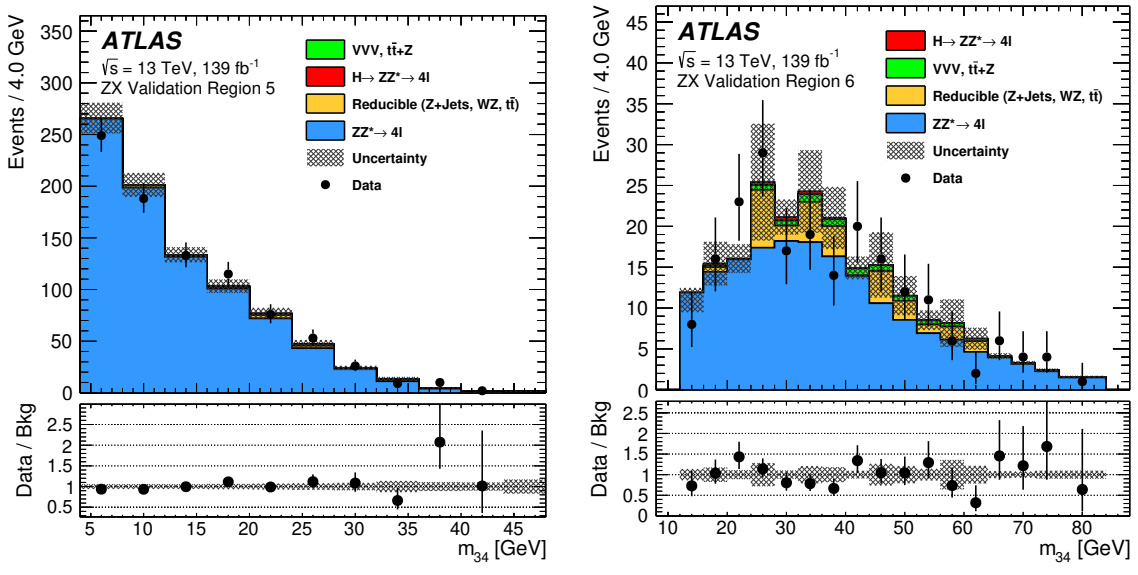

(a) (b)

Figure 8. Distributions of m_{34} in the two validation regions for the $H \to ZX \to 4\ell$ analysis. (a) VR5: $m_{4\ell} < 115\,\text{GeV}$; (b) VR6: $130\,\text{GeV} < m_{4\ell} < 170\,\text{GeV}$. The shaded band represents the total uncertainty of the (pre-fit) prediction. The lower panels show the ratio of the observed data to the MC predictions. The uncertainties of the plotted data are asymmetric and are calculated using eqs. (40.76) of ref. [160].

JHEP03(2022)041

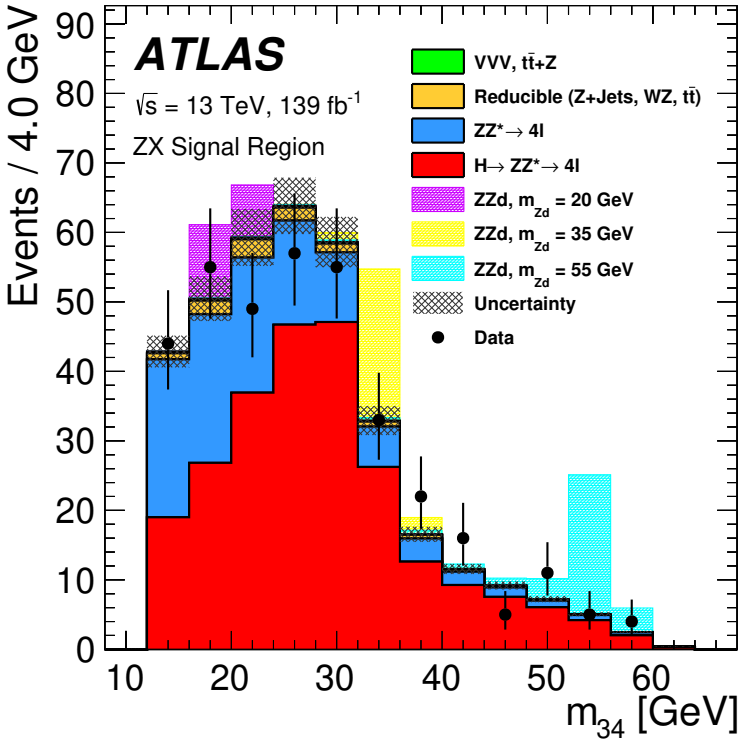

Figure 9. Distribution of m_{34} for data and background events in the mass range 115 GeV $< m_{4\ell} <$ 130 GeV after the $H \to ZX \to 4\ell$ selection. The background normalization is taken from the fit (see text); the shaded band represents the total uncertainty of the background prediction. Three signal points for the $H \to ZZ_d \to 4\ell$ model are shown, stacked on top of the background histograms. The signal yields are normalized with $\sigma(pp \to H \to ZZ_{\rm d} \to 4\ell) = \frac{1}{10}\sigma_{\rm SM}(pp \to H \to ZZ^* \to 4\ell) =$ 0.69 fb. The uncertainties of the plotted data are asymmetric and are calculated using eqs. (40.76) of ref. [160].

A total of 356 events are observed with an expected background of 320 ± 17. Figure 10 shows the observed local p-values for the background-only hypothesis. The profile-likelihood ratio is again used as the test statistic. Different final states are not distinguished in the fit; distributions used are summed over all channels. The normalization of the $H \to ZZ^*$ background is allowed to float (as an unconstrained nuisance parameter, see section 10.1.2), with a resulting normalization of 1.2 ± 0.16. The largest excess, with a local significance of around 2σ, is at about $m_X = 39$ GeV.

These results are slightly different from the corresponding results from the ATLAS SM $H \to ZZ^* \to 4\ell$ analysis [173], which observed 310 events and found a signal strength of $\sigma_{\rm fid}/\sigma_{\rm fid,SM} = 0.96 \pm 0.11$. The difference is largely due to the differences in quadruplet handling mentioned in section 5.6, and also due to differences in the definitions of the isolation and impact parameter selections. When this analysis is repeated using the quadruplet definition of ref. [173], the resulting normalization of the $H \to ZZ^*$ background is 1.12 ± 0.15.

JHEP03(2022)041

Process	Yield (±stat. ± syst.)		
	$2\ell 2\mu$	$2\ell 2e$	Total
$H \to ZZ^* \to 4\ell$	$127.9 \pm 0.1 \pm 3.6$	$76 \pm 0.1 \pm 10$	$204 \pm 0.2 \pm 12$
$ZZ^* \to 4\ell$	$70.2 \pm 0.2 \pm 1.9$	$33.0 \pm 0.2 \pm 3.6$	$103.3 \pm 0.3 \pm 4.6$
Reducible	$4.9 \pm 0.1 \pm 0.3$	$5.8 \pm 0.3 \pm 0.6$	$10.7 \pm 0.3 \pm 1.0$
$VVV, t\bar{t} + Z$	$1.1 \pm 0.1 \pm 0.04$	$0.7 \pm 0.1 \pm 0.1$	$1.8 \pm 0.1 \pm 0.1$
Total	$204.1 \pm 0.3 \pm 5.5$	$116 \pm 0.5 \pm 14$	$320 \pm 0.5 \pm 17$
Data	237	119	356

Table 5. Expected and observed numbers of events in each channel after the $H \to ZX \to 4\ell$ event selection defined by the mass range 115 GeV $< m_{4\ell} <$ 130 GeV. The background normalization is prior to the fit (see text). The systematic uncertainties of the background estimates are highly correlated between the different sources of background (see section 6).

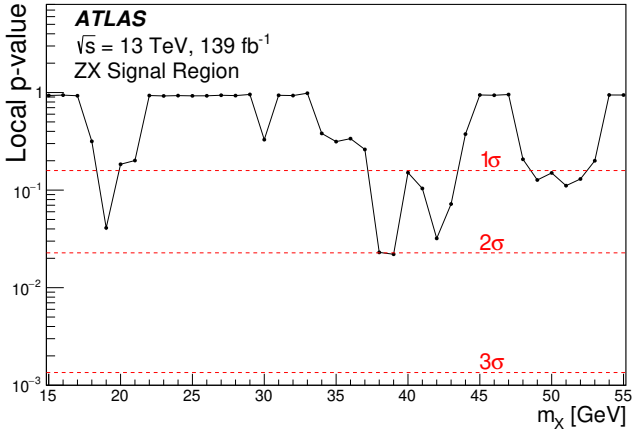

Figure 10. Observed local p-values under the background-only hypothesis for the process $H \to ZX \to 4\ell$.

10 Limits and interpretation

No significant excess is observed above SM background predictions for any of the analyses considered. Therefore, the results are interpreted in terms of exclusion limits. Firstly, model-independent limits are placed on fiducial cross sections. Model-dependent exclusion limits are then set for the benchmark models described in section 2.

For the HM and LM $H \to XX \to 4\ell$ analyses, evaluating the limits entails parameterizing the signal distribution as a function of both $\langle m_{\ell\ell} \rangle$ and m_X, while the $H \to ZX \to 4\ell$ analysis requires the parameterization to be a function of m_{34} and m_X. Since simulated events are generated only at discrete values of m_X, the signal templates are interpolated between m_X values. For the HM and ZX analyses, this is done using moment morphing [174]. The distributions at the generated values of m_X are used as templates, and the normalization is determined from interpolation of the simulated signal yields. For the LM analysis, Gaussian distributions are fit to the $\langle m_{\ell\ell} \rangle$ distributions at each generated m_X, and the fit parameters are interpolated in m_X.

JHEP03(2022)041

	Single Z (ZX) analysis $H \to XZ \to 4\ell$ ($\ell = e, \mu$)	High-mass (HM) analysis $H \to XX \to 4\ell$ ($\ell = e, \mu$)	Low-mass (LM) analysis $H \to XX \to 4\mu$
Mass range	$15\,\text{GeV} < m_X < 55\,\text{GeV}$	$15\,\text{GeV} < m_X < 60\,\text{GeV}$	$1\,\text{GeV} < m_X < 15\,\text{GeV}$
Electrons	$p_\text{T} > 7\,\text{GeV}$ $\quad |\eta| < 2.5$		
Muons	$p_\text{T} > 5\,\text{GeV}$ $\quad |\eta| < 2.7$		
Quadruplet	Three leading-p_T leptons satisfying $p_\text{T} > 20\,\text{GeV}$, 15 GeV, 10 GeV		
	$\Delta R > 0.10\,(0.20)$ between same-flavour (different-flavour) leptons		—
	—	$m_{34}/m_{12} > 0.85 - 0.1125 f(m_{12})$	$m_{34}/m_{12} > 0.85$
	$50\,\text{GeV} < m_{12} < 106\,\text{GeV}$ $12\,\text{GeV} < m_{34} < 115\,\text{GeV}$ $m_{14,23} > 5\,\text{GeV}$ ($4e/4\mu$)	$10\,\text{GeV} < m_{12,34} < 64\,\text{GeV}$ For $4e$ and 4μ channels: $5\,\text{GeV} < m_{14,23} < 75\,\text{GeV}$	$1.2\,\text{GeV} < m_{12,34} < 20\,\text{GeV}$
	—	Reject event if $m_{12,34,14,23}$ in either: $(m_{J/\psi} - 0.25\,\text{GeV})$ to $(m_{\psi(2S)} + 0.30\,\text{GeV})$, or $(m_{\Upsilon(1S)} - 0.70\,\text{GeV})$ to $(m_{\Upsilon(3S)} + 0.75\,\text{GeV})$	
	—	—	Reject event if $m_{12,34}$ in either 2 GeV to 4.4 GeV, or 8 GeV to 12 GeV
	$115\,\text{GeV} < m_{4\ell} < 130\,\text{GeV}$	—	—

Table 6. Summary of the fiducial phase-space definitions, appropriate for $H \to XX \to 4\ell$ or $H \to ZX \to 4\ell$, where X is a promptly decaying, on-shell, narrow resonance.

The data are described statistically by a likelihood function consisting of a Poisson factor for each histogram bin, summed over each channel, along with a Gaussian constraint for each nuisance parameter [175]:

$$\mathcal{L}(N, \alpha) = \prod_i \text{Pois}\left(\sum_j N_{ij}; \sum_j \mu S_{ij}(\alpha) + B_{ij}(\alpha)\right) \prod_k \text{Gaus}(\alpha_k; s_k, \sigma_k),$$

where N_{ij} is the number of observed events observed in bin i for channel j, α is the set of nuisance parameters, $S_{ij}(\alpha)$ and $B_{ij}(\alpha)$ are the predicted numbers of signal and background events for each bin and channel, μ is the signal strength, and s_k and σ_k are mean and width of the Gaussian constraint for nuisance parameter α_k. Systematic uncertainties are modelled via nuisance parameters which are profiled in the calculation of the test statistic; the effect of systematic uncertainties on the limits is small.

10.1 Limits on fiducial and total cross sections

Model-independent cross-section limits for the HM, LM, and ZX analyses are derived in fiducial regions defined using generator-level quantities. These fiducial selections, shown in table 6, are designed to mimic the signal region selection requirements. In order to account for the effects of quasi-collinear electromagnetic radiation from the leptons within the detector resolution, the four-momenta of prompt photons close to a lepton ($\Delta R < 0.1$) are added to the four-momentum of that lepton [176].

The fiducial selections are used to factorize the effects of the event selection into a largely model-independent 'efficiency' and a model-dependent 'acceptance'. The efficiency

JHEP03(2022)041

for a given channel is defined as the fraction of events passing the fiducial selection (using generator-level quantities) that also pass the full event selection (using reconstructed quantities). This mostly depends on the lepton reconstruction, but not on the model used. Systematic uncertainties relevant to the reconstruction of leptons are propagated to the efficiency. For a given theoretical signal model, the acceptance for a channel c is defined as

$$\alpha_c = \frac{N^c_{\text{fid}}}{N^c_{\text{tot}}},$$

where N^c_{fid} is the yield for channel c within the fiducial region (at generator level) and N^c_{tot} is the total yield for channel c (simply the total generator-level yield for the channel). The efficiency may thus be used to find a model-independent fiducial cross-section limit, which may then be converted to a model-dependent total cross-section limit using the acceptance.

10.1.1 HM and LM limits

The efficiencies within the fiducial regions for the HM and LM analyses are shown in figure 11(a). These were calculated using the benchmark $H \to Z_{\text{d}}Z_{\text{d}}$ model, but the efficiencies are mostly model-independent: for $H \to aa \to 4\mu$ over the range $1\,\text{GeV} < m_a < 15\,\text{GeV}$ the efficiencies are the same as for $H \to Z_{\text{d}}Z_{\text{d}} \to 4\mu$ to within a relative difference of 3%. The difference in efficiency between different final states is mainly due to the fact that the efficiencies for reconstruction, identification, and selection are lower for electrons than for muons. These efficiencies are used to compute 95% confidence level (CL) upper limits on the cross section within the fiducial region, using the CL_s frequentist formalism [177] with the profile-likelihood-ratio test statistic [178]. The resulting limits are shown in figure 12. These limits should be applicable to any models of the SM Higgs boson decaying into four leptons via two intermediate bosons that are narrow, on-shell, and that decay promptly. The model-dependent acceptances for the HM and LM analyses are shown in figure 11(b) for the $H \to Z_{\text{d}}Z_{\text{d}}$ and $H \to aa \to 4\mu$ models. The resulting upper limit on the product of the total cross section and decay branching ratio for the benchmark model, $\sigma(gg \to H \to Z_{\text{d}}Z_{\text{d}} \to 4\ell)$, for the HM analysis is shown in figure 13, while figure 14 shows upper limits on $\sigma(gg \to H \to Z_{\text{d}}Z_{\text{d}} \to 4\mu)$ and $\sigma(gg \to H \to aa \to 4\mu)$ for both the HM and LM analyses. These results are independent of assumptions about the decay branching ratios of the Z_{d} and a bosons. In particular, figure 14(b) also applies to the scalar case $\sigma(gg \to H \to ss \to 4\mu)$.

10.1.2 ZX limits

For limits involving ZX processes, the normalization of the non-resonant $ZZ^* \to 4\ell$ background is validated using control samples, but the normalization of the remaining significant background, $H \to ZZ^* \to 4\ell$, is allowed to float in the limit determination as an unconstrained nuisance parameter. The model-independent efficiency within the fiducial region is shown in figure 15(a), and the resulting 95% CL upper limit on the fiducial region cross section is shown in figure 16. The fiducial region acceptance for the $H \to ZZ_{\text{d}} \to 4\ell$ process is shown in figure 15(b), and the upper limits on the product of the total cross section and decay branching ratio for the benchmark models, $\sigma(gg \to H \to ZZ_{\text{d}} \to 4\ell)$ and $\sigma(gg \to H \to Za \to 2\ell 2\mu)$, are shown in figure 17.

JHEP03(2022)041

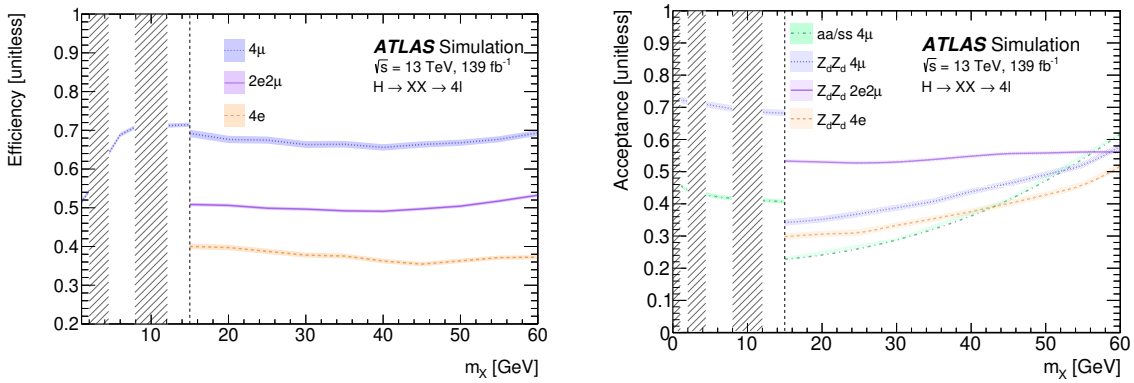

(a) **(b)**

Figure 11. (a) Model-independent per-channel efficiencies ϵ_c calculated in the fiducial volumes described in the $1\,\text{GeV} < m_X < 15\,\text{GeV}$ and $15\,\text{GeV} < m_X < 60\,\text{GeV}$ columns of table 6 (i.e. separate phase spaces are defined for m_X above and below 15 GeV). (b) Model-dependent per-channel fiducial region acceptances for the $H \to Z_\text{d}Z_\text{d} \to 4\ell$ and $H \to aa \to 4\mu$ processes. The shaded areas are the quarkonia veto regions.

10.2 Limits on branching ratios

A (model-dependent) cross-section limit may be converted to a branching ratio limit using the relations:

$$\mathcal{B}(H \to XX \to 4\ell) = \frac{\sigma_{H\to XX\to 4\ell}}{\sigma_H},$$
$$\mathcal{B}(H \to XX) = \frac{\mathcal{B}(H \to XX \to 4\ell)}{\sum_{\ell_1=e,\mu}\sum_{\ell_2=e,\mu}[\mathcal{B}(X \to 2\ell_1)\mathcal{B}(X \to 2\ell_2)]},$$

where $\sigma_{H\to XX\to 4\ell}$ is the model-dependent total cross section, σ_H is the SM Higgs boson production cross section for the ggF process (48.58 pb for $m_H = 125\,\text{GeV}$ [123]), and $\mathcal{B}(X \to 2\ell)$ is the model-dependent branching ratio for each decay to one lepton flavour. The branching ratios for $Z_\text{d} \to \ell\ell$ and $a \to \mu\mu$ are taken from the benchmark models [21, 22], where for the $Z_\text{d} \to \ell\ell$ case, the branching ratios for the two lepton flavours are taken to be equal. For the $a \to \mu\mu$ case, the branching ratio varies considerably in a model-dependent way over the range of m_a considered here. The resulting branching ratio limits are shown in figure 18.

10.3 Limits on Higgs mixing

The branching ratio limit can also be interpreted as a limit on the effective Higgs mixing parameter κ', defined as

$$\kappa' = \kappa\frac{m_H^2}{|m_H^2 - m_S^2|},$$

where κ is the Higgs portal coupling and m_S is the mass of the dark Higgs boson. Using κ' rather than κ combines the dependencies on κ and m_S into a single parameter. Then,

JHEP03(2022)041

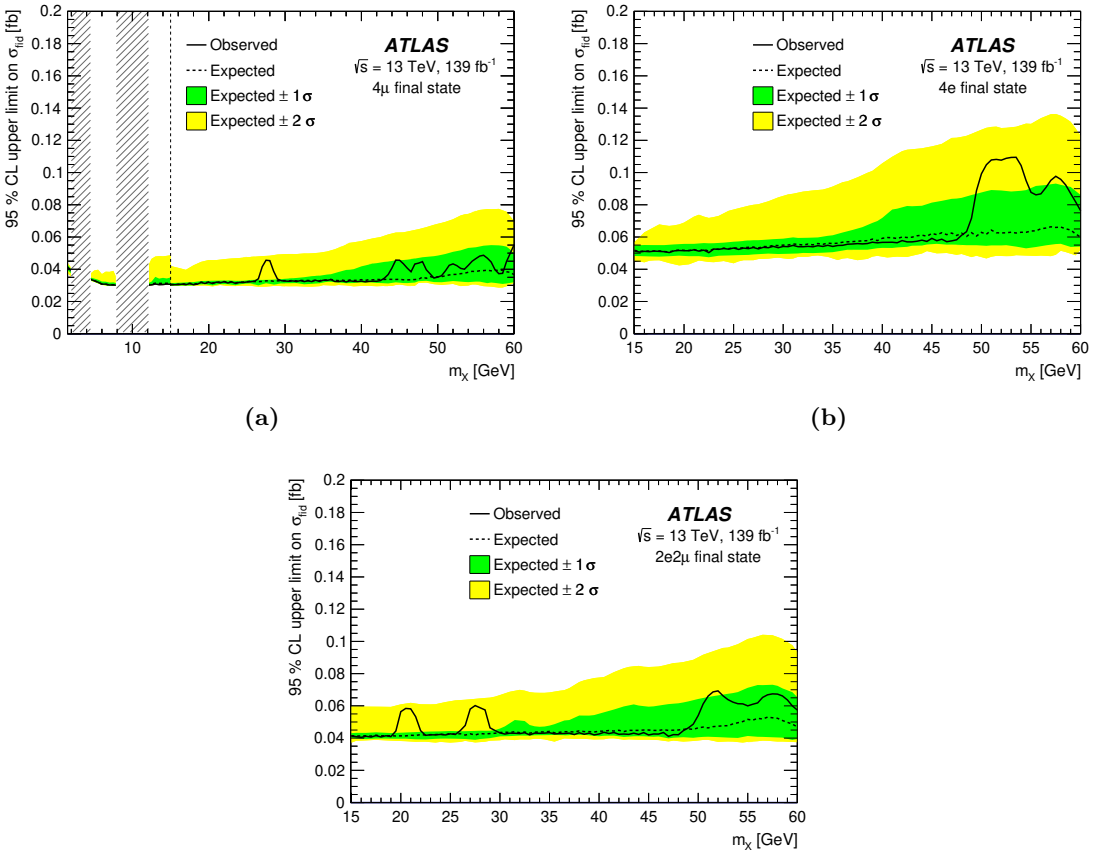

Figure 12. Per-channel upper limits at 95% CL on fiducial cross sections for the $H \to XX \to 4\ell$ process, for the (a) 4μ, (b) $4e$, and (c) $2e2\mu$ final states. The step change in the 4μ channel at $m_X = 15\,\text{GeV}$ is due to the change in efficiency caused by the change in fiducial phase-space definition. The shaded areas are the quarkonia veto regions.

according to eq. (2.33) of ref. [21] and assuming $m_S > m_H/2$:

$$\kappa'^2 = \frac{\Gamma_{\text{SM}}}{f(m_{Z_\text{d}})} \frac{\mathcal{B}(H \to Z_\text{d} Z_\text{d})}{1 - \mathcal{B}(H \to Z_\text{d} Z_\text{d})},$$

where Γ_{SM} is the SM width of the 125 GeV Higgs boson,

$$f(m_{Z_\text{d}}) = \frac{v^2}{32\pi m_H} \sqrt{1 - \frac{4m_{Z_\text{d}}^2}{m_H^2}} \frac{\left(m_H^2 + 2m_{Z_\text{d}}^2\right)^2 - 8\left(m_H^2 - m_{Z_\text{d}}^2\right) m_{Z_\text{d}}^2}{m_H^4},$$

and $v \approx 246\,\text{GeV}$ is the vacuum expectation value of the Higgs field. The resulting limit is shown in figure 19.

The $H \to ZZ_\text{d}$ analysis can also be used to set limits on the Z_d mixing parameter ϵ and on the Z–Z_d mass mixing parameter δ, as described in refs. [21, 42]. These are shown in figure 20, assuming the SM Higgs boson production cross section.

JHEP03(2022)041

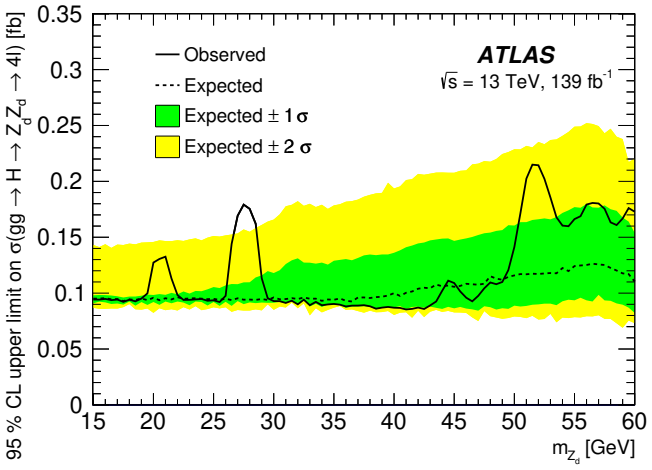

Figure 13. Observed and expected upper limits at 95% CL for the cross section of the $H \to Z_\mathrm{d}Z_\mathrm{d} \to 4\ell$ process, assuming SM Higgs boson production via the gluon-gluon fusion process. All final states are combined. HAHM parameters were set to $\kappa = \epsilon = 10^{-4}$.

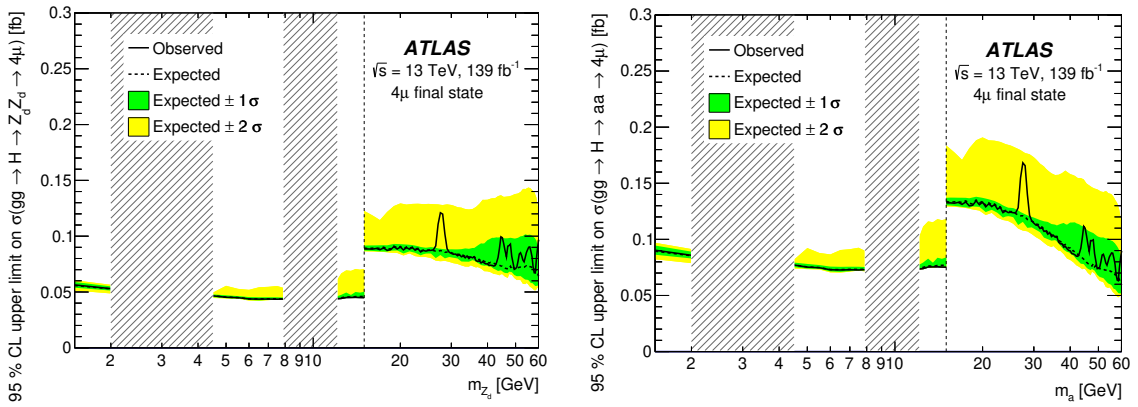

(a) **(b)**

Figure 14. Observed and expected upper limits at 95% CL for the cross sections of the (a) $H \to Z_\mathrm{d}Z_\mathrm{d} \to 4\mu$ and (b) $H \to aa \to 4\mu$ processes, assuming SM Higgs boson production via the gluon-gluon fusion process. The shaded areas are the quarkonia veto regions. HAHM parameters were set to $\kappa = \epsilon = 10^{-4}$. The step changes at $m_{Z_\mathrm{d}} = 15\,\mathrm{GeV}$ are due to the change in selection from the LM to the HM analysis.

JHEP03(2022)041

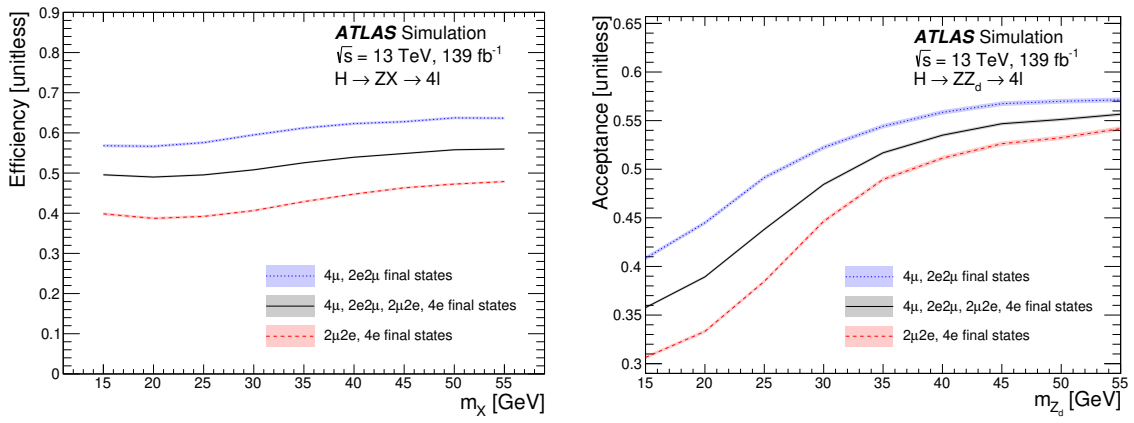

(a) **(b)**

Figure 15. (a) Model-independent efficiencies ϵ_c for the $H \to ZX$ process for different combinations of the final states calculated in the fiducial volumes described in table 6. (b) Model-dependent per-channel fiducial region acceptances for the $H \to ZZ_{\mathrm{d}} \to 4\ell$ process for different combinations of the final states.

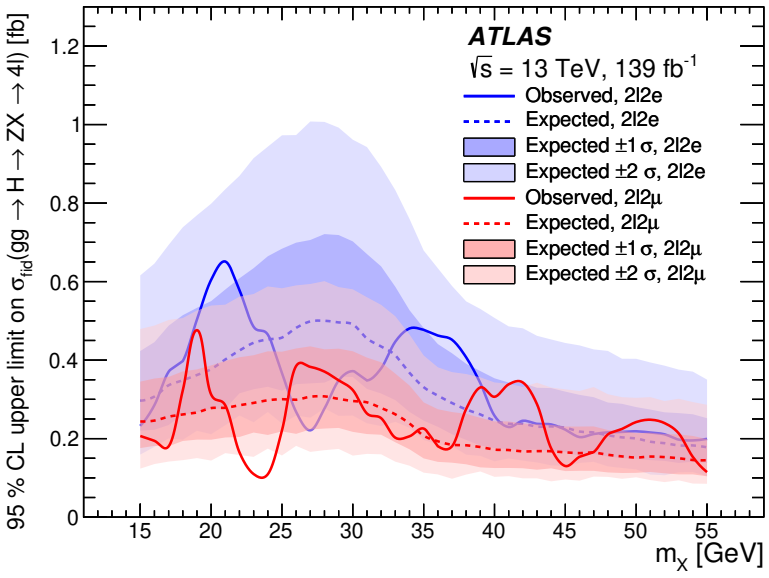

Figure 16. Per-channel upper limit at 95% CL on the fiducial cross section for the $H \to ZX \to 4\ell$ process.

JHEP03(2022)041

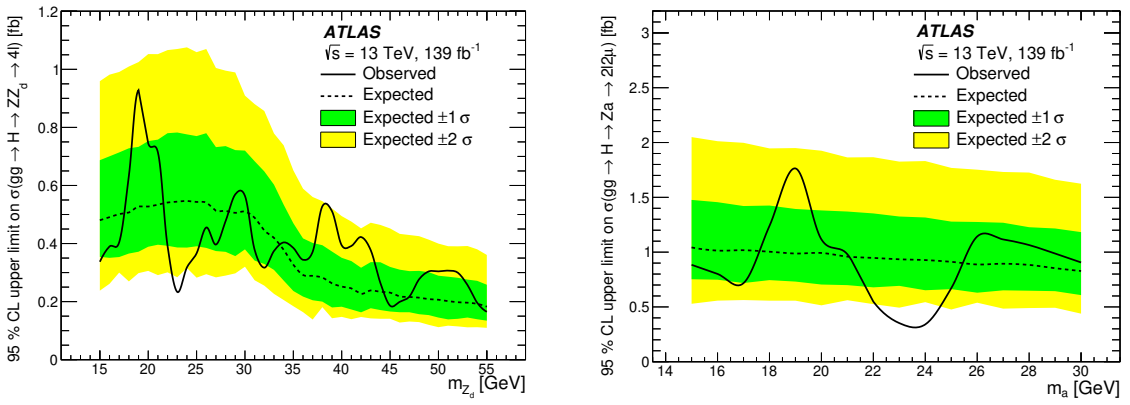

(a) **(b)**

Figure 17. Observed and expected upper limits at 95% CL for the cross sections of the (a) $H \to ZZ_{\mathrm{d}} \to 4\ell$ and (b) $H \to Za \to 2\ell 2\mu$ processes, assuming SM Higgs boson production via the gluon-gluon fusion process. All final states are combined. HAHM parameters were set to $\epsilon = 10^{-4}$ and $\kappa = 10^{-10}$.

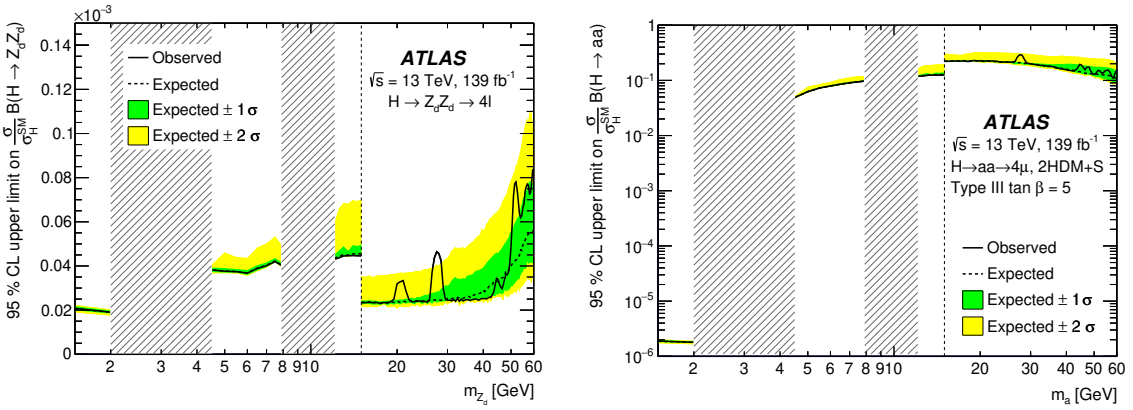

(a) **(b)**

Figure 18. 95% CL upper limits on the cross section times the model-dependent branching ratio divided by the SM Higgs boson production cross section for (a) the $H \to Z_{\mathrm{d}}Z_{\mathrm{d}}$ process for the benchmark HAHM with $\kappa = \epsilon = 10^{-4}$ and (b) the $H \to aa$ process for the benchmark 2HDM+S model. The shaded areas are the quarkonia veto regions. The step changes at $m_{Z_{\mathrm{d}}} = 15\,\mathrm{GeV}$ are due to the change in selection from the LM to the HM analysis.

JHEP03(2022)041

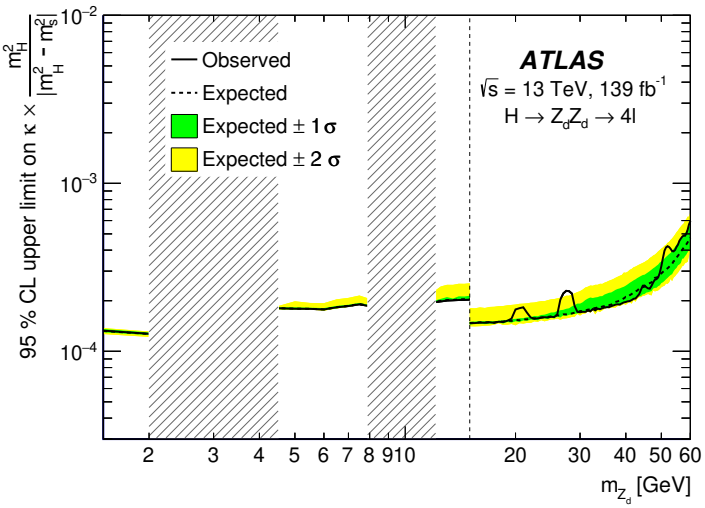

Figure 19. Upper limit at 95% CL on the effective Higgs mixing parameter $\kappa' = \kappa m_H^2/|m_H^2 - m_S^2|$, with ϵ set to 10^{-4}. The step change at $m_{Z_\mathrm{d}} = 15\,\mathrm{GeV}$ is due to the change in selection from the LM to the HM analysis. The shaded areas are the quarkonia veto regions.

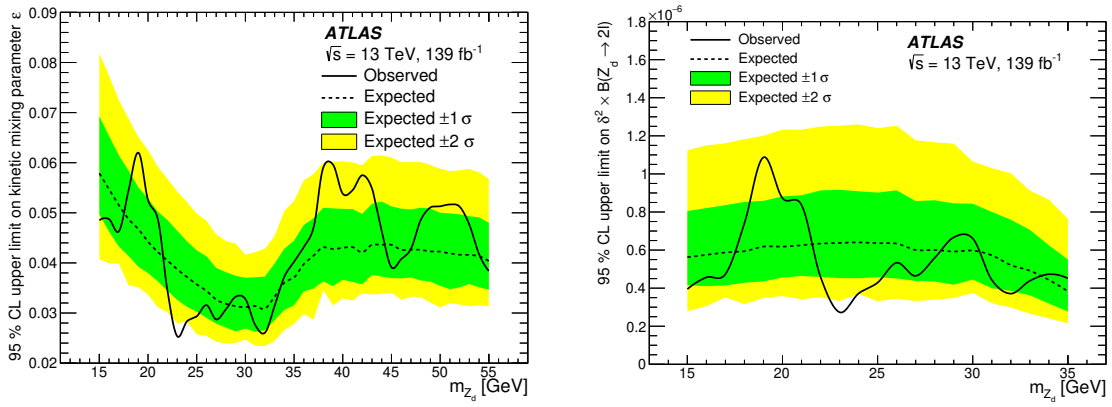

(a) **(b)**

Figure 20. Upper limit at 95% CL on (a) the Z_d mixing parameter ϵ, with κ set to 10^{-10}, and (b) the Z–Z_d mass mixing parameter $\delta^2 \times \mathcal{B}(Z_\mathrm{d} \to \ell\ell)$, assuming the SM Higgs boson production cross section.

JHEP03(2022)041

11 Conclusion

Searches have been conducted for exotic decays of the Standard Model Higgs boson into two new spin-1 particles $H \to Z_\mathrm{d}Z_\mathrm{d}$, two new spin-0 particles $H \to aa$, or a Z boson along with a single Z_d or a. The searches used $139\,\mathrm{fb}^{-1}$ of proton-proton collision data at $\sqrt{s} = 13\,\mathrm{TeV}$ recorded by the ATLAS experiment at the LHC during the period 2015–2018. The first search is for the process $H \to XX \to 4\ell$, where X is either Z_d or a, with $15\,\mathrm{GeV} < m_X < 60\,\mathrm{GeV}$. The second search is for the process $H \to XX \to 4\mu$, with $1\,\mathrm{GeV} < m_X < 15\,\mathrm{GeV}$. The third search is for the process $H \to ZX \to 4\ell$, with $15\,\mathrm{GeV} < m_X < 55\,\mathrm{GeV}$. The data are found to be consistent with the predicted backgrounds in the three aforementioned searches, and limits on fiducial and total cross sections are set.

Specializing to the benchmark models, upper limits are set on the branching ratio of the Higgs boson to $Z_\mathrm{d}Z_\mathrm{d}$ and aa as a function of intermediate boson mass, assuming gluon-gluon fusion Standard Model Higgs production and prompt decay of the Z_d /a bosons. Furthermore, assuming the Hidden Abelian Higgs Model introduced at the Higgs portal level with very weak kinetic mixing, limits are set on the mixing parameters κ', ϵ, and δ.

The limits presented in this paper improve on those from the previous ATLAS search by factors between two and four due to a larger data sample, improved lepton reconstruction and identification, and a better optimized event selection. In addition to the improvements on the results from the previous search, this paper also presents limits on total cross sections and on the dark Higgs boson mixing parameters.

Acknowledgments

We thank CERN for the very successful operation of the LHC, as well as the support staff from our institutions without whom ATLAS could not be operated efficiently.

We acknowledge the support of ANPCyT, Argentina; YerPhI, Armenia; ARC, Australia; BMWFW and FWF, Austria; ANAS, Azerbaijan; SSTC, Belarus; CNPq and FAPESP, Brazil; NSERC, NRC and CFI, Canada; CERN; ANID, Chile; CAS, MOST and NSFC, China; Minciencias, Colombia; MEYS CR, Czech Republic; DNRF and DNSRC, Denmark; IN2P3-CNRS and CEA-DRF/IRFU, France; SRNSFG, Georgia; BMBF, HGF and MPG, Germany; GSRI, Greece; RGC and Hong Kong SAR, China; ISF and Benoziyo Center, Israel; INFN, Italy; MEXT and JSPS, Japan; CNRST, Morocco; NWO, Netherlands; RCN, Norway; MEiN, Poland; FCT, Portugal; MNE/IFA, Romania; JINR; MES of Russia and NRC KI, Russian Federation; MESTD, Serbia; MSSR, Slovakia; ARRS and MIZŠ, Slovenia; DSI/NRF, South Africa; MICINN, Spain; SRC and Wallenberg Foundation, Sweden; SERI, SNSF and Cantons of Bern and Geneva, Switzerland; MOST, Taiwan; TAEK, Turkey; STFC, United Kingdom; DOE and NSF, United States of America. In addition, individual groups and members have received support from BCKDF, CANARIE, Compute Canada and CRC, Canada; COST, ERC, ERDF, Horizon 2020 and Marie Skłodowska-Curie Actions, European Union; Investissements d'Avenir Labex, Investissements d'Avenir Idex and ANR, France; DFG and AvH Foundation, Germany; Herakleitos, Thales and Aristeia programmes co-financed by EU-ESF and the Greek NSRF, Greece; BSF-NSF and GIF, Israel; Norwegian

JHEP03(2022)041

Financial Mechanism 2014–2021, Norway; NCN and NAWA, Poland; La Caixa Banking Foundation, CERCA Programme Generalitat de Catalunya and PROMETEO and GenT Programmes Generalitat Valenciana, Spain; Göran Gustafssons Stiftelse, Sweden; The Royal Society and Leverhulme Trust, United Kingdom.

The crucial computing support from all WLCG partners is acknowledged gratefully, in particular from CERN, the ATLAS Tier-1 facilities at TRIUMF (Canada), NDGF (Denmark, Norway, Sweden), CC-IN2P3 (France), KIT/GridKA (Germany), INFN-CNAF (Italy), NL-T1 (Netherlands), PIC (Spain), ASGC (Taiwan), RAL (U.K.) and BNL (U.S.A.), the Tier-2 facilities worldwide and large non-WLCG resource providers. Major contributors of computing resources are listed in ref. [179].

A HM signal region optimization

The signal region for the HM analysis in ref. [43] was defined by $m_{34}/m_{12} > 0.85$. This was the result of an optimization that assumes the Z_d width is narrow, as expected in the HAHM, so that the observed width will be dominated by the detector performance. A $\pm 2\sigma$ change in the energy measurement gives about a 15% change in the lepton-pair invariant mass, motivating the coefficient of 0.85 in the selection. However, the background is low, especially in the lower mass region, so it is possible to widen the signal region somewhat relative to the background without significant loss of sensitivity. This is further motivated by models such as the one discussed in chapter 7 of ref. [180]. Accordingly, the signal region selection was re-optimized to allow for a larger Z_d width.

The selection widens up to 3.5σ at the low end of the dilepton mass spectrum, where the background is the lowest, but narrows to the previous value of 2σ for higher masses. So the form of the selection is

$$m_{34}/m_{12} > 0.85 - 0.1125 f(m_{12}),$$

where $f(m_{12})$ is a modulating function that is 1 at the lowest mass and goes to 0 at higher masses.

The form of the modulating function is taken from the shape of the average dilepton mass spectrum in the background. The function fit to this shape consists of an exponential tail matched with half of a Gaussian:

$$F(x) = \begin{cases} B_1 + B_2(x - X) + h\,\mathrm{e}^{\frac{-(x-X)^2}{2\sigma^2}}, & x > X - T \\ B_1 + B_2(x - X) + h\,\mathrm{e}^{\frac{T(2x-2X+T)}{2\sigma^2}}, & x < X - T \end{cases}.$$

The fit parameters, with x given in GeV, are $h = 3.73$, $X = 51.6$, $\sigma = 16.6$, $B_1 = -2.62$, $B_2 = -0.0266$, and $T = 6.39$, with the maximum of $F(x)$ occurring at $x_\mathrm{max} = 49.64\,\mathrm{GeV}$. The modulating function is then defined by

$$f(m_{12}) = \begin{cases} 1 - \dfrac{F(m_{12}) - F(10)}{F(x_\mathrm{max}) - F(10)}, & m_{12} < x_\mathrm{max} \\ 0, & m_{12} > x_\mathrm{max} \end{cases}.$$

The final shape of the re-optimized signal region is shown in figure 3(b).

JHEP03(2022)041

Open Access. This article is distributed under the terms of the Creative Commons Attribution License (CC-BY 4.0), which permits any use, distribution and reproduction in any medium, provided the original author(s) and source are credited.

References

[1] ATLAS collaboration, *Observation of a new particle in the search for the Standard Model Higgs boson with the ATLAS detector at the LHC*, *Phys. Lett. B* **716** (2012) 1 [arXiv:1207.7214] [INSPIRE].

[2] CMS collaboration, *Observation of a new boson at a mass of* 125 *GeV with the CMS experiment at the LHC*, *Phys. Lett. B* **716** (2012) 30 [arXiv:1207.7235] [INSPIRE].

[3] A. Martin, J. Shelton and J. Unwin, *Fitting the Galactic Center Gamma-Ray Excess with Cascade Annihilations*, *Phys. Rev. D* **90** (2014) 103513 [arXiv:1405.0272] [INSPIRE].

[4] J.M. Cline, G. Dupuis, Z. Liu and W. Xue, *The windows for kinetically mixed Z'-mediated dark matter and the galactic center gamma ray excess*, *JHEP* **08** (2014) 131 [arXiv:1405.7691] [INSPIRE].

[5] ATLAS collaboration, *Measurements of the Higgs boson production and decay rates and coupling strengths using pp collision data at* $\sqrt{s} = 7$ *and* 8 *TeV in the ATLAS experiment*, *Eur. Phys. J. C* **76** (2016) 6 [arXiv:1507.04548] [INSPIRE].

[6] CMS collaboration, *Precise determination of the mass of the Higgs boson and tests of compatibility of its couplings with the standard model predictions using proton collisions at* 7 *and* 8 *TeV*, *Eur. Phys. J. C* **75** (2015) 212 [arXiv:1412.8662] [INSPIRE].

[7] ATLAS and CMS collaborations, *Measurements of the Higgs boson production and decay rates and constraints on its couplings from a combined ATLAS and CMS analysis of the LHC pp collision data at* $\sqrt{s} = 7$ *and* 8 *TeV*, *JHEP* **08** (2016) 045 [arXiv:1606.02266] [INSPIRE].

[8] R.E. Shrock and M. Suzuki, *Invisible Decays of Higgs Bosons*, *Phys. Lett. B* **110** (1982) 250 [INSPIRE].

[9] M.J. Strassler and K.M. Zurek, *Echoes of a hidden valley at hadron colliders*, *Phys. Lett. B* **651** (2007) 374 [hep-ph/0604261] [INSPIRE].

[10] R.M. Schabinger and J.D. Wells, *Minimal spontaneously broken hidden sector and its impact on Higgs boson physics at the CERN Large Hadron Collider*, *Phys. Rev. D* **72** (2005) 093007 [hep-ph/0509209] [INSPIRE].

[11] B. Patt and F. Wilczek, *Higgs-field portal into hidden sectors*, hep-ph/0605188 [INSPIRE].

[12] S. Profumo, M.J. Ramsey-Musolf and G. Shaughnessy, *Singlet Higgs phenomenology and the electroweak phase transition*, *JHEP* **08** (2007) 010 [arXiv:0705.2425] [INSPIRE].

[13] N. Blinov, J. Kozaczuk, D.E. Morrissey and C. Tamarit, *Electroweak Baryogenesis from Exotic Electroweak Symmetry Breaking*, *Phys. Rev. D* **92** (2015) 035012 [arXiv:1504.05195] [INSPIRE].

[14] G. Burdman, Z. Chacko, H.-S. Goh and R. Harnik, *Folded supersymmetry and the LEP paradox*, *JHEP* **02** (2007) 009 [hep-ph/0609152] [INSPIRE].

[15] N. Craig, A. Katz, M. Strassler and R. Sundrum, *Naturalness in the Dark at the LHC*, *JHEP* **07** (2015) 105 [arXiv:1501.05310] [INSPIRE].

JHEP03(2022)041

[16] D. Curtin and C.B. Verhaaren, *Discovering Uncolored Naturalness in Exotic Higgs Decays*, *JHEP* **12** (2015) 072 [arXiv:1506.06141] [INSPIRE].

[17] P. Fayet, *Light spin-1/2 or spin-0 dark matter particles*, *Phys. Rev. D* **70** (2004) 023514 [hep-ph/0403226] [INSPIRE].

[18] D.P. Finkbeiner and N. Weiner, *Exciting dark matter and the INTEGRAL/SPI 511 keV signal*, *Phys. Rev. D* **76** (2007) 083519 [astro-ph/0702587] [INSPIRE].

[19] N. Arkani-Hamed, D.P. Finkbeiner, T.R. Slatyer and N. Weiner, *A theory of dark matter*, *Phys. Rev. D* **79** (2009) 015014 [arXiv:0810.0713] [INSPIRE].

[20] E. Dudas, Y. Mambrini, S. Pokorski and A. Romagnoni, *Extra* U(1) *as natural source of a monochromatic gamma ray line*, *JHEP* **10** (2012) 123 [arXiv:1205.1520] [INSPIRE].

[21] D. Curtin, R. Essig, S. Gori and J. Shelton, *Illuminating dark photons with high-energy colliders*, *JHEP* **02** (2015) 157 [arXiv:1412.0018] [INSPIRE].

[22] D. Curtin et al., *Exotic decays of the 125 GeV Higgs boson*, *Phys. Rev. D* **90** (2014) 075004 [arXiv:1312.4992] [INSPIRE].

[23] H. Davoudiasl, H.-S. Lee, I. Lewis and W.J. Marciano, *Higgs decays as a window into the dark sector*, *Phys. Rev. D* **88** (2013) 015022 [arXiv:1304.4935] [INSPIRE].

[24] H. Davoudiasl, H.-S. Lee and W.J. Marciano, *"Dark" Z implications for parity violation, rare meson decays, and Higgs physics*, *Phys. Rev. D* **85** (2012) 115019 [arXiv:1203.2947] [INSPIRE].

[25] J.D. Wells, *How to Find a Hidden World at the Large Hadron Collider*, arXiv:0803.1243 [INSPIRE].

[26] S. Gopalakrishna, S. Jung and J.D. Wells, *Higgs boson decays to four fermions through an abelian hidden sector*, *Phys. Rev. D* **78** (2008) 055002 [arXiv:0801.3456] [INSPIRE].

[27] J.A. Evans, S. Gori and J. Shelton, *Looking for the WIMP Next Door*, *JHEP* **02** (2018) 100 [arXiv:1712.03974] [INSPIRE].

[28] V. Silveira and A. Zee, *Scalar Phantoms*, *Phys. Lett. B* **161** (1985) 136 [INSPIRE].

[29] M. Pospelov, A. Ritz and M.B. Voloshin, *Secluded WIMP Dark Matter*, *Phys. Lett. B* **662** (2008) 53 [arXiv:0711.4866] [INSPIRE].

[30] P. Draper, T. Liu, C.E.M. Wagner, L.-T. Wang and H. Zhang, *Dark Light-Higgs Bosons*, *Phys. Rev. Lett.* **106** (2011) 121805 [arXiv:1009.3963] [INSPIRE].

[31] S. Ipek, D. McKeen and A.E. Nelson, *Renormalizable model for the Galactic Center gamma-ray excess from dark matter annihilation*, *Phys. Rev. D* **90** (2014) 055021 [arXiv:1404.3716] [INSPIRE].

[32] D. Clowe et al., *A direct empirical proof of the existence of dark matter*, *Astrophys. J. Lett.* **648** (2006) L109 [astro-ph/0608407] [INSPIRE].

[33] PAMELA collaboration, *An anomalous positron abundance in cosmic rays with energies* 1.5–100 *GeV*, *Nature* **458** (2009) 607 [arXiv:0810.4995] [INSPIRE].

[34] J. Chang et al., *An excess of cosmic ray electrons at energies of* 300–800 *GeV*, *Nature* **456** (2008) 362 [INSPIRE].

[35] AMS collaboration, *High Statistics Measurement of the Positron Fraction in Primary Cosmic Rays of* 0.5–500 *GeV with the Alpha Magnetic Spectrometer on the International Space Station*, *Phys. Rev. Lett.* **113** (2014) 121101 [INSPIRE].

JHEP03(2022)041

[36] B.A. Dobrescu and K.T. Matchev, *Light axion within the next-to-minimal supersymmetric standard model*, *JHEP* **09** (2000) 031 [hep-ph/0008192] [INSPIRE].

[37] U. Ellwanger, J.F. Gunion, C. Hugonie and S. Moretti, *Towards a No-Lose Theorem for NMSSM Higgs Discovery at the LHC*, hep-ph/0305109 [INSPIRE].

[38] R. Dermíšek and J.F. Gunion, *Escaping the Large Fine-Tuning and Little Hierarchy Problems in the Next to Minimal Supersymmetric Model and $h \to aa$ Decays*, *Phys. Rev. Lett.* **95** (2005) 041801 [hep-ph/0502105] [INSPIRE].

[39] S. Chang, R. Dermíšek, J.F. Gunion and N. Weiner, *Nonstandard Higgs Boson Decays*, *Ann. Rev. Nucl. Part. Sci.* **58** (2008) 75 [arXiv:0801.4554] [INSPIRE].

[40] D.E. Morrissey and A. Pierce, *Modified Higgs boson phenomenology from gauge or gaugino mediation in the next-to-minimal supersymmetric standard model*, *Phys. Rev. D* **78** (2008) 075029 [arXiv:0807.2259] [INSPIRE].

[41] S. Dawson, C. Englert and T. Plehn, *Higgs physics: It ain't over till it is over*, *Phys. Rept.* **816** (2019) 1 [arXiv:1808.01324] [INSPIRE].

[42] ATLAS collaboration, *Search for new light gauge bosons in Higgs boson decays to four-lepton final states in pp collisions at $\sqrt{s} = 8$ TeV with the ATLAS detector at the LHC*, *Phys. Rev. D* **92** (2015) 092001 [arXiv:1505.07645] [INSPIRE].

[43] ATLAS collaboration, *Search for Higgs boson decays to beyond-the-Standard-Model light bosons in four-lepton events with the ATLAS detector at $\sqrt{s} = 13$ TeV*, *JHEP* **06** (2018) 166 [arXiv:1802.03388] [INSPIRE].

[44] ATLAS collaboration, *Search for Higgs boson decays into two new low-mass spin-0 particles in the 4b channel with the ATLAS detector using pp collisions at $\sqrt{s} = 13$ TeV*, *Phys. Rev. D* **102** (2020) 112006 [arXiv:2005.12236] [INSPIRE].

[45] ATLAS collaboration, *Search for Higgs boson decays into pairs of light (pseudo)scalar particles in the $\gamma\gamma jj$ final state in pp collisions at $\sqrt{s} = 13$ TeV with the ATLAS detector*, *Phys. Lett. B* **782** (2018) 750 [arXiv:1803.11145] [INSPIRE].

[46] ATLAS collaboration, *Search for the Higgs boson produced in association with a vector boson and decaying into two spin-zero particles in the $H \to aa \to 4b$ channel in pp collisions at $\sqrt{s} = 13$ TeV with the ATLAS detector*, *JHEP* **10** (2018) 031 [arXiv:1806.07355] [INSPIRE].

[47] ATLAS collaboration, *Search for Higgs boson decays into a pair of light bosons in the $bb\mu\mu$ final state in pp collision at $\sqrt{s} = 13$ TeV with the ATLAS detector*, *Phys. Lett. B* **790** (2019) 1 [arXiv:1807.00539] [INSPIRE].

[48] ATLAS collaboration, *Search for Higgs bosons decaying to aa in the $\mu\mu\tau\tau$ final state in pp collisions at $\sqrt{s} = 8$ TeV with the ATLAS experiment*, *Phys. Rev. D* **92** (2015) 052002 [arXiv:1505.01609] [INSPIRE].

[49] CMS collaboration, *A search for pair production of new light bosons decaying into muons*, *Phys. Lett. B* **752** (2016) 146 [arXiv:1506.00424] [INSPIRE].

[50] CMS collaboration, *Search for light bosons in decays of the 125 GeV Higgs boson in proton-proton collisions at $\sqrt{s} = 8$ TeV*, *JHEP* **10** (2017) 076 [arXiv:1701.02032] [INSPIRE].

[51] CMS collaboration, *Search for a light pseudoscalar Higgs boson in the boosted $\mu\mu\tau\tau$ final state in proton-proton collisions at $\sqrt{s} = 13$ TeV*, *JHEP* **08** (2020) 139 [arXiv:2005.08694] [INSPIRE].

JHEP03(2022)041

[52] CMS collaboration, *Search for long-lived particles decaying into muon pairs in proton-proton collisions at* $\sqrt{s} = 13$ *TeV*, submitted to *JHEP* (2021) [arXiv:2112.13769] [INSPIRE].

[53] LHCb collaboration, *Search for Dark Photons Produced in* 13 *TeV pp Collisions*, *Phys. Rev. Lett.* **120** (2018) 061801 [arXiv:1710.02867] [INSPIRE].

[54] ATLAS collaboration, *Combination of Searches for Invisible Higgs Boson Decays with the ATLAS Experiment*, *Phys. Rev. Lett.* **122** (2019) 231801 [arXiv:1904.05105] [INSPIRE].

[55] CMS collaboration, *Search for invisible decays of a Higgs boson produced through vector boson fusion in proton-proton collisions at* $\sqrt{s} = 13$ *TeV*, *Phys. Lett. B* **793** (2019) 520 [arXiv:1809.05937] [INSPIRE].

[56] J. Alexander et al., *Dark Sectors 2016 Workshop: Community Report*, arXiv:1608.08632 [INSPIRE].

[57] P. Galison and A. Manohar, *Two Z's or not two Z's?*, *Phys. Lett. B* **136** (1984) 279 [INSPIRE].

[58] B. Holdom, *Two* U(1)*'s and* ϵ *charge shifts*, *Phys. Lett. B* **166** (1986) 196 [INSPIRE].

[59] K.R. Dienes, C.F. Kolda and J. March-Russell, *Kinetic mixing and the supersymmetric gauge hierarchy*, *Nucl. Phys. B* **492** (1997) 104 [hep-ph/9610479] [INSPIRE].

[60] ATLAS collaboration, *Search for long-lived neutral particles decaying into lepton jets in proton-proton collisions at* $\sqrt{s} = 8$ *TeV with the ATLAS detector*, *JHEP* **11** (2014) 088 [arXiv:1409.0746] [INSPIRE].

[61] ATLAS collaboration, *A search for prompt lepton-jets in pp collisions at* $\sqrt{s} = 8$ *TeV with the ATLAS detector*, *JHEP* **02** (2016) 062 [arXiv:1511.05542] [INSPIRE].

[62] ATLAS collaboration, *Search for massive, long-lived particles using multitrack displaced vertices or displaced lepton pairs in pp collisions at* $\sqrt{s} = 8$ *TeV with the ATLAS detector*, *Phys. Rev. D* **92** (2015) 072004 [arXiv:1504.05162] [INSPIRE].

[63] CMS collaboration, *Search for long-lived particles that decay into final states containing two electrons or two muons in proton-proton collisions at* $\sqrt{s} = 8$ *TeV*, *Phys. Rev. D* **91** (2015) 052012 [arXiv:1411.6977] [INSPIRE].

[64] ATLAS collaboration, *Search for long-lived particles in final states with displaced dimuon vertices in pp collisions at* $\sqrt{s} = 13$ *TeV with the ATLAS detector*, *Phys. Rev. D* **99** (2019) 012001 [arXiv:1808.03057] [INSPIRE].

[65] ATLAS collaboration, *Search for displaced vertices of oppositely charged leptons from decays of long-lived particles in pp collisions at* $\sqrt{s} = 13$ *TeV with the ATLAS detector*, *Phys. Lett. B* **801** (2020) 135114 [arXiv:1907.10037] [INSPIRE].

[66] ATLAS collaboration, *Search for light long-lived neutral particles produced in pp collisions at* $\sqrt{s} = 13$ *TeV and decaying into collimated leptons or light hadrons with the ATLAS detector*, *Eur. Phys. J. C* **80** (2020) 450 [arXiv:1909.01246] [INSPIRE].

[67] ATLAS collaboration, *Constraints on mediator-based dark matter and scalar dark energy models using* $\sqrt{s} = 13$ *TeV pp collision data collected by the ATLAS detector*, *JHEP* **05** (2019) 142 [arXiv:1903.01400] [INSPIRE].

[68] CMS collaboration, *A search for pair production of new light bosons decaying into muons in proton-proton collisions at* 13 *TeV*, *Phys. Lett. B* **796** (2019) 131 [arXiv:1812.00380] [INSPIRE].

JHEP03(2022)041

[69] A. Hook, E. Izaguirre and J.G. Wacker, *Model Independent Bounds on Kinetic Mixing*, *Adv. High Energy Phys.* **2011** (2011) 859762 [arXiv:1006.0973] [INSPIRE].

[70] M. Pospelov, *Secluded* U(1) *below the weak scale*, *Phys. Rev. D* **80** (2009) 095002 [arXiv:0811.1030] [INSPIRE].

[71] I. Hoenig, G. Samach and D. Tucker-Smith, *Searching for dilepton resonances below the Z mass at the LHC*, *Phys. Rev. D* **90** (2014) 075016 [arXiv:1408.1075] [INSPIRE].

[72] NA48/2 collaboration, *Precise measurement of the* $K^{\pm} \to \pi^{\pm} e^{+} e^{-}$ *decay*, *Phys. Lett. B* **677** (2009) 246 [arXiv:0903.3130] [INSPIRE].

[73] BABAR collaboration, *Search for Low-Mass Dark-Sector Higgs Bosons*, *Phys. Rev. Lett.* **108** (2012) 211801 [arXiv:1202.1313] [INSPIRE].

[74] E.M. Riordan et al., *Search for short-lived axions in an electron-beam-dump experiment*, *Phys. Rev. Lett.* **59** (1987) 755 [INSPIRE].

[75] J.D. Bjorken et al., *Search for Neutral Metastable Penetrating Particles Produced in the SLAC Beam Dump*, *Phys. Rev. D* **38** (1988) 3375 [INSPIRE].

[76] A. Bross, M. Crisler, S.H. Pordes, J. Volk, S. Errede and J. Wrbanek, *A Search for Shortlived Particles Produced in an Electron Beam Dump*, *Phys. Rev. Lett.* **67** (1991) 2942 [INSPIRE].

[77] E787 collaboration, *Further search for the decay* $K^{+} \to \pi^{+} \nu \bar{\nu}$ *in the momentum region* $P < 195\, MeV/c$, *Phys. Rev. D* **70** (2004) 037102 [hep-ex/0403034] [INSPIRE].

[78] A. Belyaev, J. Pivarski, A. Safonov, S. Senkin and A. Tatarinov, *LHC discovery potential of the lightest NMSSM Higgs in the* $h_1 \to a_1 a_1 \to 4\mu$ *channel*, *Phys. Rev. D* **81** (2010) 075021 [arXiv:1002.1956] [INSPIRE].

[79] J.F. Gunion, B. Grzadkowski, H.E. Haber and J. Kalinowski, *Limits from LEP Data on CP-Violating Nonminimal Higgs Sectors*, *Phys. Rev. Lett.* **79** (1997) 982 [hep-ph/9704410] [INSPIRE].

[80] G. Bélanger, B. Dumont, U. Ellwanger, J.F. Gunion and S. Kraml, *Global fit to Higgs signal strengths and couplings and implications for extended Higgs sectors*, *Phys. Rev. D* **88** (2013) 075008 [arXiv:1306.2941] [INSPIRE].

[81] J.R. Ellis, J.F. Gunion, H.E. Haber, L. Roszkowski and F. Zwirner, *Higgs Bosons in a Nonminimal Supersymmetric Model*, *Phys. Rev. D* **39** (1989) 844 [INSPIRE].

[82] R. Dermíšek and J.F. Gunion, *Next-to-minimal supersymmetric model close to the R-symmetry limit and naturalness in* $h \to aa$ *decays for* $m_a < 2m_b$, *Phys. Rev. D* **75** (2007) 075019 [hep-ph/0611142] [INSPIRE].

[83] G.F. Giudice and A. Masiero, *A natural solution to the* μ*-problem in supergravity theories*, *Phys. Lett. B* **206** (1988) 480 [INSPIRE].

[84] CMS collaboration, *Search for light pseudoscalar boson pairs produced from decays of the* 125 *GeV Higgs boson in final states with two muons and two nearby tracks in pp collisions at* $\sqrt{s} = 13$ *TeV*, *Phys. Lett. B* **800** (2020) 135087 [arXiv:1907.07235] [INSPIRE].

[85] CMS collaboration, *Search for an exotic decay of the Higgs boson to a pair of light pseudoscalars in the final state with two muons and two b quarks in pp collisions at* 13 *TeV*, *Phys. Lett. B* **795** (2019) 398 [arXiv:1812.06359] [INSPIRE].

[86] CMS collaboration, *Search for an exotic decay of the Higgs boson to a pair of light pseudoscalars in the final state with two b quarks and two* τ *leptons in proton-proton collisions at* $\sqrt{s} = 13$ *TeV*, *Phys. Lett. B* **785** (2018) 462 [arXiv:1805.10191] [INSPIRE].

JHEP03(2022)041

[87] CMS collaboration, *Search for an exotic decay of the Higgs boson to a pair of light pseudoscalars in the final state of two muons and two τ leptons in proton-proton collisions at $\sqrt{s} = 13$ TeV*, *JHEP* **11** (2018) 018 [arXiv:1805.04865] [INSPIRE].

[88] ATLAS collaboration, *Search for new phenomena in events with at least three photons collected in pp collisions at $\sqrt{s} = 8$ TeV with the ATLAS detector*, *Eur. Phys. J. C* **76** (2016) 210 [arXiv:1509.05051] [INSPIRE].

[89] CMS collaboration, *Search for a very light NMSSM Higgs boson produced in decays of the 125 GeV scalar boson and decaying into τ leptons in pp collisions at $\sqrt{s} = 8$ TeV*, *JHEP* **01** (2016) 079 [arXiv:1510.06534] [INSPIRE].

[90] D0 collaboration, *Search for NMSSM Higgs bosons in the $h \to aa \to \mu\mu\mu\mu$, $\mu\mu\tau\tau$ channels using p anti-p collisions at $\sqrt{s} = 1.96$ TeV*, *Phys. Rev. Lett.* **103** (2009) 061801 [arXiv:0905.3381] [INSPIRE].

[91] ATLAS collaboration, *The ATLAS Experiment at the CERN Large Hadron Collider*, 2008 *JINST* **3** S08003 [INSPIRE].

[92] ATLAS collaboration, *ATLAS Insertable B-Layer: Technical Design Report*, CERN-LHCC-2010-013; ATLAS-TDR-19 (2010) [*Addendum* ATLAS-TDR-19-ADD-1; CERN-LHCC-2012-009 (2012)].

[93] ATLAS IBL collaboration, *Production and integration of the ATLAS Insertable B-Layer*, 2018 *JINST* **13** T05008 [arXiv:1803.00844] [INSPIRE].

[94] ATLAS collaboration, *Performance of the ATLAS trigger system in 2015*, *Eur. Phys. J. C* **77** (2017) 317 [arXiv:1611.09661] [INSPIRE].

[95] ATLAS collaboration, *The ATLAS Collaboration Software and Firmware*, ATL-SOFT-PUB-2021-001 (2021).

[96] GEANT4 collaboration, GEANT4 — *a simulation toolkit*, *Nucl. Instrum. Meth. A* **506** (2003) 250 [INSPIRE].

[97] ATLAS collaboration, *The ATLAS Simulation Infrastructure*, *Eur. Phys. J. C* **70** (2010) 823 [arXiv:1005.4568] [INSPIRE].

[98] ATLAS collaboration, *The simulation principle and performance of the ATLAS fast calorimeter simulation FastCaloSim*, ATL-PHYS-PUB-2010-013 (2010).

[99] ATLAS collaboration, *Electron and photon performance measurements with the ATLAS detector using the 2015–2017 LHC proton-proton collision data*, 2019 *JINST* **14** P12006 [arXiv:1908.00005] [INSPIRE].

[100] ATLAS collaboration, *Electron reconstruction and identification in the ATLAS experiment using the 2015 and 2016 LHC proton-proton collision data at $\sqrt{s} = 13$ TeV*, *Eur. Phys. J. C* **79** (2019) 639 [arXiv:1902.04655] [INSPIRE].

[101] ATLAS collaboration, *Muon reconstruction and identification efficiency in ATLAS using the full Run 2 pp collision data set at $\sqrt{s} = 13$ TeV*, *Eur. Phys. J. C* **81** (2021) 578 [arXiv:2012.00578] [INSPIRE].

[102] ATLAS collaboration, *Electron and photon energy calibration with the ATLAS detector using 2015–2016 LHC proton-proton collision data*, 2019 *JINST* **14** P03017 [arXiv:1812.03848] [INSPIRE].

[103] J. Alwall et al., *The automated computation of tree-level and next-to-leading order differential cross sections, and their matching to parton shower simulations*, *JHEP* **07** (2014) 079 [arXiv:1405.0301] [INSPIRE].

JHEP03(2022)041

[104] K. Hamilton, P. Nason, E. Re and G. Zanderighi, *NNLOPS simulation of Higgs boson production*, *JHEP* **10** (2013) 222 [arXiv:1309.0017] [INSPIRE].

[105] K. Hamilton, P. Nason and G. Zanderighi, *Finite quark-mass effects in the NNLOPS POWHEG+MiNLO Higgs generator*, *JHEP* **05** (2015) 140 [arXiv:1501.04637] [INSPIRE].

[106] S. Alioli, P. Nason, C. Oleari and E. Re, *A general framework for implementing NLO calculations in shower Monte Carlo programs: the POWHEG BOX*, *JHEP* **06** (2010) 043 [arXiv:1002.2581] [INSPIRE].

[107] P. Nason, *A new method for combining NLO QCD with shower Monte Carlo algorithms*, *JHEP* **11** (2004) 040 [hep-ph/0409146] [INSPIRE].

[108] S. Frixione, P. Nason and C. Oleari, *Matching NLO QCD computations with parton shower simulations: the POWHEG method*, *JHEP* **11** (2007) 070 [arXiv:0709.2092] [INSPIRE].

[109] T. Sjöstrand et al., *An introduction to PYTHIA 8.2*, *Comput. Phys. Commun.* **191** (2015) 159 [arXiv:1410.3012] [INSPIRE].

[110] D.J. Lange, *The EvtGen particle decay simulation package*, *Nucl. Instrum. Meth. A* **462** (2001) 152 [INSPIRE].

[111] SHERPA collaboration, *Event generation with Sherpa 2.2*, *SciPost Phys.* **7** (2019) 034 [arXiv:1905.09127] [INSPIRE].

[112] R.D. Ball et al., *Parton distributions with LHC data*, *Nucl. Phys. B* **867** (2013) 244 [arXiv:1207.1303] [INSPIRE].

[113] ATLAS collaboration, *ATLAS Pythia 8 tunes to 7 TeV data*, ATL-PHYS-PUB-2014-021 (2014).

[114] ATLAS collaboration, *Measurement of the Z/γ^* boson transverse momentum distribution in pp collisions at $\sqrt{s} = 7$ TeV with the ATLAS detector*, *JHEP* **09** (2014) 145 [arXiv:1406.3660] [INSPIRE].

[115] J. Butterworth et al., *PDF4LHC recommendations for LHC Run II*, *J. Phys. G* **43** (2016) 023001 [arXiv:1510.03865] [INSPIRE].

[116] H.-L. Lai et al., *New parton distributions for collider physics*, *Phys. Rev. D* **82** (2010) 074024 [arXiv:1007.2241] [INSPIRE].

[117] K. Hamilton, P. Nason and G. Zanderighi, *MINLO: multi-scale improved NLO*, *JHEP* **10** (2012) 155 [arXiv:1206.3572] [INSPIRE].

[118] J.M. Campbell, R.K. Ellis, R. Frederix, P. Nason, C. Oleari and C. Williams, *NLO Higgs boson production plus one and two jets using the POWHEG BOX, MadGraph4 and MCFM*, *JHEP* **07** (2012) 092 [arXiv:1202.5475] [INSPIRE].

[119] K. Hamilton, P. Nason, C. Oleari and G. Zanderighi, *Merging $H/W/Z + 0$ and 1 jet at NLO with no merging scale: a path to parton shower + NNLO matching*, *JHEP* **05** (2013) 082 [arXiv:1212.4504] [INSPIRE].

[120] S. Catani and M. Grazzini, *Next-to-Next-to-Leading-Order Subtraction Formalism in Hadron Collisions and its Application to Higgs-Boson Production at the Large Hadron Collider*, *Phys. Rev. Lett.* **98** (2007) 222002 [hep-ph/0703012] [INSPIRE].

[121] ATLAS collaboration, *Study of higher-order QCD corrections in the $gg \to H \to VV$ process*, ATL-PHYS-PUB-2016-006 (2016).

JHEP03(2022)041

[122] LHC Higgs Cross Section Working Group collaboration, *Handbook of LHC Higgs Cross Sections: 4. Deciphering the Nature of the Higgs Sector*, arXiv:1610.07922 [INSPIRE].

[123] C. Anastasiou et al., *High precision determination of the gluon fusion Higgs boson cross-section at the LHC*, *JHEP* **05** (2016) 058 [arXiv:1602.00695] [INSPIRE].

[124] C. Anastasiou, C. Duhr, F. Dulat, F. Herzog and B. Mistlberger, *Higgs Boson Gluon-Fusion Production in QCD at Three Loops*, *Phys. Rev. Lett.* **114** (2015) 212001 [arXiv:1503.06056] [INSPIRE].

[125] F. Dulat, A. Lazopoulos and B. Mistlberger, *iHixs 2 — Inclusive Higgs cross sections*, *Comput. Phys. Commun.* **233** (2018) 243 [arXiv:1802.00827] [INSPIRE].

[126] R.V. Harlander and K.J. Ozeren, *Finite top mass effects for hadronic Higgs production at next-to-next-to-leading order*, *JHEP* **11** (2009) 088 [arXiv:0909.3420] [INSPIRE].

[127] R.V. Harlander and K.J. Ozeren, *Top mass effects in Higgs production at next-to-next-to-leading order QCD: Virtual corrections*, *Phys. Lett. B* **679** (2009) 467 [arXiv:0907.2997] [INSPIRE].

[128] R.V. Harlander, H. Mantler, S. Marzani and K.J. Ozeren, *Higgs production in gluon fusion at next-to-next-to-leading order QCD for finite top mass*, *Eur. Phys. J. C* **66** (2010) 359 [arXiv:0912.2104] [INSPIRE].

[129] M. Czakon, R.V. Harlander, J. Klappert and M. Niggetiedt, *Exact Top-Quark Mass Dependence in Hadronic Higgs Production*, *Phys. Rev. Lett.* **127** (2021) 162002 [arXiv:2105.04436] [INSPIRE].

[130] A. Pak, M. Rogal and M. Steinhauser, *Finite top quark mass effects in NNLO Higgs boson production at LHC*, *JHEP* **02** (2010) 025 [arXiv:0911.4662] [INSPIRE].

[131] S. Actis, G. Passarino, C. Sturm and S. Uccirati, *NLO electroweak corrections to Higgs boson production at hadron colliders*, *Phys. Lett. B* **670** (2008) 12 [arXiv:0809.1301] [INSPIRE].

[132] S. Actis, G. Passarino, C. Sturm and S. Uccirati, *NNLO computational techniques: The cases $H \to \gamma\gamma$ and $H \to gg$*, *Nucl. Phys. B* **811** (2009) 182 [arXiv:0809.3667] [INSPIRE].

[133] M. Bonetti, K. Melnikov and L. Tancredi, *Higher order corrections to mixed QCD-EW contributions to Higgs boson production in gluon fusion*, *Phys. Rev. D* **97** (2018) 056017 [*Erratum ibid.* **97** (2018) 099906] [arXiv:1801.10403] [INSPIRE].

[134] P. Nason and C. Oleari, *NLO Higgs boson production via vector-boson fusion matched with shower in POWHEG*, *JHEP* **02** (2010) 037 [arXiv:0911.5299] [INSPIRE].

[135] M. Ciccolini, A. Denner and S. Dittmaier, *Strong and Electroweak Corrections to the Production of a Higgs Boson + 2 Jets via Weak Interactions at the Large Hadron Collider*, *Phys. Rev. Lett.* **99** (2007) 161803 [arXiv:0707.0381] [INSPIRE].

[136] M. Ciccolini, A. Denner and S. Dittmaier, *Electroweak and QCD corrections to Higgs production via vector-boson fusion at the CERN LHC*, *Phys. Rev. D* **77** (2008) 013002 [arXiv:0710.4749] [INSPIRE].

[137] P. Bolzoni, F. Maltoni, S.-O. Moch and M. Zaro, *Higgs Boson Production via Vector-Boson Fusion at Next-to-Next-to-Leading Order in QCD*, *Phys. Rev. Lett.* **105** (2010) 011801 [arXiv:1003.4451] [INSPIRE].

[138] G. Luisoni, P. Nason, C. Oleari and F. Tramontano, *$HW^{\pm}/HZ + 0$ and 1 jet at NLO with the POWHEG BOX interfaced to GoSam and their merging within MiNLO*, *JHEP* **10** (2013) 083 [arXiv:1306.2542] [INSPIRE].

JHEP03(2022)041

[139] M.L. Ciccolini, S. Dittmaier and M. Krämer, *Electroweak radiative corrections to associated WH and ZH production at hadron colliders*, *Phys. Rev. D* **68** (2003) 073003 [hep-ph/0306234] [INSPIRE].

[140] O. Brein, A. Djouadi and R. Harlander, *NNLO QCD corrections to the Higgs-strahlung processes at hadron colliders*, *Phys. Lett. B* **579** (2004) 149 [hep-ph/0307206] [INSPIRE].

[141] G. Ferrera, M. Grazzini and F. Tramontano, *Associated Higgs-W-Boson Production at Hadron Colliders: A Fully Exclusive QCD Calculation at NNLO*, *Phys. Rev. Lett.* **107** (2011) 152003 [arXiv:1107.1164] [INSPIRE].

[142] O. Brein, R. Harlander, M. Wiesemann and T. Zirke, *Top-quark mediated effects in hadronic Higgs-Strahlung*, *Eur. Phys. J. C* **72** (2012) 1868 [arXiv:1111.0761] [INSPIRE].

[143] G. Ferrera, M. Grazzini and F. Tramontano, *Higher-order QCD effects for associated WH production and decay at the LHC*, *JHEP* **04** (2014) 039 [arXiv:1312.1669] [INSPIRE].

[144] G. Ferrera, M. Grazzini and F. Tramontano, *Associated ZH production at hadron colliders: the fully differential NNLO QCD calculation*, *Phys. Lett. B* **740** (2015) 51 [arXiv:1407.4747] [INSPIRE].

[145] J.M. Campbell, R.K. Ellis and C. Williams, *Associated production of a Higgs boson at NNLO*, *JHEP* **06** (2016) 179 [arXiv:1601.00658] [INSPIRE].

[146] ATLAS collaboration, *Modelling of the $t\bar{t}H$ and $t\bar{t}V$ ($V = W, Z$) processes for $\sqrt{s} = 13$ TeV ATLAS analyses*, ATL-PHYS-PUB-2016-005 (2016).

[147] B.A. Kniehl, *Associated Production of Higgs and Z Bosons From Gluon Fusion in Hadron Collisions*, *Phys. Rev. D* **42** (1990) 2253 [INSPIRE].

[148] ATLAS collaboration, *Multi-Boson Simulation for 13 TeV ATLAS Analyses*, ATL-PHYS-PUB-2017-005 (2017).

[149] T. Gleisberg and S. Hoeche, *Comix, a new matrix element generator*, *JHEP* **12** (2008) 039 [arXiv:0808.3674] [INSPIRE].

[150] S. Schumann and F. Krauss, *A parton shower algorithm based on Catani-Seymour dipole factorisation*, *JHEP* **03** (2008) 038 [arXiv:0709.1027] [INSPIRE].

[151] S. Hoeche, F. Krauss, M. Schonherr and F. Siegert, *A critical appraisal of NLO+PS matching methods*, *JHEP* **09** (2012) 049 [arXiv:1111.1220] [INSPIRE].

[152] S. Hoeche, F. Krauss, M. Schonherr and F. Siegert, *QCD matrix elements + parton showers. The NLO case*, *JHEP* **04** (2013) 027 [arXiv:1207.5030] [INSPIRE].

[153] S. Catani, F. Krauss, R. Kuhn and B.R. Webber, *QCD Matrix Elements + Parton Showers*, *JHEP* **11** (2001) 063 [hep-ph/0109231] [INSPIRE].

[154] S. Hoeche, F. Krauss, S. Schumann and F. Siegert, *QCD matrix elements and truncated showers*, *JHEP* **05** (2009) 053 [arXiv:0903.1219] [INSPIRE].

[155] F. Buccioni et al., *OpenLoops 2*, *Eur. Phys. J. C* **79** (2019) 866 [arXiv:1907.13071] [INSPIRE].

[156] F. Cascioli, P. Maierhofer and S. Pozzorini, *Scattering Amplitudes with Open Loops*, *Phys. Rev. Lett.* **108** (2012) 111601 [arXiv:1111.5206] [INSPIRE].

[157] A. Denner, S. Dittmaier and L. Hofer, COLLIER*: A fortran-based complex one-loop library in extended regularizations*, *Comput. Phys. Commun.* **212** (2017) 220 [arXiv:1604.06792] [INSPIRE].

JHEP03(2022)041

[158] F. Caola, K. Melnikov, R. Röntsch and L. Tancredi, *QCD corrections to ZZ production in gluon fusion at the LHC*, *Phys. Rev. D* **92** (2015) 094028 [arXiv:1509.06734] [INSPIRE].

[159] ATLAS collaboration, *Studies on top-quark Monte Carlo modelling for Top2016*, ATL-PHYS-PUB-2016-020 (2016).

[160] PARTICLE DATA GROUP collaboration, *Review of Particle Physics*, *PTEP* **2020** (2020) 083C01 [INSPIRE].

[161] ATLAS collaboration, *ATLAS data preparation in run 2*, *J. Phys. Conf. Ser.* **898** (2017) 042050 [INSPIRE].

[162] ATLAS collaboration, *Selection of jets produced in* 13 *TeV proton-proton collisions with the ATLAS detector*, ATLAS-CONF-2015-029 (2015).

[163] ATLAS collaboration, *Vertex Reconstruction Performance of the ATLAS Detector at* $\sqrt{s} = 13$ *TeV*, ATL-PHYS-PUB-2015-026 (2015).

[164] ATLAS collaboration, *Performance of electron and photon triggers in ATLAS during LHC Run 2*, *Eur. Phys. J. C* **80** (2020) 47 [arXiv:1909.00761] [INSPIRE].

[165] ATLAS collaboration, *Performance of the ATLAS muon triggers in Run 2*, 2020 *JINST* **15** P09015 [arXiv:2004.13447] [INSPIRE].

[166] ATLAS collaboration, *The ATLAS Inner Detector Trigger performance in pp collisions at* 13 *TeV during LHC Run 2*, CERN-EP-2021-076 (2021).

[167] W. Lampl et al., *Calorimeter Clustering Algorithms: Description and Performance*, ATL-LARG-PUB-2008-002, ATL-COM-LARG-2008-003 (2008).

[168] ATLAS collaboration, *Measurement of the Higgs boson coupling properties in the* $H \to ZZ^* \to 4\ell$ *decay channel at* $\sqrt{s} = 13$ *TeV with the ATLAS detector*, *JHEP* **03** (2018) 095 [arXiv:1712.02304] [INSPIRE].

[169] ATLAS collaboration, *Luminosity determination in pp collisions at* $\sqrt{s} = 13$ *TeV using the ATLAS detector at the LHC*, ATLAS-CONF-2019-021 (2019).

[170] G. Avoni et al., *The new LUCID-2 detector for luminosity measurement and monitoring in atlas*, 2018 *JINST* **13** P07017 [INSPIRE].

[171] LHC HIGGS CROSS SECTION WORKING GROUP collaboration, *Handbook of LHC Higgs Cross Sections: 1. Inclusive Observables*, CERN-2011-002 (2011) [arXiv:1101.0593] [INSPIRE].

[172] ATLAS collaboration, *Measurement of inclusive and differential cross sections in the* $H \to ZZ^* \to 4\ell$ *decay channel in pp collisions at* $\sqrt{s} = 13$ *TeV with the ATLAS detector*, *JHEP* **10** (2017) 132 [arXiv:1708.02810] [INSPIRE].

[173] ATLAS collaboration, *Measurements of the Higgs boson inclusive and differential fiducial cross sections in the* 4ℓ *decay channel at* $\sqrt{s} = 13$ *TeV*, *Eur. Phys. J. C* **80** (2020) 942 [arXiv:2004.03969] [INSPIRE].

[174] M. Baak, S. Gadatsch, R. Harrington and W. Verkerke, *Interpolation between multi-dimensional histograms using a new non-linear moment morphing method*, *Nucl. Instrum. Meth. A* **771** (2015) 39 [arXiv:1410.7388] [INSPIRE].

[175] ROOT collaboration, *HistFactory: A tool for creating statistical models for use with RooFit and RooStats*, CERN-OPEN-2012-016 (2012).

JHEP03(2022)041

[176] ATLAS collaboration, *Proposal for particle-level object and observable definitions for use in physics measurements at the LHC*, ATL-PHYS-PUB-2015-013 (2015).

[177] A.L. Read, *Presentation of search results: the CL_S technique*, *J. Phys. G* **28** (2002) 2693 [INSPIRE].

[178] G. Cowan, K. Cranmer, E. Gross and O. Vitells, *Asymptotic formulae for likelihood-based tests of new physics*, *Eur. Phys. J. C* **71** (2011) 1554 [*Erratum ibid.* **73** (2013) 2501] [arXiv:1007.1727] [INSPIRE].

[179] ATLAS collaboration, *ATLAS Computing Acknowledgements*, ATL-SOFT-PUB-2021-003 (2021).

[180] J. Alimena et al., *Searching for long-lived particles beyond the Standard Model at the Large Hadron Collider*, *J. Phys. G* **47** (2020) 090501 [arXiv:1903.04497] [INSPIRE].

JHEP03(2022)041

The ATLAS collaboration

G. Aad[98], B. Abbott[124], D.C. Abbott[99], A. Abed Abud[34], K. Abeling[51], D.K. Abhayasinghe[91], S.H. Abidi[27], A. Aboulhorma[33e], H. Abramowicz[157], H. Abreu[156], Y. Abulaiti[5], A.C. Abusleme Hoffman[142a], B.S. Acharya[64a,64b,o], B. Achkar[51], L. Adam[96], C. Adam Bourdarios[4], L. Adamczyk[81a], L. Adamek[162], S.V. Addepalli[24], J. Adelman[116], A. Adiguzel[11c,ac], S. Adorni[52], T. Adye[139], A.A. Affolder[141], Y. Afik[34], C. Agapopoulou[62], M.N. Agaras[12], J. Agarwala[68a,68b], A. Aggarwal[114], C. Agheorghiesei[25c], J.A. Aguilar-Saavedra[135f,135a,ab], A. Ahmad[34], F. Ahmadov[77], W.S. Ahmed[100], X. Ai[44], G. Aielli[71a,71b], I. Aizenberg[175], S. Akatsuka[83], M. Akbiyik[96], T.P.A. Åkesson[94], A.V. Akimov[107], K. Al Khoury[37], G.L. Alberghi[21b], J. Albert[171], P. Albicocco[49], M.J. Alconada Verzini[86], S. Alderweireldt[48], M. Aleksa[34], I.N. Aleksandrov[77], C. Alexa[25b], T. Alexopoulos[9], A. Alfonsi[115], F. Alfonsi[21b], M. Alhroob[124], B. Ali[137], S. Ali[154], M. Aliev[161], G. Alimonti[66a], C. Allaire[34], B.M.M. Allbrooke[152], P.P. Allport[19], A. Aloisio[67a,67b], F. Alonso[86], C. Alpigiani[144], E. Alunno Camelia[71a,71b], M. Alvarez Estevez[95], M.G. Alviggi[67a,67b], Y. Amaral Coutinho[78b], A. Ambler[100], L. Ambroz[130], C. Amelung[34], D. Amidei[102], S.P. Amor Dos Santos[135a], S. Amoroso[44], K.R. Amos[169], C.S. Amrouche[52], V. Ananiev[129], C. Anastopoulos[145], N. Andari[140], T. Andeen[10], J.K. Anders[18], S.Y. Andrean[43a,43b], A. Andreazza[66a,66b], S. Angelidakis[8], A. Angerami[37], A.V. Anisenkov[117b,117a], A. Annovi[69a], C. Antel[52], M.T. Anthony[145], E. Antipov[125], M. Antonelli[49], D.J.A. Antrim[16], F. Anulli[70a], M. Aoki[79], J.A. Aparisi Pozo[169], M.A. Aparo[152], L. Aperio Bella[44], N. Aranzabal[34], V. Araujo Ferraz[78a], C. Arcangeletti[49], A.T.H. Arce[47], E. Arena[88], J-F. Arguin[106], S. Argyropoulos[50], J.-H. Arling[44], A.J. Armbruster[34], A. Armstrong[166], O. Arnaez[162], H. Arnold[34], Z.P. Arrubarrena Tame[110], G. Artoni[130], H. Asada[112], K. Asai[122], S. Asai[159], N.A. Asbah[57], E.M. Asimakopoulou[167], L. Asquith[152], J. Assahsah[33d], K. Assamagan[27], R. Astalos[26a], R.J. Atkin[31a], M. Atkinson[168], N.B. Atlay[17], H. Atmani[58b], P.A. Atmasiddha[102], K. Augsten[137], S. Auricchio[67a,67b], V.A. Austrup[177], G. Avner[156], G. Avolio[34], M.K. Ayoub[13c], G. Azuelos[106,aj], D. Babal[26a], H. Bachacou[140], K. Bachas[158], A. Bachiu[32], F. Backman[43a,43b], A. Badea[57], P. Bagnaia[70a,70b], H. Bahrasemani[148], A.J. Bailey[169], V.R. Bailey[168], J.T. Baines[139], C. Bakalis[9], O.K. Baker[178], P.J. Bakker[115], E. Bakos[14], D. Bakshi Gupta[7], S. Balaji[153], R. Balasubramanian[115], E.M. Baldin[117b,117a], P. Balek[138], E. Ballabene[66a,66b], F. Balli[140], L.M. Baltes[59a], W.K. Balunas[130], J. Balz[96], E. Banas[82], M. Bandieramonte[134], A. Bandyopadhyay[22], S. Bansal[22], L. Barak[157], E.L. Barberio[101], D. Barberis[53b,53a], M. Barbero[98], G. Barbour[92], K.N. Barends[31a], T. Barillari[111], M-S. Barisits[34], J. Barkeloo[127], T. Barklow[149], B.M. Barnett[139], R.M. Barnett[16], A. Baroncelli[58a], G. Barone[27], A.J. Barr[130], L. Barranco Navarro[43a,43b], F. Barreiro[95], J. Barreiro Guimarães da Costa[13a], U. Barron[157], S. Barsov[133], F. Bartels[59a], R. Bartoldus[149], G. Bartolini[98], A.E. Barton[87], P. Bartos[26a], A. Basalaev[44], A. Basan[96], M. Baselga[44], I. Bashta[72a,72b], A. Bassalat[62,ag], M.J. Basso[162], C.R. Basson[97], R.L. Bates[55], S. Batlamous[33e], J.R. Batley[30], B. Batool[147], M. Battaglia[141], M. Bauce[70a,70b], F. Bauer[140,*], P. Bauer[22], H.S. Bawa[29], A. Bayirli[11c], J.B. Beacham[47], T. Beau[131], P.H. Beauchemin[165], F. Becherer[50], P. Bechtle[22], H.P. Beck[18,q], K. Becker[173], C. Becot[44], A.J. Beddall[11a], V.A. Bednyakov[77], C.P. Bee[151], T.A. Beermann[34], M. Begalli[78b], M. Begel[27], A. Behera[151], J.K. Behr[44], C. Beirao Da Cruz E Silva[34], J.F. Beirer[51,34], F. Beisiegel[22], M. Belfkir[4], G. Bella[157], L. Bellagamba[21b], A. Bellerive[32], P. Bellos[19], K. Beloborodov[117b,117a], K. Belotskiy[108], N.L. Belyaev[108], D. Benchekroun[33a], Y. Benhammou[157], D.P. Benjamin[27], M. Benoit[27], J.R. Bensinger[24], S. Bentvelsen[115], L. Beresford[34], M. Beretta[49], D. Berge[17], E. Bergeaas Kuutmann[167], N. Berger[4], B. Bergmann[137], L.J. Bergsten[24], J. Beringer[16], S. Berlendis[6], G. Bernardi[131], C. Bernius[149], F.U. Bernlochner[22], T. Berry[91], P. Berta[138], A. Berthold[46], I.A. Bertram[87], O. Bessidskaia Bylund[177], S. Bethke[111], A. Betti[40], A.J. Bevan[90],

JHEP03(2022)041

S. Bhatta[151], D.S. Bhattacharya[172], P. Bhattarai[24], V.S. Bhopatkar[5], R. Bi[134], R.M. Bianchi[134], O. Biebel[110], R. Bielski[127], N.V. Biesuz[69a,69b], M. Biglietti[72a], T.R.V. Billoud[137], M. Bindi[51], A. Bingul[11d], C. Bini[70a,70b], S. Biondi[21b,21a], A. Biondini[88], C.J. Birch-sykes[97], G.A. Bird[19,139], M. Birman[175], T. Bisanz[34], J.P. Biswal[2], D. Biswas[176,j], A. Bitadze[97], C. Bittrich[46], K. Bjørke[129], I. Bloch[44], C. Blocker[24], A. Blue[55], U. Blumenschein[90], J. Blumenthal[96], G.J. Bobbink[115], V.S. Bobrovnikov[117b,117a], M. Boehler[50], D. Bogavac[12], A.G. Bogdanchikov[117b,117a], C. Bohm[43a], V. Boisvert[91], P. Bokan[44], T. Bold[81a], M. Bomben[131], M. Bona[90], M. Boonekamp[140], C.D. Booth[91], A.G. Borbély[55], H.M. Borecka-Bielska[106], L.S. Borgna[92], G. Borissov[87], D. Bortoletto[130], D. Boscherini[21b], M. Bosman[12], J.D. Bossio Sola[34], K. Bouaouda[33a], J. Boudreau[134], E.V. Bouhova-Thacker[87], D. Boumediene[36], R. Bouquet[131], A. Boveia[123], J. Boyd[34], D. Boye[27], I.R. Boyko[77], A.J. Bozson[91], J. Bracinik[19], N. Brahimi[58d,58c], G. Brandt[177], O. Brandt[30], F. Braren[44], B. Brau[99], J.E. Brau[127], W.D. Breaden Madden[55], K. Brendlinger[44], R. Brener[175], L. Brenner[34], R. Brenner[167], S. Bressler[175], B. Brickwedde[96], D.L. Briglin[19], D. Britton[55], D. Britzger[111], I. Brock[22], R. Brock[103], G. Brooijmans[37], W.K. Brooks[142e], E. Brost[27], P.A. Bruckman de Renstrom[82], B. Brüers[44], D. Bruncko[26b], A. Bruni[21b], G. Bruni[21b], M. Bruschi[21b], N. Bruscino[70a,70b], L. Bryngemark[149], T. Buanes[15], Q. Buat[151], P. Buchholz[147], A.G. Buckley[55], I.A. Budagov[77], M.K. Bugge[129], O. Bulekov[108], B.A. Bullard[57], S. Burdin[88], C.D. Burgard[44], A.M. Burger[125], B. Burghgrave[7], J.T.P. Burr[44], C.D. Burton[10], J.C. Burzynski[148], E.L. Busch[37], V. Büscher[96], P.J. Bussey[55], J.M. Butler[23], C.M. Buttar[55], J.M. Butterworth[92], W. Buttinger[139], C.J. Buxo Vazquez[103], A.R. Buzykaev[117b,117a], G. Cabras[21b], S. Cabrera Urbán[169], D. Caforio[54], H. Cai[134], V.M.M. Cairo[149], O. Cakir[3a], N. Calace[34], P. Calafiura[16], G. Calderini[131], P. Calfayan[63], G. Callea[55], L.P. Caloba[78b], D. Calvet[36], S. Calvet[36], T.P. Calvet[98], M. Calvetti[69a,69b], R. Camacho Toro[131], S. Camarda[34], D. Camarero Munoz[95], P. Camarri[71a,71b], M.T. Camerlingo[72a,72b], D. Cameron[129], C. Camincher[171], M. Campanelli[92], A. Camplani[38], V. Canale[67a,67b], A. Canesse[100], M. Cano Bret[75], J. Cantero[125], Y. Cao[168], F. Capocasa[24], M. Capua[39b,39a], A. Carbone[66a,66b], R. Cardarelli[71a], J.C.J. Cardenas[7], F. Cardillo[169], G. Carducci[39b,39a], T. Carli[34], G. Carlino[67a], B.T. Carlson[134], E.M. Carlson[171,163a], L. Carminati[66a,66b], M. Carnesale[70a,70b], R.M.D. Carney[149], S. Caron[114], E. Carquin[142e], S. Carrá[44], G. Carratta[21b,21a], J.W.S. Carter[162], T.M. Carter[48], D. Casadei[31c], M.P. Casado[12,g], A.F. Casha[162], E.G. Castiglia[178], F.L. Castillo[59a], L. Castillo Garcia[12], V. Castillo Gimenez[169], N.F. Castro[135a,135e], A. Catinaccio[34], J.R. Catmore[129], A. Cattai[34], V. Cavaliere[27], N. Cavalli[21b,21a], V. Cavasinni[69a,69b], E. Celebi[11b], F. Celli[130], M.S. Centonze[65a,65b], K. Cerny[126], A.S. Cerqueira[78a], A. Cerri[152], L. Cerrito[71a,71b], F. Cerutti[16], A. Cervelli[21b], S.A. Cetin[11b], Z. Chadi[33a], D. Chakraborty[116], M. Chala[135f], J. Chan[176], W.S. Chan[115], W.Y. Chan[88], J.D. Chapman[30], B. Chargeishvili[155b], D.G. Charlton[19], T.P. Charman[90], M. Chatterjee[18], S. Chekanov[5], S.V. Chekulaev[163a], G.A. Chelkov[77,ae], A. Chen[102], B. Chen[157], B. Chen[171], C. Chen[58a], C.H. Chen[76], H. Chen[13c], H. Chen[27], J. Chen[58c], J. Chen[24], S. Chen[132], S.J. Chen[13c], X. Chen[58c], X. Chen[13b], Y. Chen[58a], Y-H. Chen[44], C.L. Cheng[176], H.C. Cheng[60a], A. Cheplakov[77], E. Cheremushkina[44], E. Cherepanova[77], R. Cherkaoui El Moursli[33e], E. Cheu[6], K. Cheung[61], L. Chevalier[140], V. Chiarella[49], G. Chiarelli[69a], G. Chiodini[65a], A.S. Chisholm[19], A. Chitan[25b], Y.H. Chiu[171], M.V. Chizhov[77,s], K. Choi[10], A.R. Chomont[70a,70b], Y. Chou[99], Y.S. Chow[115], T. Chowdhury[31f], L.D. Christopher[31f], M.C. Chu[60a], X. Chu[13a,13d], J. Chudoba[136], J.J. Chwastowski[82], D. Cieri[111], K.M. Ciesla[82], V. Cindro[89], I.A. Cioară[25b], A. Ciocio[16], F. Cirotto[67a,67b], Z.H. Citron[175,k], M. Citterio[66a], D.A. Ciubotaru[25b], B.M. Ciungu[162], A. Clark[52], P.J. Clark[48], J.M. Clavijo Columbie[44], S.E. Clawson[97], C. Clement[43a,43b], L. Clissa[21b,21a], Y. Coadou[98], M. Cobal[64a,64c], A. Coccaro[53b], J. Cochran[76], R.F. Coelho Barrue[135a], R. Coelho Lopes De Sa[99], S. Coelli[66a], H. Cohen[157], A.E.C. Coimbra[34], B. Cole[37], J. Collot[56], P. Conde Muiño[135a,135g], S.H. Connell[31c],

JHEP03(2022)041

I.A. Connelly[55], E.I. Conroy[130], F. Conventi[67a,ak], H.G. Cooke[19], A.M. Cooper-Sarkar[130], F. Cormier[170], L.D. Corpe[34], M. Corradi[70a,70b], E.E. Corrigan[94], F. Corriveau[100,y], M.J. Costa[169], F. Costanza[4], D. Costanzo[145], B.M. Cote[123], G. Cowan[91], J.W. Cowley[30], K. Cranmer[121], S. Crépé-Renaudin[56], F. Crescioli[131], M. Cristinziani[147], M. Cristoforetti[73a,73b,b], V. Croft[165], G. Crosetti[39b,39a], A. Cueto[34], T. Cuhadar Donszelmann[166], H. Cui[13a,13d], A.R. Cukierman[149], W.R. Cunningham[55], F. Curcio[39b,39a], P. Czodrowski[34], M.M. Czurylo[59b], M.J. Da Cunha Sargedas De Sousa[58a], J.V. Da Fonseca Pinto[78b], C. Da Via[97], W. Dabrowski[81a], T. Dado[45], S. Dahbi[31f], T. Dai[102], C. Dallapiccola[99], M. Dam[38], G. D'amen[27], V. D'Amico[72a,72b], J. Damp[96], J.R. Dandoy[132], M.F. Daneri[28], M. Danninger[148], V. Dao[34], G. Darbo[53b], S. Darmora[5], A. Dattagupta[127], S. D'Auria[66a,66b], C. David[163b], T. Davidek[138], D.R. Davis[47], B. Davis-Purcell[32], I. Dawson[90], K. De[7], R. De Asmundis[67a], M. De Beurs[115], S. De Castro[21b,21a], N. De Groot[114], P. de Jong[115], H. De la Torre[103], A. De Maria[13c], D. De Pedis[70a], A. De Salvo[70a], U. De Sanctis[71a,71b], M. De Santis[71a,71b], A. De Santo[152], J.B. De Vivie De Regie[56], D.V. Dedovich[77], J. Degens[115], A.M. Deiana[40], J. Del Peso[95], Y. Delabat Diaz[44], F. Deliot[140], C.M. Delitzsch[6], M. Della Pietra[67a,67b], D. Della Volpe[52], A. Dell'Acqua[34], L. Dell'Asta[66a,66b], M. Delmastro[4], P.A. Delsart[56], S. Demers[178], M. Demichev[77], S.P. Denisov[118], L. D'Eramo[116], D. Derendarz[82], J.E. Derkaoui[33d], F. Derue[131], P. Dervan[88], K. Desch[22], K. Dette[162], C. Deutsch[22], P.O. Deviveiros[34], F.A. Di Bello[70a,70b], A. Di Ciaccio[71a,71b], L. Di Ciaccio[4], A. Di Domenico[70a,70b], C. Di Donato[67a,67b], A. Di Girolamo[34], G. Di Gregorio[69a,69b], A. Di Luca[73a,73b], B. Di Micco[72a,72b], R. Di Nardo[72a,72b], C. Diaconu[98], F.A. Dias[115], T. Dias Do Vale[135a], M.A. Diaz[142a], F.G. Diaz Capriles[22], J. Dickinson[16], M. Didenko[169], E.B. Diehl[102], J. Dietrich[17], S. Díez Cornell[44], C. Diez Pardos[147], A. Dimitrievska[16], W. Ding[13b], J. Dingfelder[22], I-M. Dinu[25b], S.J. Dittmeier[59b], F. Dittus[34], F. Djama[98], T. Djobava[155b], J.I. Djuvsland[15], M.A.B. Do Vale[143], D. Dodsworth[24], C. Doglioni[94], J. Dolejsi[138], Z. Dolezal[138], M. Donadelli[78c], B. Dong[58c], J. Donini[36], A. D'onofrio[13c], M. D'Onofrio[88], J. Dopke[139], A. Doria[67a], M.T. Dova[86], A.T. Doyle[55], E. Drechsler[148], E. Dreyer[148], T. Dreyer[51], A.S. Drobac[165], D. Du[58a], T.A. du Pree[115], F. Dubinin[107], M. Dubovsky[26a], A. Dubreuil[52], E. Duchovni[175], G. Duckeck[110], O.A. Ducu[34,25b], D. Duda[111], A. Dudarev[34], M. D'uffizi[97], L. Duflot[62], M. Dührssen[34], C. Dülsen[177], A.E. Dumitriu[25b], M. Dunford[59a], S. Dungs[45], K. Dunne[43a,43b], A. Duperrin[98], H. Duran Yildiz[3a], M. Düren[54], A. Durglishvili[155b], B. Dutta[44], B.L. Dwyer[116], G.I. Dyckes[16], M. Dyndal[81a], S. Dysch[97], B.S. Dziedzic[82], B. Eckerova[26a], M.G. Eggleston[47], E. Egidio Purcino De Souza[78b], L.F. Ehrke[52], T. Eifert[7], G. Eigen[15], K. Einsweiler[16], T. Ekelof[167], Y. El Ghazali[33b], H. El Jarrari[33e], A. El Moussaouy[33a], V. Ellajosyula[167], M. Ellert[167], F. Ellinghaus[177], A.A. Elliot[90], N. Ellis[34], J. Elmsheuser[27], M. Elsing[34], D. Emeliyanov[139], A. Emerman[37], Y. Enari[159], J. Erdmann[45], A. Ereditato[18], P.A. Erland[82], M. Errenst[177], M. Escalier[62], C. Escobar[169], O. Estrada Pastor[169], E. Etzion[157], G. Evans[135a], H. Evans[63], M.O. Evans[152], A. Ezhilov[133], F. Fabbri[55], L. Fabbri[21b,21a], G. Facini[173], V. Fadeyev[141], R.M. Fakhrutdinov[118], S. Falciano[70a], P.J. Falke[22], S. Falke[34], J. Faltova[138], Y. Fan[13a], Y. Fang[13a], G. Fanourakis[42], M. Fanti[66a,66b], M. Faraj[58c], A. Farbin[7], A. Farilla[72a], E.M. Farina[68a,68b], T. Farooque[103], S.M. Farrington[48], P. Farthouat[34], F. Fassi[33e], D. Fassouliotis[8], M. Faucci Giannelli[71a,71b], W.J. Fawcett[30], L. Fayard[62], O.L. Fedin[133,p], M. Feickert[168], L. Feligioni[98], A. Fell[145], C. Feng[58b], M. Feng[13b], M.J. Fenton[166], A.B. Fenyuk[118], S.W. Ferguson[41], J. Ferrando[44], A. Ferrari[167], P. Ferrari[115], R. Ferrari[68a], D. Ferrere[52], C. Ferretti[102], F. Fiedler[96], A. Filipčič[89], F. Filthaut[114], M.C.N. Fiolhais[135a,135c,a], L. Fiorini[169], F. Fischer[147], W.C. Fisher[103], T. Fitschen[19], I. Fleck[147], P. Fleischmann[102], T. Flick[177], B.M. Flierl[110], L. Flores[132], M. Flores[31d], L.R. Flores Castillo[60a], F.M. Follega[73a,73b], N. Fomin[15], J.H. Foo[162], B.C. Forland[63], A. Formica[140], F.A. Förster[12], A.C. Forti[97], E. Fortin[98], M.G. Foti[130], L. Fountas[8], D. Fournier[62], H. Fox[87], P. Francavilla[69a,69b], S. Francescato[57], M. Franchini[21b,21a],

JHEP03(2022)041

S. Franchino[59a], D. Francis[34], L. Franco[4], L. Franconi[18], M. Franklin[57], G. Frattari[70a,70b], A.C. Freegard[90], P.M. Freeman[19], W.S. Freund[78b], E.M. Freundlich[45], D. Froidevaux[34], J.A. Frost[130], Y. Fu[58a], M. Fujimoto[122], E. Fullana Torregrosa[169], J. Fuster[169], A. Gabrielli[21b,21a], A. Gabrielli[34], P. Gadow[44], G. Gagliardi[53b,53a], L.G. Gagnon[16], G.E. Gallardo[130], E.J. Gallas[130], B.J. Gallop[139], R. Gamboa Goni[90], K.K. Gan[123], S. Ganguly[159], J. Gao[58a], Y. Gao[48], Y.S. Gao[29,m], F.M. Garay Walls[142a], C. García[169], J.E. García Navarro[169], J.A. García Pascual[13a], M. Garcia-Sciveres[16], R.W. Gardner[35], D. Garg[75], R.B. Garg[149], S. Gargiulo[50], C.A. Garner[162], V. Garonne[129], S.J. Gasiorowski[144], P. Gaspar[78b], G. Gaudio[68a], P. Gauzzi[70a,70b], I.L. Gavrilenko[107], A. Gavrilyuk[119], C. Gay[170], G. Gaycken[44], E.N. Gazis[9], A.A. Geanta[25b], C.M. Gee[141], C.N.P. Gee[139], J. Geisen[94], M. Geisen[96], C. Gemme[53b], M.H. Genest[56], S. Gentile[70a,70b], S. George[91], W.F. George[19], T. Geralis[42], L.O. Gerlach[51], P. Gessinger-Befurt[34], M. Ghasemi Bostanabad[171], A. Ghosh[166], A. Ghosh[75], B. Giacobbe[21b], S. Giagu[70a,70b], N. Giangiacomi[162], P. Giannetti[69a], A. Giannini[67a,67b], S.M. Gibson[91], M. Gignac[141], D.T. Gil[81b], B.J. Gilbert[37], D. Gillberg[32], G. Gilles[115], N.E.K. Gillwald[44], D.M. Gingrich[2,aj], M.P. Giordani[64a,64c], P.F. Giraud[140], G. Giugliarelli[64a,64c], D. Giugni[66a], F. Giuli[71a,71b], I. Gkialas[8,h], P. Gkountoumis[9], L.K. Gladilin[109], C. Glasman[95], G.R. Gledhill[127], M. Glisic[127], I. Gnesi[39b,d], M. Goblirsch-Kolb[24], D. Godin[106], S. Goldfarb[101], T. Golling[52], D. Golubkov[118], J.P. Gombas[103], A. Gomes[135a,135b], R. Goncalves Gama[51], R. Gonçalo[135a,135c], G. Gonella[127], L. Gonella[19], A. Gongadze[77], F. Gonnella[19], J.L. Gonski[37], S. González de la Hoz[169], S. Gonzalez Fernandez[12], R. Gonzalez Lopez[88], C. Gonzalez Renteria[16], R. Gonzalez Suarez[167], S. Gonzalez-Sevilla[52], G.R. Gonzalvo Rodriguez[169], R.Y. González Andana[142a], L. Goossens[34], N.A. Gorasia[19], P.A. Gorbounov[119], H.A. Gordon[27], B. Gorini[34], E. Gorini[65a,65b], A. Gorišek[89], A.T. Goshaw[47], M.I. Gostkin[77], C.A. Gottardo[114], M. Gouighri[33b], V. Goumarre[44], A.G. Goussiou[144], N. Govender[31c], C. Goy[4], I. Grabowska-Bold[81a], K. Graham[32], E. Gramstad[129], S. Grancagnolo[17], M. Grandi[152], V. Gratchev[133], P.M. Gravila[25f], F.G. Gravili[65a,65b], H.M. Gray[16], C. Grefe[22], I.M. Gregor[44], P. Grenier[149], K. Grevtsov[44], C. Grieco[12], N.A. Grieser[124], A.A. Grillo[141], K. Grimm[29,l], S. Grinstein[12,v], J.-F. Grivaz[62], S. Groh[96], E. Gross[175], J. Grosse-Knetter[51], C. Grud[102], A. Grummer[113], J.C. Grundy[130], L. Guan[102], W. Guan[176], C. Gubbels[170], J. Guenther[34], J.G.R. Guerrero Rojas[169], F. Guescini[111], D. Guest[17], R. Gugel[96], A. Guida[44], T. Guillemin[4], S. Guindon[34], J. Guo[58c], L. Guo[62], Y. Guo[102], R. Gupta[44], S. Gurbuz[22], G. Gustavino[124], M. Guth[52], P. Gutierrez[124], L.F. Gutierrez Zagazeta[132], C. Gutschow[92], C. Guyot[140], C. Gwenlan[130], C.B. Gwilliam[88], E.S. Haaland[129], A. Haas[121], M. Habedank[44], C. Haber[16], H.K. Hadavand[7], A. Hadef[96], S. Hadzic[111], M. Haleem[172], J. Haley[125], J.J. Hall[145], G. Halladjian[103], G.D. Hallewell[98], L. Halser[18], K. Hamano[171], H. Hamdaoui[33e], M. Hamer[22], G.N. Hamity[48], K. Han[58a], L. Han[13c], L. Han[58a], S. Han[16], Y.F. Han[162], K. Hanagaki[79,t], M. Hance[141], M.D. Hank[35], R. Hankache[97], E. Hansen[94], J.B. Hansen[38], J.D. Hansen[38], M.C. Hansen[22], P.H. Hansen[38], K. Hara[164], T. Harenberg[177], S. Harkusha[104], Y.T. Harris[130], P.F. Harrison[173], N.M. Hartman[149], N.M. Hartmann[110], Y. Hasegawa[146], A. Hasib[48], S. Hassani[140], S. Haug[18], R. Hauser[103], M. Havranek[137], C.M. Hawkes[19], R.J. Hawkings[34], S. Hayashida[112], D. Hayden[103], C. Hayes[102], R.L. Hayes[170], C.P. Hays[130], J.M. Hays[90], H.S. Hayward[88], S.J. Haywood[139], F. He[58a], Y. He[160], Y. He[131], M.P. Heath[48], V. Hedberg[94], A.L. Heggelund[129], N.D. Hehir[90], C. Heidegger[50], K.K. Heidegger[50], W.D. Heidorn[76], J. Heilman[32], S. Heim[44], T. Heim[16], B. Heinemann[44,ah], J.G. Heinlein[132], J.J. Heinrich[127], L. Heinrich[34], J. Hejbal[136], L. Helary[44], A. Held[121], C.M. Helling[141], S. Hellman[43a,43b], C. Helsens[34], R.C.W. Henderson[87], L. Henkelmann[30], A.M. Henriques Correia[34], H. Herde[149], Y. Hernández Jiménez[151], H. Herr[96], M.G. Herrmann[110], T. Herrmann[46], G. Herten[50], R. Hertenberger[110], L. Hervas[34], N.P. Hessey[163a], H. Hibi[80], S. Higashino[79], E. Higón-Rodriguez[169], K.H. Hiller[44], S.J. Hillier[19], M. Hils[46], I. Hinchliffe[16], F. Hinterkeuser[22],

JHEP03(2022)041

M. Hirose[128], S. Hirose[164], D. Hirschbuehl[177], B. Hiti[89], O. Hladik[136], J. Hobbs[151], R. Hobincu[25e], N. Hod[175], M.C. Hodgkinson[145], B.H. Hodkinson[30], A. Hoecker[34], J. Hofer[44], D. Hohn[50], T. Holm[22], T.R. Holmes[35], M. Holzbock[111], L.B.A.H. Hommels[30], B.P. Honan[97], J. Hong[58c], T.M. Hong[134], Y. Hong[51], J.C. Honig[50], A. Hönle[111], B.H. Hooberman[168], W.H. Hopkins[5], Y. Horii[112], L.A. Horyn[35], S. Hou[154], J. Howarth[55], J. Hoya[86], M. Hrabovsky[126], A. Hrynevich[105], T. Hryn'ova[4], P.J. Hsu[61], S.-C. Hsu[144], Q. Hu[37], S. Hu[58c], Y.F. Hu[13a,13d,al], D.P. Huang[92], X. Huang[13c], Y. Huang[58a], Y. Huang[13a], Z. Hubacek[137], F. Hubaut[98], M. Huebner[22], F. Huegging[22], T.B. Huffman[130], M. Huhtinen[34], S.K. Huiberts[15], R. Hulsken[56], N. Huseynov[77,z], J. Huston[103], J. Huth[57], R. Hyneman[149], S. Hyrych[26a], G. Iacobucci[52], G. Iakovidis[27], I. Ibragimov[147], L. Iconomidou-Fayard[62], P. Iengo[34], R. Iguchi[159], T. Iizawa[52], Y. Ikegami[79], A. Ilg[18], N. Ilic[162], H. Imam[33a], T. Ingebretsen Carlson[43a,43b], G. Introzzi[68a,68b], M. Iodice[72a], V. Ippolito[70a,70b], M. Ishino[159], W. Islam[176], C. Issever[17,44], S. Istin[11c,am], J.M. Iturbe Ponce[60a], R. Iuppa[73a,73b], A. Ivina[175], J.M. Izen[41], V. Izzo[67a], P. Jacka[136], P. Jackson[1], R.M. Jacobs[44], B.P. Jaeger[148], C.S. Jagfeld[110], G. Jäkel[177], K. Jakobs[50], T. Jakoubek[175], J. Jamieson[55], K.W. Janas[81a], G. Jarlskog[94], A.E. Jaspan[88], N. Javadov[77,z], T. Javůrek[34], M. Javurkova[99], F. Jeanneau[140], L. Jeanty[127], J. Jejelava[155a,aa], P. Jenni[50,e], S. Jézéquel[4], J. Jia[151], Z. Jia[13c], Y. Jiang[58a], S. Jiggins[48], J. Jimenez Pena[111], S. Jin[13c], A. Jinaru[25b], O. Jinnouchi[160], H. Jivan[31f], P. Johansson[145], K.A. Johns[6], C.A. Johnson[63], D.M. Jones[30], E. Jones[173], R.W.L. Jones[87], T.J. Jones[88], J. Jovicevic[14], X. Ju[16], J.J. Junggeburth[34], A. Juste Rozas[12,v], S. Kabana[142d], A. Kaczmarska[82], M. Kado[70a,70b], H. Kagan[123], M. Kagan[149], A. Kahn[37], A. Kahn[132], C. Kahra[96], T. Kaji[174], E. Kajomovitz[156], C.W. Kalderon[27], A. Kamenshchikov[118], M. Kaneda[159], N.J. Kang[141], S. Kang[76], Y. Kano[112], D. Kar[31f], K. Karava[130], M.J. Kareem[163b], I. Karkanias[158], S.N. Karpov[77], Z.M. Karpova[77], V. Kartvelishvili[87], A.N. Karyukhin[118], E. Kasimi[158], C. Kato[58d], J. Katzy[44], K. Kawade[146], K. Kawagoe[85], T. Kawaguchi[112], T. Kawamoto[140], G. Kawamura[51], E.F. Kay[171], F.I. Kaya[165], S. Kazakos[12], V.F. Kazanin[117b,117a], Y. Ke[151], J.M. Keaveney[31a], R. Keeler[171], J.S. Keller[32], D. Kelsey[152], J.J. Kempster[19], J. Kendrick[19], K.E. Kennedy[37], O. Kepka[136], S. Kersten[177], B.P. Kerševan[89], S. Ketabchi Haghighat[162], M. Khandoga[131], A. Khanov[125], A.G. Kharlamov[117b,117a], T. Kharlamova[117b,117a], E.E. Khoda[144], T.J. Khoo[17], G. Khoriauli[172], E. Khramov[77], J. Khubua[155b], S. Kido[80], M. Kiehn[34], A. Kilgallon[127], E. Kim[160], Y.K. Kim[35], N. Kimura[92], A. Kirchhoff[51], D. Kirchmeier[46], C. Kirfel[22], J. Kirk[139], A.E. Kiryunin[111], T. Kishimoto[159], D.P. Kisliuk[162], C. Kitsaki[9], O. Kivernyk[22], T. Klapdor-Kleingrothaus[50], M. Klassen[59a], C. Klein[32], L. Klein[172], M.H. Klein[102], M. Klein[88], U. Klein[88], P. Klimek[34], A. Klimentov[27], F. Klimpel[111], T. Klingl[22], T. Klioutchnikova[34], F.F. Klitzner[110], P. Kluit[115], S. Kluth[111], E. Kneringer[74], T.M. Knight[162], A. Knue[50], D. Kobayashi[85], R. Kobayashi[83], M. Kobel[46], M. Kocian[149], T. Kodama[159], P. Kodys[138], D.M. Koeck[152], P.T. Koenig[22], T. Koffas[32], N.M. Köhler[34], M. Kolb[140], I. Koletsou[4], T. Komarek[126], K. Köneke[50], A.X.Y. Kong[1], T. Kono[122], V. Konstantinides[92], N. Konstantinidis[92], B. Konya[94], R. Kopeliansky[63], S. Koperny[81a], K. Korcyl[82], K. Kordas[158], G. Koren[157], A. Korn[92], S. Korn[51], I. Korolkov[12], E.V. Korolkova[145], N. Korotkova[109], B. Kortman[115], O. Kortner[111], S. Kortner[111], W.H. Kostecka[116], V.V. Kostyukhin[147,161], A. Kotsokechagia[62], A. Kotwal[47], A. Koulouris[34], A. Kourkoumeli-Charalampidi[68a,68b], C. Kourkoumelis[8], E. Kourlitis[5], O. Kovanda[152], R. Kowalewski[171], W. Kozanecki[140], A.S. Kozhin[118], V.A. Kramarenko[109], G. Kramberger[89], P. Kramer[96], D. Krasnopevtsev[58a], M.W. Krasny[131], A. Krasznahorkay[34], J.A. Kremer[96], J. Kretzschmar[88], K. Kreul[17], P. Krieger[162], F. Krieter[110], S. Krishnamurthy[99], A. Krishnan[59b], M. Krivos[138], K. Krizka[16], K. Kroeninger[45], H. Kroha[111], J. Kroll[136], J. Kroll[132], K.S. Krowpman[103], U. Kruchonak[77], H. Krüger[22], N. Krumnack[76], M.C. Kruse[47], J.A. Krzysiak[82], A. Kubota[160], O. Kuchinskaia[161], S. Kuday[3a], D. Kuechler[44], J.T. Kuechler[44], S. Kuehn[34], T. Kuhl[44], V. Kukhtin[77], Y. Kulchitsky[104,ad], S. Kuleshov[142c], M. Kumar[31f], N. Kumari[98],

JHEP03(2022)041

M. Kuna[56], A. Kupco[136], T. Kupfer[45], O. Kuprash[50], H. Kurashige[80], L.L. Kurchaninov[163a], Y.A. Kurochkin[104], A. Kurova[108], M.G. Kurth[13a,13d], E.S. Kuwertz[34], M. Kuze[160], A.K. Kvam[144], J. Kvita[126], T. Kwan[100], K.W. Kwok[60a], C. Lacasta[169], F. Lacava[70a,70b], H. Lacker[17], D. Lacour[131], N.N. Lad[92], E. Ladygin[77], R. Lafaye[4], B. Laforge[131], T. Lagouri[142d], S. Lai[51], I.K. Lakomiec[81a], N. Lalloue[56], J.E. Lambert[124], S. Lammers[63], W. Lampl[6], C. Lampoudis[158], E. Lançon[27], U. Landgraf[50], M.P.J. Landon[90], V.S. Lang[50], J.C. Lange[51], R.J. Langenberg[99], A.J. Lankford[166], F. Lanni[27], K. Lantzsch[22], A. Lanza[68a], A. Lapertosa[53b,53a], J.F. Laporte[140], T. Lari[66a], F. Lasagni Manghi[21b], M. Lassnig[34], V. Latonova[136], T.S. Lau[60a], A. Laudrain[96], A. Laurier[32], M. Lavorgna[67a,67b], S.D. Lawlor[91], Z. Lawrence[97], M. Lazzaroni[66a,66b], B. Le[97], B. Leban[89], A. Lebedev[76], M. LeBlanc[34], T. LeCompte[5], F. Ledroit-Guillon[56], A.C.A. Lee[92], G.R. Lee[15], L. Lee[57], S.C. Lee[154], S. Lee[76], L.L. Leeuw[31c], B. Lefebvre[163a], H.P. Lefebvre[91], M. Lefebvre[171], C. Leggett[16], K. Lehmann[148], N. Lehmann[18], G. Lehmann Miotto[34], W.A. Leight[44], A. Leisos[158,u], M.A.L. Leite[78c], C.E. Leitgeb[44], R. Leitner[138], K.J.C. Leney[40], T. Lenz[22], S. Leone[69a], C. Leonidopoulos[48], A. Leopold[150], C. Leroy[106], R. Les[103], C.G. Lester[30], M. Levchenko[133], J. Levêque[4], D. Levin[102], L.J. Levinson[175], D.J. Lewis[19], B. Li[13b], B. Li[58b], C. Li[58a], C-Q. Li[58c,58d], H. Li[58a], H. Li[58b], H. Li[58b], J. Li[58c], K. Li[144], L. Li[58c], M. Li[13a,13d], Q.Y. Li[58a], S. Li[58d,58c,c], T. Li[58b], X. Li[44], Y. Li[44], Z. Li[58b], Z. Li[130], Z. Li[100], Z. Li[88], Z. Liang[13a], M. Liberatore[44], B. Liberti[71a], K. Lie[60c], J. Lieber Marin[78b], K. Lin[103], R.A. Linck[63], R.E. Lindley[6], J.H. Lindon[2], A. Linss[44], E. Lipeles[132], A. Lipniacka[15], T.M. Liss[168,ai], A. Lister[170], J.D. Little[7], B. Liu[13a], B.X. Liu[148], J.B. Liu[58a], J.K.K. Liu[35], K. Liu[58d,58c], M. Liu[58a], M.Y. Liu[58a], P. Liu[13a], X. Liu[58a], Y. Liu[44], Y. Liu[13c,13d], Y.L. Liu[102], Y.W. Liu[58a], M. Livan[68a,68b], J. Llorente Merino[148], S.L. Lloyd[90], E.M. Lobodzinska[44], P. Loch[6], S. Loffredo[71a,71b], T. Lohse[17], K. Lohwasser[145], M. Lokajicek[136], J.D. Long[168], I. Longarini[70a,70b], L. Longo[34], R. Longo[168], I. Lopez Paz[12], A. Lopez Solis[44], J. Lorenz[110], N. Lorenzo Martinez[4], A.M. Lory[110], A. Lösle[50], X. Lou[43a,43b], X. Lou[13a], A. Lounis[62], J. Love[5], P.A. Love[87], J.J. Lozano Bahilo[169], G. Lu[13a], M. Lu[58a], S. Lu[132], Y.J. Lu[61], H.J. Lubatti[144], C. Luci[70a,70b], F.L. Lucio Alves[13c], A. Lucotte[56], F. Luehring[63], I. Luise[151], L. Luminari[70a], O. Lundberg[150], B. Lund-Jensen[150], N.A. Luongo[127], M.S. Lutz[157], D. Lynn[27], H. Lyons[88], R. Lysak[136], E. Lytken[94], F. Lyu[13a], V. Lyubushkin[77], T. Lyubushkina[77], H. Ma[27], L.L. Ma[58b], Y. Ma[92], D.M. Mac Donell[171], G. Maccarrone[49], C.M. Macdonald[145], J.C. MacDonald[145], R. Madar[36], W.F. Mader[46], M. Madugoda Ralalage Don[125], N. Madysa[46], J. Maeda[80], T. Maeno[27], M. Maerker[46], V. Magerl[50], J. Magro[64a,64c], D.J. Mahon[37], C. Maidantchik[78b], A. Maio[135a,135b,135d], K. Maj[81a], O. Majersky[26a], S. Majewski[127], N. Makovec[62], V. Maksimovic[14], B. Malaescu[131], Pa. Malecki[82], V.P. Maleev[133], F. Malek[56], D. Malito[39b,39a], U. Mallik[75], C. Malone[30], S. Maltezos[9], S. Malyukov[77], J. Mamuzic[169], G. Mancini[49], J.P. Mandalia[90], I. Mandić[89], L. Manhaes de Andrade Filho[78a], I.M. Maniatis[158], M. Manisha[140], J. Manjarres Ramos[46], K.H. Mankinen[94], A. Mann[110], A. Manousos[74], B. Mansoulie[140], I. Manthos[158], S. Manzoni[115], X. Mapekula[31c], A. Marantis[158,u], G. Marchiori[131], M. Marcisovsky[136], L. Marcoccia[71a,71b], C. Marcon[94], M. Marjanovic[124], Z. Marshall[16], S. Marti-Garcia[169], T.A. Martin[173], V.J. Martin[48], B. Martin dit Latour[15], L. Martinelli[70a,70b], M. Martinez[12,v], P. Martinez Agullo[169], V.I. Martinez Outschoorn[99], S. Martin-Haugh[139], V.S. Martoiu[25b], A.C. Martyniuk[92], A. Marzin[34], S.R. Maschek[111], L. Masetti[96], T. Mashimo[159], J. Masik[97], A.L. Maslennikov[117b,117a], L. Massa[21b], P. Massarotti[67a,67b], P. Mastrandrea[69a,69b], A. Mastroberardino[39b,39a], T. Masubuchi[159], D. Matakias[27], T. Mathisen[167], A. Matic[110], N. Matsuzawa[159], J. Maurer[25b], B. Maček[89], D.A. Maximov[117b,117a], R. Mazini[154], I. Maznas[158], S.M. Mazza[141], C. Mc Ginn[27], J.P. Mc Gowan[100], S.P. Mc Kee[102], T.G. McCarthy[111], W.P. McCormack[16], E.F. McDonald[101], A.E. McDougall[115], J.A. Mcfayden[152], G. Mchedlidze[155b], M.A. McKay[40], K.D. McLean[171], S.J. McMahon[139], P.C. McNamara[101], R.A. McPherson[171,y],

JHEP03(2022)041

J.E. Mdhluli[31f], Z.A. Meadows[99], S. Meehan[34], T. Megy[36], S. Mehlhase[110], A. Mehta[88], B. Meirose[41], D. Melini[156], B.R. Mellado Garcia[31f], A.H. Melo[51], F. Meloni[44], A. Melzer[22], E.D. Mendes Gouveia[135a], A.M. Mendes Jacques Da Costa[19], H.Y. Meng[162], L. Meng[34], S. Menke[111], M. Mentink[34], E. Meoni[39b,39a], C. Merlassino[130], P. Mermod[52,*], L. Merola[67a,67b], C. Meroni[66a], G. Merz[102], O. Meshkov[107,109], J.K.R. Meshreki[147], J. Metcalfe[5], A.S. Mete[5], C. Meyer[63], J-P. Meyer[140], M. Michetti[17], R.P. Middleton[139], L. Mijović[48], G. Mikenberg[175], M. Mikestikova[136], M. Mikuž[89], H. Mildner[145], A. Milic[162], C.D. Milke[40], D.W. Miller[35], L.S. Miller[32], A. Milov[175], D.A. Milstead[43a,43b], T. Min[13c], A.A. Minaenko[118], I.A. Minashvili[155b], L. Mince[55], A.I. Mincer[121], B. Mindur[81a], M. Mineev[77], Y. Minegishi[159], Y. Mino[83], L.M. Mir[12], M. Miralles Lopez[169], M. Mironova[130], T. Mitani[174], V.A. Mitsou[169], M. Mittal[58c], O. Miu[162], P.S. Miyagawa[90], Y. Miyazaki[85], A. Mizukami[79], J.U. Mjörnmark[94], T. Mkrtchyan[59a], M. Mlynarikova[116], T. Moa[43a,43b], S. Mobius[51], K. Mochizuki[106], P. Moder[44], P. Mogg[110], A.F. Mohammed[13a], S. Mohapatra[37], G. Mokgatitswane[31f], B. Mondal[147], S. Mondal[137], K. Mönig[44], E. Monnier[98], L. Monsonis Romero[169], A. Montalbano[148], J. Montejo Berlingen[34], M. Montella[123], F. Monticelli[86], N. Morange[62], A.L. Moreira De Carvalho[135a], M. Moreno Llácer[169], C. Moreno Martinez[12], P. Morettini[53b], S. Morgenstern[173], D. Mori[148], M. Morii[57], M. Morinaga[159], V. Morisbak[129], A.K. Morley[34], A.P. Morris[92], L. Morvaj[34], P. Moschovakos[34], B. Moser[115], M. Mosidze[155b], T. Moskalets[50], P. Moskvitina[114], J. Moss[29,n], E.J.W. Moyse[99], S. Muanza[98], J. Mueller[134], R. Mueller[18], D. Muenstermann[87], G.A. Mullier[94], J.J. Mullin[132], D.P. Mungo[66a,66b], J.L. Munoz Martinez[12], F.J. Munoz Sanchez[97], M. Murin[97], P. Murin[26b], W.J. Murray[173,139], A. Murrone[66a,66b], J.M. Muse[124], M. Muškinja[16], C. Mwewa[27], A.G. Myagkov[118,ae], A.J. Myers[7], A.A. Myers[134], G. Myers[63], M. Myska[137], B.P. Nachman[16], O. Nackenhorst[45], A.Nag Nag[46], K. Nagai[130], K. Nagano[79], J.L. Nagle[27], E. Nagy[98], A.M. Nairz[34], Y. Nakahama[112], K. Nakamura[79], H. Nanjo[128], F. Napolitano[59a], R. Narayan[40], E.A. Narayanan[113], I. Naryshkin[133], M. Naseri[32], C. Nass[22], T. Naumann[44], G. Navarro[20a], J. Navarro-Gonzalez[169], R. Nayak[157], P.Y. Nechaeva[107], F. Nechansky[44], T.J. Neep[19], A. Negri[68a,68b], M. Negrini[21b], C. Nellist[114], C. Nelson[100], K. Nelson[102], S. Nemecek[136], M. Nessi[34,f], M.S. Neubauer[168], F. Neuhaus[96], J. Neundorf[44], R. Newhouse[170], P.R. Newman[19], C.W. Ng[134], Y.S. Ng[17], Y.W.Y. Ng[166], B. Ngair[33e], H.D.N. Nguyen[106], R.B. Nickerson[130], R. Nicolaidou[140], D.S. Nielsen[38], J. Nielsen[141], M. Niemeyer[51], N. Nikiforou[10], V. Nikolaenko[118,ae], I. Nikolic-Audit[131], K. Nikolopoulos[19], P. Nilsson[27], H.R. Nindhito[52], A. Nisati[70a], N. Nishu[2], R. Nisius[111], T. Nitta[174], T. Nobe[159], D.L. Noel[30], Y. Noguchi[83], I. Nomidis[131], M.A. Nomura[27], M.B. Norfolk[145], R.R.B. Norisam[92], J. Novak[89], T. Novak[44], O. Novgorodova[46], L. Novotny[137], R. Novotny[113], L. Nozka[126], K. Ntekas[166], E. Nurse[92], F.G. Oakham[32,aj], J. Ocariz[131], A. Ochi[80], I. Ochoa[135a], J.P. Ochoa-Ricoux[142a], S. Oda[85], S. Odaka[79], S. Oerdek[167], A. Ogrodnik[81a], A. Oh[97], C.C. Ohm[150], H. Oide[160], R. Oishi[159], M.L. Ojeda[44], Y. Okazaki[83], M.W. O'Keefe[88], Y. Okumura[159], A. Olariu[25b], L.F. Oleiro Seabra[135a], S.A. Olivares Pino[142d], D. Oliveira Damazio[27], D. Oliveira Goncalves[78a], J.L. Oliver[166], M.J.R. Olsson[166], A. Olszewski[82], J. Olszowska[82], Ö.O. Öncel[22], D.C. O'Neil[148], A.P. O'neill[130], A. Onofre[135a,135e], P.U.E. Onyisi[10], R.G. Oreamuno Madriz[116], M.J. Oreglia[35], G.E. Orellana[86], D. Orestano[72a,72b], N. Orlando[12], R.S. Orr[162], V. O'Shea[55], R. Ospanov[58a], G. Otero y Garzon[28], H. Otono[85], P.S. Ott[59a], G.J. Ottino[16], M. Ouchrif[33d], J. Ouellette[27], F. Ould-Saada[129], A. Ouraou[140,*], Q. Ouyang[13a], M. Owen[55], R.E. Owen[139], K.Y. Oyulmaz[11c], V.E. Ozcan[11c], N. Ozturk[7], S. Ozturk[11c], J. Pacalt[126], H.A. Pacey[30], K. Pachal[47], A. Pacheco Pages[12], C. Padilla Aranda[12], S. Pagan Griso[16], G. Palacino[63], S. Palazzo[48], S. Palestini[34], M. Palka[81b], P. Palni[81a], D.K. Panchal[10], C.E. Pandini[52], J.G. Panduro Vazquez[91], P. Pani[44], G. Panizzo[64a,64c], L. Paolozzi[52], C. Papadatos[106], S. Parajuli[40], A. Paramonov[5], C. Paraskevopoulos[9], D. Paredes Hernandez[60b], S.R. Paredes Saenz[130], B. Parida[175], T.H. Park[162], A.J. Parker[29],

JHEP03(2022)041

M.A. Parker[30], F. Parodi[53b,53a], E.W. Parrish[116], J.A. Parsons[37], U. Parzefall[50], L. Pascual Dominguez[157], V.R. Pascuzzi[16], F. Pasquali[115], E. Pasqualucci[70a], S. Passaggio[53b], F. Pastore[91], P. Pasuwan[43a,43b], J.R. Pater[97], A. Pathak[176], J. Patton[88], T. Pauly[34], J. Pearkes[149], M. Pedersen[129], L. Pedraza Diaz[114], R. Pedro[135a], T. Peiffer[51], S.V. Peleganchuk[117b,117a], O. Penc[136], C. Peng[60b], H. Peng[58a], M. Penzin[161], B.S. Peralva[78a], A.P. Pereira Peixoto[135a], L. Pereira Sanchez[43a,43b], D.V. Perepelitsa[27], E. Perez Codina[163a], M. Perganti[9], L. Perini[66a,66b], H. Pernegger[34], S. Perrella[34], A. Perrevoort[115], K. Peters[44], R.F.Y. Peters[97], B.A. Petersen[34], T.C. Petersen[38], E. Petit[98], V. Petousis[137], C. Petridou[158], P. Petroff[62], F. Petrucci[72a,72b], A. Petrukhin[147], M. Pettee[178], N.E. Pettersson[34], K. Petukhova[138], A. Peyaud[140], R. Pezoa[142e], L. Pezzotti[34], G. Pezzullo[178], T. Pham[101], P.W. Phillips[139], M.W. Phipps[168], G. Piacquadio[151], E. Pianori[16], F. Piazza[66a,66b], A. Picazio[99], R. Piegaia[28], D. Pietreanu[25b], J.E. Pilcher[35], A.D. Pilkington[97], M. Pinamonti[64a,64c], J.L. Pinfold[2], C. Pitman Donaldson[92], D.A. Pizzi[32], L. Pizzimento[71a,71b], A. Pizzini[115], M.-A. Pleier[27], V. Plesanovs[50], V. Pleskot[138], E. Plotnikova[77], P. Podberezko[117b,117a], R. Poettgen[94], R. Poggi[52], L. Poggioli[131], I. Pogrebnyak[103], D. Pohl[22], I. Pokharel[51], G. Polesello[68a], A. Poley[148,163a], A. Policicchio[70a,70b], R. Polifka[138], A. Polini[21b], C.S. Pollard[130], Z.B. Pollock[123], V. Polychronakos[27], D. Ponomarenko[108], L. Pontecorvo[34], S. Popa[25a], G.A. Popeneciu[25d], L. Portales[4], D.M. Portillo Quintero[163a], S. Pospisil[137], P. Postolache[25c], K. Potamianos[130], I.N. Potrap[77], C.J. Potter[30], H. Potti[1], T. Poulsen[44], J. Poveda[169], T.D. Powell[145], G. Pownall[44], M.E. Pozo Astigarraga[34], A. Prades Ibanez[169], P. Pralavorio[98], M.M. Prapa[42], S. Prell[76], D. Price[97], M. Primavera[65a], M.A. Principe Martin[95], M.L. Proffitt[144], N. Proklova[108], K. Prokofiev[60c], F. Prokoshin[77], S. Protopopescu[27], J. Proudfoot[5], M. Przybycien[81a], D. Pudzha[133], P. Puzo[62], D. Pyatiizbyantseva[108], J. Qian[102], Y. Qin[97], T. Qiu[90], A. Quadt[51], M. Queitsch-Maitland[34], G. Rabanal Bolanos[57], F. Ragusa[66a,66b], J.A. Raine[52], S. Rajagopalan[27], K. Ran[13a,13d], D.F. Rassloff[59a], D.M. Rauch[44], S. Rave[96], B. Ravina[55], I. Ravinovich[175], M. Raymond[34], A.L. Read[129], N.P. Readioff[145], D.M. Rebuzzi[68a,68b], G. Redlinger[27], K. Reeves[41], D. Reikher[157], A. Reiss[96], A. Rej[147], C. Rembser[34], A. Renardi[44], M. Renda[25b], M.B. Rendel[111], A.G. Rennie[55], S. Resconi[66a], M. Ressegotti[53b,53a], E.D. Resseguie[16], S. Rettie[92], B. Reynolds[123], E. Reynolds[19], M. Rezaei Estabragh[177], O.L. Rezanova[117b,117a], P. Reznicek[138], E. Ricci[73a,73b], R. Richter[111], S. Richter[44], E. Richter-Was[81b], M. Ridel[131], P. Rieck[111], P. Riedler[34], O. Rifki[44], M. Rijssenbeek[151], A. Rimoldi[68a,68b], M. Rimoldi[44], L. Rinaldi[21b,21a], T.T. Rinn[168], M.P. Rinnagel[110], G. Ripellino[150], I. Riu[12], P. Rivadeneira[44], J.C. Rivera Vergara[171], F. Rizatdinova[125], E. Rizvi[90], C. Rizzi[52], B.A. Roberts[173], B.R. Roberts[16], S.H. Robertson[100,y], M. Robin[44], D. Robinson[30], C.M. Robles Gajardo[142e], M. Robles Manzano[96], A. Robson[55], A. Rocchi[71a,71b], C. Roda[69a,69b], S. Rodriguez Bosca[59a], A. Rodriguez Rodriguez[50], A.M. Rodríguez Vera[163b], S. Roe[34], A.R. Roepe[124], J. Roggel[177], O. Røhne[129], R.A. Rojas[171], B. Roland[50], C.P.A. Roland[63], J. Roloff[27], A. Romaniouk[108], M. Romano[21b], A.C. Romero Hernandez[168], N. Rompotis[88], M. Ronzani[121], L. Roos[131], S. Rosati[70a], B.J. Rosser[132], E. Rossi[162], E. Rossi[4], E. Rossi[67a,67b], L.P. Rossi[53b], L. Rossini[44], R. Rosten[123], M. Rotaru[25b], B. Rottler[50], D. Rousseau[62], D. Rousso[30], G. Rovelli[68a,68b], A. Roy[10], A. Rozanov[98], Y. Rozen[156], X. Ruan[31f], A.J. Ruby[88], T.A. Ruggeri[1], F. Rühr[50], A. Ruiz-Martinez[169], A. Rummler[34], Z. Rurikova[50], N.A. Rusakovich[77], H.L. Russell[34], L. Rustige[36], J.P. Rutherfoord[6], E.M. Rüttinger[145], M. Rybar[138], E.B. Rye[129], A. Ryzhov[118], J.A. Sabater Iglesias[44], P. Sabatini[169], L. Sabetta[70a,70b], H.F-W. Sadrozinski[141], R. Sadykov[77], F. Safai Tehrani[70a], B. Safarzadeh Samani[152], M. Safdari[149], S. Saha[100], M. Sahinsoy[111], A. Sahu[177], M. Saimpert[140], M. Saito[159], T. Saito[159], D. Salamani[34], G. Salamanna[72a,72b], A. Salnikov[149], J. Salt[169], A. Salvador Salas[12], D. Salvatore[39b,39a], F. Salvatore[152], A. Salzburger[34], D. Sammel[50], D. Sampsonidis[158], D. Sampsonidou[58d,58c], J. Sánchez[169], A. Sanchez Pineda[4],

JHEP03(2022)041

V. Sanchez Sebastian[169], H. Sandaker[129], C.O. Sander[44], I.G. Sanderswood[87], J.A. Sandesara[99], M. Sandhoff[177], C. Sandoval[20b], D.P.C. Sankey[139], M. Sannino[53b,53a], A. Sansoni[49], C. Santoni[36], H. Santos[135a,135b], S.N. Santpur[16], A. Santra[175], K.A. Saoucha[145], A. Sapronov[77], J.G. Saraiva[135a,135d], J. Sardain[98], O. Sasaki[79], K. Sato[164], C. Sauer[59b], F. Sauerburger[50], E. Sauvan[4], P. Savard[162,aj], R. Sawada[159], C. Sawyer[139], L. Sawyer[93], I. Sayago Galvan[169], C. Sbarra[21b], A. Sbrizzi[21b,21a], T. Scanlon[92], J. Schaarschmidt[144], P. Schacht[111], D. Schaefer[35], U. Schäfer[96], A.C. Schaffer[62], D. Schaile[110], R.D. Schamberger[151], E. Schanet[110], C. Scharf[17], N. Scharmberg[97], V.A. Schegelsky[133], D. Scheirich[138], F. Schenck[17], M. Schernau[166], C. Schiavi[53b,53a], L.K. Schildgen[22], Z.M. Schillaci[24], E.J. Schioppa[65a,65b], M. Schioppa[39b,39a], B. Schlag[96], K.E. Schleicher[50], S. Schlenker[34], K. Schmieden[96], C. Schmitt[96], S. Schmitt[44], L. Schoeffel[140], A. Schoening[59b], P.G. Scholer[50], E. Schopf[130], M. Schott[96], J. Schovancova[34], S. Schramm[52], F. Schroeder[177], H-C. Schultz-Coulon[59a], M. Schumacher[50], B.A. Schumm[141], Ph. Schune[140], A. Schwartzman[149], T.A. Schwarz[102], Ph. Schwemling[140], R. Schwienhorst[103], A. Sciandra[141], G. Sciolla[24], F. Scuri[69a], F. Scutti[101], C.D. Sebastiani[88], K. Sedlaczek[45], P. Seema[17], S.C. Seidel[113], A. Seiden[141], B.D. Seidlitz[27], T. Seiss[35], C. Seitz[44], J.M. Seixas[78b], G. Sekhniaidze[67a], S.J. Sekula[40], L. Selem[4], N. Semprini-Cesari[21b,21a], S. Sen[47], C. Serfon[27], L. Serin[62], L. Serkin[64a,64b], M. Sessa[72a,72b], H. Severini[124], S. Sevova[149], F. Sforza[53b,53a], A. Sfyrla[52], E. Shabalina[51], R. Shaheen[150], J.D. Shahinian[132], N.W. Shaikh[43a,43b], D. Shaked Renous[175], L.Y. Shan[13a], M. Shapiro[16], A. Sharma[34], A.S. Sharma[1], S. Sharma[44], P.B. Shatalov[119], K. Shaw[152], S.M. Shaw[97], P. Sherwood[92], L. Shi[92], C.O. Shimmin[178], Y. Shimogama[174], J.D. Shinner[91], I.P.J. Shipsey[130], S. Shirabe[52], M. Shiyakova[77], J. Shlomi[175], M.J. Shochet[35], J. Shojaii[101], D.R. Shope[150], S. Shrestha[123], E.M. Shrif[31f], M.J. Shroff[171], E. Shulga[175], P. Sicho[136], A.M. Sickles[168], E. Sideras Haddad[31f], O. Sidiropoulou[34], A. Sidoti[21b], F. Siegert[46], Dj. Sijacki[14], J.M. Silva[19], M.V. Silva Oliveira[34], S.B. Silverstein[43a], S. Simion[62], R. Simoniello[34], N.D. Simpson[94], S. Simsek[11b], P. Sinervo[162], V. Sinetckii[109], S. Singh[148], S. Singh[162], S. Sinha[44], S. Sinha[31f], M. Sioli[21b,21a], I. Siral[127], S.Yu. Sivoklokov[109], J. Sjölin[43a,43b], A. Skaf[51], E. Skorda[94], P. Skubic[124], M. Slawinska[82], K. Sliwa[165], V. Smakhtin[175], B.H. Smart[139], J. Smiesko[138], S.Yu. Smirnov[108], Y. Smirnov[108], L.N. Smirnova[109,r], O. Smirnova[94], E.A. Smith[35], H.A. Smith[130], M. Smizanska[87], K. Smolek[137], A. Smykiewicz[82], A.A. Snesarev[107], H.L. Snoek[115], S. Snyder[27], R. Sobie[171,y], A. Soffer[157], F. Sohns[51], C.A. Solans Sanchez[34], E.Yu. Soldatov[108], U. Soldevila[169], A.A. Solodkov[118], S. Solomon[50], A. Soloshenko[77], O.V. Solovyanov[118], V. Solovyev[133], P. Sommer[145], H. Son[165], A. Sonay[12], W.Y. Song[163b], A. Sopczak[137], A.L. Sopio[92], F. Sopkova[26b], S. Sottocornola[68a,68b], R. Soualah[64a,64c], A.M. Soukharev[117b,117a], Z. Soumaimi[33e], D. South[44], S. Spagnolo[65a,65b], M. Spalla[111], M. Spangenberg[173], F. Spanò[91], D. Sperlich[50], T.M. Spieker[59a], G. Spigo[34], M. Spina[152], D.P. Spiteri[55], M. Spousta[138], A. Stabile[66a,66b], R. Stamen[59a], M. Stamenkovic[115], A. Stampekis[19], M. Standke[22], E. Stanecka[82], B. Stanislaus[34], M.M. Stanitzki[44], M. Stankaityte[130], B. Stapf[44], E.A. Starchenko[118], G.H. Stark[141], J. Stark[98], D.M. Starko[163b], P. Staroba[136], P. Starovoitov[59a], S. Stärz[100], R. Staszewski[82], G. Stavropoulos[42], P. Steinberg[27], A.L. Steinhebel[127], B. Stelzer[148,163a], H.J. Stelzer[134], O. Stelzer-Chilton[163a], H. Stenzel[54], T.J. Stevenson[152], G.A. Stewart[34], M.C. Stockton[34], G. Stoicea[25b], M. Stolarski[135a], S. Stonjek[111], A. Straessner[46], J. Strandberg[150], S. Strandberg[43a,43b], M. Strauss[124], T. Strebler[98], P. Strizenec[26b], R. Ströhmer[172], D.M. Strom[127], L.R. Strom[44], R. Stroynowski[40], A. Strubig[43a,43b], S.A. Stucci[27], B. Stugu[15], J. Stupak[124], N.A. Styles[44], D. Su[149], S. Su[58a], W. Su[58d,144,58c], X. Su[58a], K. Sugizaki[159], V.V. Sulin[107], M.J. Sullivan[88], D.M.S. Sultan[52], L. Sultanaliyeva[107], S. Sultansoy[3c], T. Sumida[83], S. Sun[102], S. Sun[176], X. Sun[97], O. Sunneborn Gudnadottir[167], C.J.E. Suster[153], M.R. Sutton[152], M. Svatos[136], M. Swiatlowski[163a], T. Swirski[172], I. Sykora[26a], M. Sykora[138], T. Sykora[138], D. Ta[96], K. Tackmann[44,w], A. Taffard[166], R. Tafirout[163a], R.H.M. Taibah[131], R. Takashima[84], K. Takeda[80],

JHEP03(2022)041

T. Takeshita[146], E.P. Takeva[48], Y. Takubo[79], M. Talby[98], A.A. Talyshev[117b,117a], K.C. Tam[60b], N.M. Tamir[157], A. Tanaka[159], J. Tanaka[159], R. Tanaka[62], J. Tang[58c], Z. Tao[170], S. Tapia Araya[76], S. Tapprogge[96], A. Tarek Abouelfadl Mohamed[103], S. Tarem[156], K. Tariq[58b], G. Tarna[25b], G.F. Tartarelli[66a], P. Tas[138], M. Tasevsky[136], E. Tassi[39b,39a], G. Tateno[159], Y. Tayalati[33e], G.N. Taylor[101], W. Taylor[163b], H. Teagle[88], A.S. Tee[176], R. Teixeira De Lima[149], P. Teixeira-Dias[91], H. Ten Kate[34], J.J. Teoh[115], K. Terashi[159], J. Terron[95], S. Terzo[12], M. Testa[49], R.J. Teuscher[162,y], N. Themistokleous[48], T. Theveneaux-Pelzer[17], O. Thielmann[177], D.W. Thomas[91], J.P. Thomas[19], E.A. Thompson[44], P.D. Thompson[19], E. Thomson[132], E.J. Thorpe[90], Y. Tian[51], V.O. Tikhomirov[107,af], Yu.A. Tikhonov[117b,117a], S. Timoshenko[108], P. Tipton[178], S. Tisserant[98], S.H. Tlou[31f], A. Tnourji[36], K. Todome[21b,21a], S. Todorova-Nova[138], S. Todt[46], M. Togawa[79], J. Tojo[85], S. Tokár[26a], K. Tokushuku[79], E. Tolley[123], R. Tombs[30], M. Tomoto[79,112], L. Tompkins[149], P. Tornambe[99], E. Torrence[127], H. Torres[46], E. Torró Pastor[169], M. Toscani[28], C. Tosciri[35], J. Toth[98,x], D.R. Tovey[145], A. Traeet[15], C.J. Treado[121], T. Trefzger[172], A. Tricoli[27], I.M. Trigger[163a], S. Trincaz-Duvoid[131], D.A. Trischuk[170], W. Trischuk[162], B. Trocmé[56], A. Trofymov[62], C. Troncon[66a], F. Trovato[152], L. Truong[31c], M. Trzebinski[82], A. Trzupek[82], F. Tsai[151], A. Tsiamis[158], P.V. Tsiareshka[104,ad], A. Tsirigotis[158,u], V. Tsiskaridze[151], E.G. Tskhadadze[155a], M. Tsopoulou[158], Y. Tsujikawa[83], I.I. Tsukerman[119], V. Tsulaia[16], S. Tsuno[79], O. Tsur[156], D. Tsybychev[151], Y. Tu[60b], A. Tudorache[25b], V. Tudorache[25b], A.N. Tuna[34], S. Turchikhin[77], I. Turk Cakir[3a], R.J. Turner[19], R. Turra[66a], P.M. Tuts[37], S. Tzamarias[158], P. Tzanis[9], E. Tzovara[96], K. Uchida[159], F. Ukegawa[164], P.A. Ulloa Poblete[142c], G. Unal[34], M. Unal[10], A. Undrus[27], G. Unel[166], F.C. Ungaro[101], K. Uno[159], J. Urban[26b], P. Urquijo[101], G. Usai[7], R. Ushioda[160], M. Usman[106], Z. Uysal[11d], V. Vacek[137], B. Vachon[100], K.O.H. Vadla[129], T. Vafeiadis[34], C. Valderanis[110], E. Valdes Santurio[43a,43b], M. Valente[163a], S. Valentinetti[21b,21a], A. Valero[169], R.A. Vallance[19], A. Vallier[98], J.A. Valls Ferrer[169], T.R. Van Daalen[144], P. Van Gemmeren[5], S. Van Stroud[92], I. Van Vulpen[115], M. Vanadia[71a,71b], W. Vandelli[34], M. Vandenbroucke[140], E.R. Vandewall[125], D. Vannicola[157], L. Vannoli[53b,53a], R. Vari[70a], E.W. Varnes[6], C. Varni[16], T. Varol[154], D. Varouchas[62], K.E. Varvell[153], M.E. Vasile[25b], L. Vaslin[36], G.A. Vasquez[171], F. Vazeille[36], D. Vazquez Furelos[12], T. Vazquez Schroeder[34], J. Veatch[51], V. Vecchio[97], M.J. Veen[115], I. Veliscek[130], L.M. Veloce[162], F. Veloso[135a,135c], S. Veneziano[70a], A. Ventura[65a,65b], A. Verbytskyi[111], M. Verducci[69a,69b], C. Vergis[22], M. Verissimo De Araujo[78b], W. Verkerke[115], A.T. Vermeulen[115], J.C. Vermeulen[115], C. Vernieri[149], P.J. Verschuuren[91], M. Vessella[99], M.L. Vesterbacka[121], M.C. Vetterli[148,aj], A. Vgenopoulos[158], N. Viaux Maira[142e], T. Vickey[145], O.E. Vickey Boeriu[145], G.H.A. Viehhauser[130], L. Vigani[59b], M. Villa[21b,21a], M. Villaplana Perez[169], E.M. Villhauer[48], E. Vilucchi[49], M.G. Vincter[32], G.S. Virdee[19], A. Vishwakarma[48], C. Vittori[21b,21a], I. Vivarelli[152], V. Vladimirov[173], E. Voevodina[111], M. Vogel[177], P. Vokac[137], J. Von Ahnen[44], E. Von Toerne[22], V. Vorobel[138], K. Vorobev[108], M. Vos[169], J.H. Vossebeld[88], M. Vozak[97], L. Vozdecky[90], N. Vranjes[14], M. Vranjes Milosavljevic[14], V. Vrba[137,*], M. Vreeswijk[115], N.K. Vu[98], R. Vuillermet[34], O.V. Vujinovic[96], I. Vukotic[35], S. Wada[164], C. Wagner[99], W. Wagner[177], S. Wahdan[177], H. Wahlberg[86], R. Wakasa[164], M. Wakida[112], V.M. Walbrecht[111], J. Walder[139], R. Walker[110], S.D. Walker[91], W. Walkowiak[147], A.M. Wang[57], A.Z. Wang[176], C. Wang[58a], C. Wang[58c], H. Wang[16], J. Wang[60a], P. Wang[40], R.-J. Wang[96], R. Wang[57], R. Wang[116], S.M. Wang[154], S. Wang[58b], T. Wang[58a], W.T. Wang[75], W.X. Wang[58a], X. Wang[13c], X. Wang[168], X. Wang[58c], Y. Wang[58a], Z. Wang[102], C. Wanotayaroj[34], A. Warburton[100], C.P. Ward[30], R.J. Ward[19], N. Warrack[55], A.T. Watson[19], M.F. Watson[19], G. Watts[144], B.M. Waugh[92], A.F. Webb[10], C. Weber[27], M.S. Weber[18], S.A. Weber[32], S.M. Weber[59a], C. Wei[58a], Y. Wei[130], A.R. Weidberg[130], J. Weingarten[45], M. Weirich[96], C. Weiser[50], T. Wenaus[27], B. Wendland[45], T. Wengler[34], S. Wenig[34], N. Wermes[22], M. Wessels[59a], K. Whalen[127], A.M. Wharton[87], A.S. White[57],

JHEP03(2022)041

A. White[7], M.J. White[1], D. Whiteson[166], L. Wickremasinghe[128], W. Wiedenmann[176], C. Wiel[46], M. Wielers[139], N. Wieseotte[96], C. Wiglesworth[38], L.A.M. Wiik-Fuchs[50], D.J. Wilbern[124], H.G. Wilkens[34], L.J. Wilkins[91], D.M. Williams[37], H.H. Williams[132], S. Williams[30], S. Willocq[99], P.J. Windischhofer[130], I. Wingerter-Seez[4], F. Winklmeier[127], B.T. Winter[50], M. Wittgen[149], M. Wobisch[93], A. Wolf[96], R. Wölker[130], J. Wollrath[166], M.W. Wolter[82], H. Wolters[135a,135c], V.W.S. Wong[170], A.F. Wongel[44], S.D. Worm[44], B.K. Wosiek[82], K.W. Woźniak[82], K. Wraight[55], J. Wu[13a,13d], S.L. Wu[176], X. Wu[52], Y. Wu[58a], Z. Wu[140,58a], J. Wuerzinger[130], T.R. Wyatt[97], B.M. Wynne[48], S. Xella[38], L. Xia[13c], M. Xia[13b], J. Xiang[60c], X. Xiao[102], M. Xie[58a], X. Xie[58a], I. Xiotidis[152], D. Xu[13a], H. Xu[58a], H. Xu[58a], L. Xu[58a], R. Xu[132], T. Xu[58a], W. Xu[102], Y. Xu[13b], Z. Xu[58b], Z. Xu[149], B. Yabsley[153], S. Yacoob[31a], N. Yamaguchi[85], Y. Yamaguchi[160], M. Yamatani[159], H. Yamauchi[164], T. Yamazaki[16], Y. Yamazaki[80], J. Yan[58c], S. Yan[130], Z. Yan[23], H.J. Yang[58c,58d], H.T. Yang[16], S. Yang[58a], T. Yang[60c], X. Yang[58a], X. Yang[13a], Y. Yang[159], Z. Yang[102,58a], W-M. Yao[16], Y.C. Yap[44], H. Ye[13c], J. Ye[40], S. Ye[27], I. Yeletskikh[77], M.R. Yexley[87], P. Yin[37], K. Yorita[174], K. Yoshihara[76], C.J.S. Young[50], C. Young[149], M. Yuan[102], R. Yuan[58b,i], X. Yue[59a], M. Zaazoua[33e], B. Zabinski[82], G. Zacharis[9], E. Zaid[48], A.M. Zaitsev[118,ae], T. Zakareishvili[155b], N. Zakharchuk[32], S. Zambito[34], D. Zanzi[50], S.V. Zeißner[45], C. Zeitnitz[177], J.C. Zeng[168], D.T. Zenger Jr[24], O. Zenin[118], T. Ženiš[26a], S. Zenz[90], S. Zerradi[33a], D. Zerwas[62], B. Zhang[13c], D.F. Zhang[145], G. Zhang[13b], J. Zhang[5], K. Zhang[13a], L. Zhang[13c], M. Zhang[168], R. Zhang[176], S. Zhang[102], X. Zhang[58c], X. Zhang[58b], Z. Zhang[62], P. Zhao[47], T. Zhao[58b], Y. Zhao[141], Z. Zhao[58a], A. Zhemchugov[77], Z. Zheng[149], D. Zhong[168], B. Zhou[102], C. Zhou[176], H. Zhou[6], N. Zhou[58c], Y. Zhou[6], C.G. Zhu[58b], C. Zhu[13a,13d], H.L. Zhu[58a], H. Zhu[13a], J. Zhu[102], Y. Zhu[58a], X. Zhuang[13a], K. Zhukov[107], V. Zhulanov[117b,117a], D. Zieminska[63], N.I. Zimine[77], S. Zimmermann[50,*], J. Zinsser[59b], M. Ziolkowski[147], L. Živković[14], A. Zoccoli[21b,21a], K. Zoch[52], T.G. Zorbas[145], O. Zormpa[42], W. Zou[37], L. Zwalinski[34]

[1] *Department of Physics, University of Adelaide, Adelaide; Australia*

[2] *Department of Physics, University of Alberta, Edmonton AB; Canada*

[3] [(a)] *Department of Physics, Ankara University, Ankara;* [(b)] *Istanbul Aydin University, Application and Research Center for Advanced Studies, Istanbul;* [(c)] *Division of Physics, TOBB University of Economics and Technology, Ankara; Turkey*

[4] *LAPP, Univ. Savoie Mont Blanc, CNRS/IN2P3, Annecy; France*

[5] *High Energy Physics Division, Argonne National Laboratory, Argonne IL; United States of America*

[6] *Department of Physics, University of Arizona, Tucson AZ; United States of America*

[7] *Department of Physics, University of Texas at Arlington, Arlington TX; United States of America*

[8] *Physics Department, National and Kapodistrian University of Athens, Athens; Greece*

[9] *Physics Department, National Technical University of Athens, Zografou; Greece*

[10] *Department of Physics, University of Texas at Austin, Austin TX; United States of America*

[11] [(a)] *Bahcesehir University, Faculty of Engineering and Natural Sciences, Istanbul;* [(b)] *Istanbul Bilgi University, Faculty of Engineering and Natural Sciences, Istanbul;* [(c)] *Department of Physics, Bogazici University, Istanbul;* [(d)] *Department of Physics Engineering, Gaziantep University, Gaziantep; Turkey*

[12] *Institut de Física d'Altes Energies (IFAE), Barcelona Institute of Science and Technology, Barcelona; Spain*

[13] [(a)] *Institute of High Energy Physics, Chinese Academy of Sciences, Beijing;* [(b)] *Physics Department, Tsinghua University, Beijing;* [(c)] *Department of Physics, Nanjing University, Nanjing;* [(d)] *University of Chinese Academy of Science (UCAS), Beijing; China*

[14] *Institute of Physics, University of Belgrade, Belgrade; Serbia*

[15] *Department for Physics and Technology, University of Bergen, Bergen; Norway*

[16] *Physics Division, Lawrence Berkeley National Laboratory and University of California, Berkeley CA; United States of America*

[17] *Institut für Physik, Humboldt Universität zu Berlin, Berlin; Germany*

JHEP03(2022)041

[18] *Albert Einstein Center for Fundamental Physics and Laboratory for High Energy Physics, University of Bern, Bern; Switzerland*
[19] *School of Physics and Astronomy, University of Birmingham, Birmingham; United Kingdom*
[20] [(a)] *Facultad de Ciencias y Centro de Investigaciónes, Universidad Antonio Nariño, Bogotá;* [(b)] *Departamento de Física, Universidad Nacional de Colombia, Bogotá; Colombia*
[21] [(a)] *Dipartimento di Fisica e Astronomia A. Righi, Università di Bologna, Bologna;* [(b)] *INFN Sezione di Bologna; Italy*
[22] *Physikalisches Institut, Universität Bonn, Bonn; Germany*
[23] *Department of Physics, Boston University, Boston MA; United States of America*
[24] *Department of Physics, Brandeis University, Waltham MA; United States of America*
[25] [(a)] *Transilvania University of Brasov, Brasov;* [(b)] *Horia Hulubei National Institute of Physics and Nuclear Engineering, Bucharest;* [(c)] *Department of Physics, Alexandru Ioan Cuza University of Iasi, Iasi;* [(d)] *National Institute for Research and Development of Isotopic and Molecular Technologies, Physics Department, Cluj-Napoca;* [(e)] *University Politehnica Bucharest, Bucharest;* [(f)] *West University in Timisoara, Timisoara; Romania*
[26] [(a)] *Faculty of Mathematics, Physics and Informatics, Comenius University, Bratislava;* [(b)] *Department of Subnuclear Physics, Institute of Experimental Physics of the Slovak Academy of Sciences, Kosice; Slovak Republic*
[27] *Physics Department, Brookhaven National Laboratory, Upton NY; United States of America*
[28] *Departamento de Física (FCEN) and IFIBA, Universidad de Buenos Aires and CONICET, Buenos Aires; Argentina*
[29] *California State University, CA; United States of America*
[30] *Cavendish Laboratory, University of Cambridge, Cambridge; United Kingdom*
[31] [(a)] *Department of Physics, University of Cape Town, Cape Town;* [(b)] *iThemba Labs, Western Cape;* [(c)] *Department of Mechanical Engineering Science, University of Johannesburg, Johannesburg;* [(d)] *National Institute of Physics, University of the Philippines Diliman (Philippines);* [(e)] *University of South Africa, Department of Physics, Pretoria;* [(f)] *School of Physics, University of the Witwatersrand, Johannesburg; South Africa*
[32] *Department of Physics, Carleton University, Ottawa ON; Canada*
[33] [(a)] *Faculté des Sciences Ain Chock, Réseau Universitaire de Physique des Hautes Energies — Université Hassan II, Casablanca;* [(b)] *Faculté des Sciences, Université Ibn-Tofail, Kénitra;* [(c)] *Faculté des Sciences Semlalia, Université Cadi Ayyad, LPHEA-Marrakech;* [(d)] *LPMR, Faculté des Sciences, Université Mohamed Premier, Oujda;* [(e)] *Faculté des sciences, Université Mohammed V, Rabat;* [(f)] *Mohammed VI Polytechnic University, Ben Guerir; Morocco*
[34] *CERN, Geneva; Switzerland*
[35] *Enrico Fermi Institute, University of Chicago, Chicago IL; United States of America*
[36] *LPC, Université Clermont Auvergne, CNRS/IN2P3, Clermont-Ferrand; France*
[37] *Nevis Laboratory, Columbia University, Irvington NY; United States of America*
[38] *Niels Bohr Institute, University of Copenhagen, Copenhagen; Denmark*
[39] [(a)] *Dipartimento di Fisica, Università della Calabria, Rende;* [(b)] *INFN Gruppo Collegato di Cosenza, Laboratori Nazionali di Frascati; Italy*
[40] *Physics Department, Southern Methodist University, Dallas TX; United States of America*
[41] *Physics Department, University of Texas at Dallas, Richardson TX; United States of America*
[42] *National Centre for Scientific Research "Demokritos", Agia Paraskevi; Greece*
[43] [(a)] *Department of Physics, Stockholm University;* [(b)] *Oskar Klein Centre, Stockholm; Sweden*
[44] *Deutsches Elektronen-Synchrotron DESY, Hamburg and Zeuthen; Germany*
[45] *Fakultät Physik, Technische Universität Dortmund, Dortmund; Germany*
[46] *Institut für Kern- und Teilchenphysik, Technische Universität Dresden, Dresden; Germany*
[47] *Department of Physics, Duke University, Durham NC; United States of America*
[48] *SUPA — School of Physics and Astronomy, University of Edinburgh, Edinburgh; United Kingdom*
[49] *INFN e Laboratori Nazionali di Frascati, Frascati; Italy*
[50] *Physikalisches Institut, Albert-Ludwigs-Universität Freiburg, Freiburg; Germany*
[51] *II. Physikalisches Institut, Georg-August-Universität Göttingen, Göttingen; Germany*

JHEP03(2022)041

[52] Département de Physique Nucléaire et Corpusculaire, Université de Genève, Genève; Switzerland
[53] [(a)] Dipartimento di Fisica, Università di Genova, Genova; [(b)] INFN Sezione di Genova; Italy
[54] II. Physikalisches Institut, Justus-Liebig-Universität Giessen, Giessen; Germany
[55] SUPA — School of Physics and Astronomy, University of Glasgow, Glasgow; United Kingdom
[56] LPSC, Université Grenoble Alpes, CNRS/IN2P3, Grenoble INP, Grenoble; France
[57] Laboratory for Particle Physics and Cosmology, Harvard University, Cambridge MA; United States of America
[58] [(a)] Department of Modern Physics and State Key Laboratory of Particle Detection and Electronics, University of Science and Technology of China, Hefei; [(b)] Institute of Frontier and Interdisciplinary Science and Key Laboratory of Particle Physics and Particle Irradiation (MOE), Shandong University, Qingdao; [(c)] School of Physics and Astronomy, Shanghai Jiao Tong University, Key Laboratory for Particle Astrophysics and Cosmology (MOE), SKLPPC, Shanghai; [(d)] Tsung-Dao Lee Institute, Shanghai; China
[59] [(a)] Kirchhoff-Institut für Physik, Ruprecht-Karls-Universität Heidelberg, Heidelberg; [(b)] Physikalisches Institut, Ruprecht-Karls-Universität Heidelberg, Heidelberg; Germany
[60] [(a)] Department of Physics, Chinese University of Hong Kong, Shatin, N.T., Hong Kong; [(b)] Department of Physics, University of Hong Kong, Hong Kong; [(c)] Department of Physics and Institute for Advanced Study, Hong Kong University of Science and Technology, Clear Water Bay, Kowloon, Hong Kong; China
[61] Department of Physics, National Tsing Hua University, Hsinchu; Taiwan
[62] IJCLab, Université Paris-Saclay, CNRS/IN2P3, 91405, Orsay; France
[63] Department of Physics, Indiana University, Bloomington IN; United States of America
[64] [(a)] INFN Gruppo Collegato di Udine, Sezione di Trieste, Udine; [(b)] ICTP, Trieste; [(c)] Dipartimento Politecnico di Ingegneria e Architettura, Università di Udine, Udine; Italy
[65] [(a)] INFN Sezione di Lecce; [(b)] Dipartimento di Matematica e Fisica, Università del Salento, Lecce; Italy
[66] [(a)] INFN Sezione di Milano; [(b)] Dipartimento di Fisica, Università di Milano, Milano; Italy
[67] [(a)] INFN Sezione di Napoli; [(b)] Dipartimento di Fisica, Università di Napoli, Napoli; Italy
[68] [(a)] INFN Sezione di Pavia; [(b)] Dipartimento di Fisica, Università di Pavia, Pavia; Italy
[69] [(a)] INFN Sezione di Pisa; [(b)] Dipartimento di Fisica E. Fermi, Università di Pisa, Pisa; Italy
[70] [(a)] INFN Sezione di Roma; [(b)] Dipartimento di Fisica, Sapienza Università di Roma, Roma; Italy
[71] [(a)] INFN Sezione di Roma Tor Vergata; [(b)] Dipartimento di Fisica, Università di Roma Tor Vergata, Roma; Italy
[72] [(a)] INFN Sezione di Roma Tre; [(b)] Dipartimento di Matematica e Fisica, Università Roma Tre, Roma; Italy
[73] [(a)] INFN-TIFPA; [(b)] Università degli Studi di Trento, Trento; Italy
[74] Institut für Astro- und Teilchenphysik, Leopold-Franzens-Universität, Innsbruck; Austria
[75] University of Iowa, Iowa City IA; United States of America
[76] Department of Physics and Astronomy, Iowa State University, Ames IA; United States of America
[77] Joint Institute for Nuclear Research, Dubna; Russia
[78] [(a)] Departamento de Engenharia Elétrica, Universidade Federal de Juiz de Fora (UFJF), Juiz de Fora; [(b)] Universidade Federal do Rio De Janeiro COPPE/EE/IF, Rio de Janeiro; [(c)] Instituto de Física, Universidade de São Paulo, São Paulo; Brazil
[79] KEK, High Energy Accelerator Research Organization, Tsukuba; Japan
[80] Graduate School of Science, Kobe University, Kobe; Japan
[81] [(a)] AGH University of Science and Technology, Faculty of Physics and Applied Computer Science, Krakow; [(b)] Marian Smoluchowski Institute of Physics, Jagiellonian University, Krakow; Poland
[82] Institute of Nuclear Physics Polish Academy of Sciences, Krakow; Poland
[83] Faculty of Science, Kyoto University, Kyoto; Japan
[84] Kyoto University of Education, Kyoto; Japan
[85] Research Center for Advanced Particle Physics and Department of Physics, Kyushu University, Fukuoka; Japan
[86] Instituto de Física La Plata, Universidad Nacional de La Plata and CONICET, La Plata; Argentina
[87] Physics Department, Lancaster University, Lancaster; United Kingdom

JHEP03(2022)041

[88] Oliver Lodge Laboratory, University of Liverpool, Liverpool; United Kingdom
[89] Department of Experimental Particle Physics, Jožef Stefan Institute and Department of Physics, University of Ljubljana, Ljubljana; Slovenia
[90] School of Physics and Astronomy, Queen Mary University of London, London; United Kingdom
[91] Department of Physics, Royal Holloway University of London, Egham; United Kingdom
[92] Department of Physics and Astronomy, University College London, London; United Kingdom
[93] Louisiana Tech University, Ruston LA; United States of America
[94] Fysiska institutionen, Lunds universitet, Lund; Sweden
[95] Departamento de Física Teorica C-15 and CIAFF, Universidad Autónoma de Madrid, Madrid; Spain
[96] Institut für Physik, Universität Mainz, Mainz; Germany
[97] School of Physics and Astronomy, University of Manchester, Manchester; United Kingdom
[98] CPPM, Aix-Marseille Université, CNRS/IN2P3, Marseille; France
[99] Department of Physics, University of Massachusetts, Amherst MA; United States of America
[100] Department of Physics, McGill University, Montreal QC; Canada
[101] School of Physics, University of Melbourne, Victoria; Australia
[102] Department of Physics, University of Michigan, Ann Arbor MI; United States of America
[103] Department of Physics and Astronomy, Michigan State University, East Lansing MI; United States of America
[104] B.I. Stepanov Institute of Physics, National Academy of Sciences of Belarus, Minsk; Belarus
[105] Research Institute for Nuclear Problems of Byelorussian State University, Minsk; Belarus
[106] Group of Particle Physics, University of Montreal, Montreal QC; Canada
[107] P.N. Lebedev Physical Institute of the Russian Academy of Sciences, Moscow; Russia
[108] National Research Nuclear University MEPhI, Moscow; Russia
[109] D.V. Skobeltsyn Institute of Nuclear Physics, M.V. Lomonosov Moscow State University, Moscow; Russia
[110] Fakultät für Physik, Ludwig-Maximilians-Universität München, München; Germany
[111] Max-Planck-Institut für Physik (Werner-Heisenberg-Institut), München; Germany
[112] Graduate School of Science and Kobayashi-Maskawa Institute, Nagoya University, Nagoya; Japan
[113] Department of Physics and Astronomy, University of New Mexico, Albuquerque NM; United States of America
[114] Institute for Mathematics, Astrophysics and Particle Physics, Radboud University/Nikhef, Nijmegen; Netherlands
[115] Nikhef National Institute for Subatomic Physics and University of Amsterdam, Amsterdam; Netherlands
[116] Department of Physics, Northern Illinois University, DeKalb IL; United States of America
[117] [(a)] Budker Institute of Nuclear Physics and NSU, SB RAS, Novosibirsk;[(b)] Novosibirsk State University Novosibirsk; Russia
[118] Institute for High Energy Physics of the National Research Centre Kurchatov Institute, Protvino; Russia
[119] Institute for Theoretical and Experimental Physics named by A.I. Alikhanov of National Research Centre "Kurchatov Institute", Moscow; Russia
[120] [(a)] New York University Abu Dhabi, Abu Dhabi;[(b)] United Arab Emirates University, Al Ain;[(c)] University of Sharjah, Sharjah; United Arab Emirates
[121] Department of Physics, New York University, New York NY; United States of America
[122] Ochanomizu University, Otsuka, Bunkyo-ku, Tokyo; Japan
[123] Ohio State University, Columbus OH; United States of America
[124] Homer L. Dodge Department of Physics and Astronomy, University of Oklahoma, Norman OK; United States of America
[125] Department of Physics, Oklahoma State University, Stillwater OK; United States of America
[126] Palacký University, Joint Laboratory of Optics, Olomouc; Czech Republic
[127] Institute for Fundamental Science, University of Oregon, Eugene, OR; United States of America
[128] Graduate School of Science, Osaka University, Osaka; Japan
[129] Department of Physics, University of Oslo, Oslo; Norway

JHEP03(2022)041

[130] Department of Physics, Oxford University, Oxford; United Kingdom
[131] LPNHE, Sorbonne Université, Université de Paris, CNRS/IN2P3, Paris; France
[132] Department of Physics, University of Pennsylvania, Philadelphia PA; United States of America
[133] Konstantinov Nuclear Physics Institute of National Research Centre "Kurchatov Institute", PNPI, St. Petersburg; Russia
[134] Department of Physics and Astronomy, University of Pittsburgh, Pittsburgh PA; United States of America
[135] [(a)] Laboratório de Instrumentação e Física Experimental de Partículas — LIP, Lisboa;[(b)] Departamento de Física, Faculdade de Ciências, Universidade de Lisboa, Lisboa;[(c)] Departamento de Física, Universidade de Coimbra, Coimbra;[(d)] Centro de Física Nuclear da Universidade de Lisboa, Lisboa;[(e)] Departamento de Física, Universidade do Minho, Braga;[(f)] Departamento de Física Teórica y del Cosmos, Universidad de Granada, Granada (Spain);[(g)] Instituto Superior Técnico, Universidade de Lisboa, Lisboa; Portugal
[136] Institute of Physics of the Czech Academy of Sciences, Prague; Czech Republic
[137] Czech Technical University in Prague, Prague; Czech Republic
[138] Charles University, Faculty of Mathematics and Physics, Prague; Czech Republic
[139] Particle Physics Department, Rutherford Appleton Laboratory, Didcot; United Kingdom
[140] IRFU, CEA, Université Paris-Saclay, Gif-sur-Yvette; France
[141] Santa Cruz Institute for Particle Physics, University of California Santa Cruz, Santa Cruz CA; United States of America
[142] [(a)] Departamento de Física, Pontificia Universidad Católica de Chile, Santiago;[(b)] Instituto de Investigación Multidisciplinario en Ciencia y Tecnología, y Departamento de Física, Universidad de La Serena;[(c)] Universidad Andres Bello, Department of Physics, Santiago;[(d)] Instituto de Alta Investigación, Universidad de Tarapacá, Arica;[(e)] Departamento de Física, Universidad Técnica Federico Santa María, Valparaíso; Chile
[143] Universidade Federal de São João del Rei (UFSJ), São João del Rei; Brazil
[144] Department of Physics, University of Washington, Seattle WA; United States of America
[145] Department of Physics and Astronomy, University of Sheffield, Sheffield; United Kingdom
[146] Department of Physics, Shinshu University, Nagano; Japan
[147] Department Physik, Universität Siegen, Siegen; Germany
[148] Department of Physics, Simon Fraser University, Burnaby BC; Canada
[149] SLAC National Accelerator Laboratory, Stanford CA; United States of America
[150] Department of Physics, Royal Institute of Technology, Stockholm; Sweden
[151] Departments of Physics and Astronomy, Stony Brook University, Stony Brook NY; United States of America
[152] Department of Physics and Astronomy, University of Sussex, Brighton; United Kingdom
[153] School of Physics, University of Sydney, Sydney; Australia
[154] Institute of Physics, Academia Sinica, Taipei; Taiwan
[155] [(a)] E. Andronikashvili Institute of Physics, Iv. Javakhishvili Tbilisi State University, Tbilisi;[(b)] High Energy Physics Institute, Tbilisi State University, Tbilisi; Georgia
[156] Department of Physics, Technion, Israel Institute of Technology, Haifa; Israel
[157] Raymond and Beverly Sackler School of Physics and Astronomy, Tel Aviv University, Tel Aviv; Israel
[158] Department of Physics, Aristotle University of Thessaloniki, Thessaloniki; Greece
[159] International Center for Elementary Particle Physics and Department of Physics, University of Tokyo, Tokyo; Japan
[160] Department of Physics, Tokyo Institute of Technology, Tokyo; Japan
[161] Tomsk State University, Tomsk; Russia
[162] Department of Physics, University of Toronto, Toronto ON; Canada
[163] [(a)] TRIUMF, Vancouver BC;[(b)] Department of Physics and Astronomy, York University, Toronto ON; Canada
[164] Division of Physics and Tomonaga Center for the History of the Universe, Faculty of Pure and Applied Sciences, University of Tsukuba, Tsukuba; Japan
[165] Department of Physics and Astronomy, Tufts University, Medford MA; United States of America

JHEP03(2022)041

[166] Department of Physics and Astronomy, University of California Irvine, Irvine CA; United States of America
[167] Department of Physics and Astronomy, University of Uppsala, Uppsala; Sweden
[168] Department of Physics, University of Illinois, Urbana IL; United States of America
[169] Instituto de Física Corpuscular (IFIC), Centro Mixto Universidad de Valencia — CSIC, Valencia; Spain
[170] Department of Physics, University of British Columbia, Vancouver BC; Canada
[171] Department of Physics and Astronomy, University of Victoria, Victoria BC; Canada
[172] Fakultät für Physik und Astronomie, Julius-Maximilians-Universität Würzburg, Würzburg; Germany
[173] Department of Physics, University of Warwick, Coventry; United Kingdom
[174] Waseda University, Tokyo; Japan
[175] Department of Particle Physics and Astrophysics, Weizmann Institute of Science, Rehovot; Israel
[176] Department of Physics, University of Wisconsin, Madison WI; United States of America
[177] Fakultät für Mathematik und Naturwissenschaften, Fachgruppe Physik, Bergische Universität Wuppertal, Wuppertal; Germany
[178] Department of Physics, Yale University, New Haven CT; United States of America

[a] Also at Borough of Manhattan Community College, City University of New York, New York NY; United States of America
[b] Also at Bruno Kessler Foundation, Trento; Italy
[c] Also at Center for High Energy Physics, Peking University; China
[d] Also at Centro Studi e Ricerche Enrico Fermi; Italy
[e] Also at CERN, Geneva; Switzerland
[f] Also at Département de Physique Nucléaire et Corpusculaire, Université de Genève, Genève; Switzerland
[g] Also at Departament de Fisica de la Universitat Autonoma de Barcelona, Barcelona; Spain
[h] Also at Department of Financial and Management Engineering, University of the Aegean, Chios; Greece
[i] Also at Department of Physics and Astronomy, Michigan State University, East Lansing MI; United States of America
[j] Also at Department of Physics and Astronomy, University of Louisville, Louisville, KY; United States of America
[k] Also at Department of Physics, Ben Gurion University of the Negev, Beer Sheva; Israel
[l] Also at Department of Physics, California State University, East Bay; United States of America
[m] Also at Department of Physics, California State University, Fresno; United States of America
[n] Also at Department of Physics, California State University, Sacramento; United States of America
[o] Also at Department of Physics, King's College London, London; United Kingdom
[p] Also at Department of Physics, St. Petersburg State Polytechnical University, St. Petersburg; Russia
[q] Also at Department of Physics, University of Fribourg, Fribourg; Switzerland
[r] Also at Faculty of Physics, M.V. Lomonosov Moscow State University, Moscow; Russia
[s] Also at Faculty of Physics, Sofia University, 'St. Kliment Ohridski', Sofia; Bulgaria
[t] Also at Graduate School of Science, Osaka University, Osaka; Japan
[u] Also at Hellenic Open University, Patras; Greece
[v] Also at Institucio Catalana de Recerca i Estudis Avancats, ICREA, Barcelona; Spain
[w] Also at Institut für Experimentalphysik, Universität Hamburg, Hamburg; Germany
[x] Also at Institute for Particle and Nuclear Physics, Wigner Research Centre for Physics, Budapest; Hungary
[y] Also at Institute of Particle Physics (IPP); Canada
[z] Also at Institute of Physics, Azerbaijan Academy of Sciences, Baku; Azerbaijan
[aa] Also at Institute of Theoretical Physics, Ilia State University, Tbilisi; Georgia
[ab] Also at Instituto de Fisica Teorica, IFT-UAM/CSIC, Madrid; Spain
[ac] Also at Istanbul University, Dept. of Physics, Istanbul; Turkey
[ad] Also at Joint Institute for Nuclear Research, Dubna; Russia

JHEP03(2022)041

[ae] Also at Moscow Institute of Physics and Technology State University, Dolgoprudny; Russia
[af] Also at National Research Nuclear University MEPhI, Moscow; Russia
[ag] Also at Physics Department, An-Najah National University, Nablus; Palestine
[ah] Also at Physikalisches Institut, Albert-Ludwigs-Universität Freiburg, Freiburg; Germany
[ai] Also at The City College of New York, New York NY; United States of America
[aj] Also at TRIUMF, Vancouver BC; Canada
[ak] Also at Università di Napoli Parthenope, Napoli; Italy
[al] Also at University of Chinese Academy of Sciences (UCAS), Beijing; China
[am] Also at Yeditepe University, Physics Department, Istanbul; Turkey
[*] Deceased

JHEP03(2022)041